

A.C. MEASUREMENTS WITH A  
DEPLETION-MODE CHARGE-FLOW TRANSISTOR

by

STEVEN LEE GARVERICK

S.B., Massachusetts Institute of Technology  
(1979)

SUBMITTED IN PARTIAL FULFILLMENT  
OF THE REQUIREMENTS FOR THE  
DEGREE OF

MASTER OF SCIENCE

at the

MASSACHUSETTS INSTITUTE OF TECHNOLOGY

September 1980

© Massachusetts Institute of Technology 1979

Signature of Author \_\_\_\_\_

Department of Electrical Engineering  
August 15, 1980

Certified by \_\_\_\_\_ *8/15/80*

*Stephen D. Senturia*  
Thesis Supervisor

Accepted by \_\_\_\_\_

Arthur C. Smith  
Chairman, Committee on Graduate Students

ARCHIVES  
MASSACHUSETTS INSTITUTE  
OF TECHNOLOGY

NOV 4 1980

LIBRARIES

A.C. MEASUREMENTS WITH A  
DEPLETION-MODE CHARGE-FLOW TRANSISTOR

by

STEVEN LEE GARVERICK

Submitted to the Department of Electrical Engineering  
on August 15, 1980 in partial fulfillment of the  
requirements for the Degree of Master of Science in  
Electrical Engineering

ABSTRACT

A new MOS device for use in measuring the dielectric properties of high-impedance materials has been developed. The device consists of a depletion-mode FET, and a planar interdigitated capacitor (lock and key) that is coated with the material of interest. One electrode of the lock and key is driven with a sinusoid, while the other is tied to the gate of the FET. The signal that reaches this floating gate electrode is a function of the dielectric properties of the material under study. This signal is monitored via the channel conductance modulation of the FET.

A measurement technique that employs a second matched FET as reference has been developed. The technique allows indirect measurement of the floating electrode voltage, by the use of external feedback circuitry that maintains matched operation by the two FET's. The gate voltage which the circuit supplies to the reference FET mirrors the floating-electrode voltage. One measurement is required to calibrate each FET pair.

The technique has been used to examine the properties of thin films of the moisture-sensitive polymer, poly ethylene oxide (PEO). A model describing the transfer function of the system has been derived, assuming surface-dominated conductance by the thin film, negligible contact impedance, and no dispersion. The model and data are in excellent agreement, making possible the extraction of the sheet resistance. The PEO thin film exhibits a sheet resistance that varies over more than four orders of magnitude, for 3% to 75% relative humidity. The study has demonstrated that the technique may be successfully employed to measure sheet resistances as high as  $10^{16}$  ohms per square.

Thesis Supervisor: Stephen D. Senturia

Title: Professor of Electrical Engineering

## ACKNOWLEDGEMENTS

The author wishes to acknowledge the efforts of Professor Stephen D. Senturia who supervised this thesis, providing constant guidance during the course of the work as well as invaluable aid in the preparation of this document. The author gratefully acknowledges the support of the MIT-Industry Polymer Processing Program who sponsored the research.

Some of the instrumentation used in this work was made available through programs sponsored by the Office of Naval Research and by the National Science Foundation. The MOS Characterization System is a gift from the Hewlett-Packard Corporation. The Microelectronics Laboratory is a central facility of the Center for Materials Science and Engineering, a Materials Research Laboratory supported in part by NSF contract number DMR-78-24185.

## TABLE OF CONTENTS

	<u>PAGE</u>
ABSTRACT .....	2
CHAPTER 1: INTRODUCTION .....	5
CHAPTER 2: BACKGROUND .....	7
A. THE LOCK AND KEY .....	7
B. THE CHARGE-FLOW TRANSISTOR .....	9
CHAPTER 3: THE NEW METHOD FOR A.C. MEASUREMENT OF DIELECTRIC PROPERTIES .....	15
A. THE DEVICE .....	15
B. THE MEASUREMENT TECHNIQUE .....	25
CHAPTER 4: ANALYSIS OF A THIN-FILM SYSTEM: POLY ETHYLENE OXIDE ...	32
CHAPTER 5: LIMITATIONS OF THE NEW TECHNIQUE .....	52
APPENDICES .....	56
A. SYMBOL DEFINITIONS .....	56
B. SOLUTION TO TRANSMISSION LINE MODEL .....	57
C. DEVICE FABRICATION PROCEDURE .....	59
D. SUPREM SIMULATION OF DEVICE FABRICATION .....	62
E. DETAILED MASK LAYOUT .....	70
F. DESCRIPTION OF THE COMPUTER PROGRAM DEWPNT .....	77
G. DESCRIPTION OF FLIP-CHIP PACKAGE .....	92
H. PLANS FOR AN IMMERSIBLE DEVICE .....	97
REFERENCES .....	101

## CHAPTER 1: INTRODUCTION

In recent years, MOS technology has been applied to the problem of making small and inexpensive sensing devices. These sensing devices are typically based upon the measurement of the electrical properties of a high-impedance film.

This project was begun with the goal of making an MOS pH sensor based upon the measurement of a pH-sensitive impedance, rather than of a D.C. potential, as is the case with current pH sensors (1). The project had three main divisions: 1) the characterization of various thin films of pH glass to determine if they exhibited an exploitable pH-sensitive admittance; 2) the development of a device structure and corresponding measurement technique suitable for use with the pH-sensitive thin film; and 3) the development of an immersible device package.

The first of the above was the subject of work done by J. Adcock (2) and R. Johns (3). Thin films of various pH-sensitive glasses, fabricated by sputtering, silk screening, and by blowing, as well as a pH-sensitive polymer were examined. The basic conclusion of their work is that there is no intrinsic pH sensitivity of the electrical admittance in any of the above samples.

While the above studies proceeded, the design of the device and its package was undertaken by the author. Because the thin films under study were primarily capacitive, the device was designed to be suitable for use in an A.C. measurement system. In addition, both the device and package design included special features for resistance against the hazards of immersion. It became obvious, however, that a pH-sensitive thin film was not going to be available.

Nevertheless, the technique that had been designed for making

A.C. measurements of high-impedance films was not limited to the field of ion sensing. On the contrary, the technique seemed to have immediate applications in the areas of moisture sensing and resin cure monitoring. To test these applications, the requirement of immersibility of the device was dropped, and a simplified version of the device was designed, built, and successfully tested.

This paper reports on the results of this work. There are essentially five contributions to be reported:

- 1) The development of a process for the fabrication of n-channel depletion-mode FET's in the MIT Microelectronics Laboratory.
- 2) A new device structure which combines a lock and key device with a floating-gate CFT, for improved sensitivity.
- 3) A measurement scheme which employs a reference FET and external feedback circuitry that allows easy measurement of the pertinent transfer function.
- 4) The addition of a stray capacitance to the existing device model to account for high-frequency behavior of the device.
- 5) The analysis of a moisture-sensitive thin-film system by systematic application of the model to the observed response.

Background on the use of MOS structures to examine high-impedance films is presented in Chapter 2. Chapter 3 follows with a description of the new device and its associated measurement technique. In Chapter 4, the technique is applied to the examination of thin-film PEO. Finally, Chapter 5 contains a discussion concerning limitations of the technique.

## CHAPTER 2: BACKGROUND

This chapter summarizes work previously done at MIT involving the characterization of high-impedance films. This work has been done with the aid of two MOS structures: 1) the lock and key, and 2) the charge-flow transistor.

### A. THE LOCK AND KEY

The lock and key is a planar, interdigitated electrode pair (Figure 1). Recent studies at MIT have employed the lock and key to measure the sheet resistance of moisture-sensitive thin films (4), and to monitor the dielectric properties of epoxy resin during cure (5).

When a thin film is applied over a lock and key, a resistor is formed. The resistor's value ideally depends only upon the sheet resistance of the thin film (in ohms per square) and the number of squares in the path between the two electrodes of the lock and key. The smaller the number of squares between electrodes, the easier it is to measure the current through the device.

For example, assume the sheet resistance of the thin film is  $10^{15}$  ohms per square, and the lock and key has 1/100th of a square between its electrodes--in other words, the ratio of the interelectrode spacing to the inner-electrode circumference is 1/100. The resistor value is  $10^{13}$  ohms. This means that the resistor will draw .1 pA from a one volt supply, a difficult current to measure. If a lock and key with 1/10,000th of a square (a practical limit) is used, the resistor value becomes  $10^{11}$  ohms. The current becomes 10 pA--still a difficult current to measure accurately, but a factor of 100 improvement over the previous case.

This example illustrates perhaps the biggest problem with the use

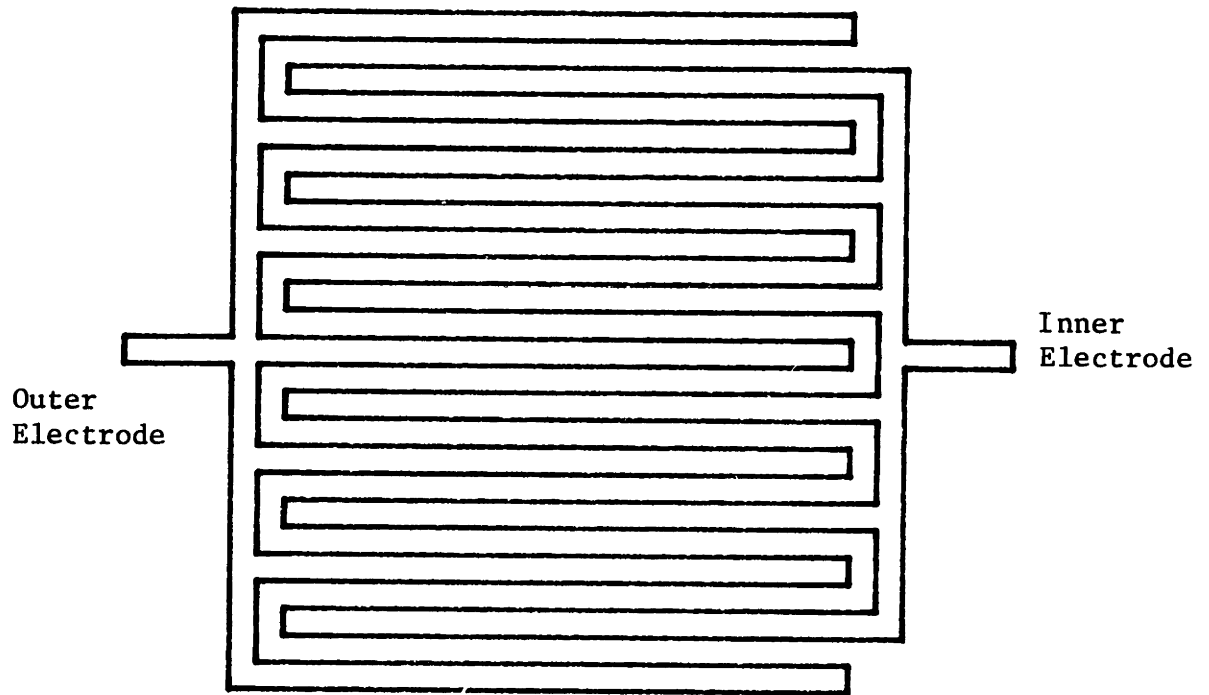


Figure 1A) Top view of lock and key

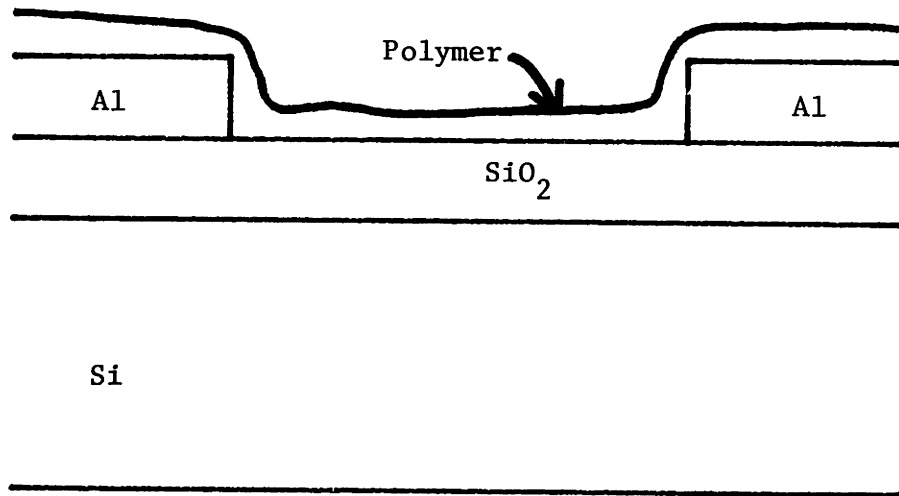


Figure 1B) Cross section of two fingers of the lock and key



of the lock and key to characterize thin films: the inability to measure sheet resistances on the order of  $10^{15}$  ohms per square and greater accurately. There are other difficulties. When the lock and key is used to make a D.C. measurement, error may result from high resistance in the contact between electrode and thin film. This problem may be avoided by making an A.C. measurement, but this leads to a new difficulty, since capacitive current may be much greater than that conducted by the thin film, even at low frequencies.

The lock and key may also be employed in the characterization of infinite-medium systems such as a curing resin. The term "infinite medium" refers to the case of a film that is thick compared to relevant device dimensions. Modeling of this type of system is much more difficult than for the thin film, since current paths are highly two dimensional. The model to be presented in this paper was developed specifically for thin-film systems and may or may not be applicable to the infinite-medium case.

#### B. THE CHARGE-FLOW TRANSISTOR

The charge-flow transistor (CFT) is an MOS-compatible sensing device (6). The floating-gate version of the CFT is depicted in Figure 2. To date, the CFT has been applied primarily to the problem of monitoring the sheet resistance of thin films (7,8).

The measurement technique is pictured in Figure 3. A voltage step greater than threshold is applied to the driven gate of the CFT. Charge migrates from the driven gate to the floating gate through the highly-resistive path of the thin film. After some delay (typically ranging from milliseconds to kiloseconds), the voltage on the floating gate reaches threshold, and the FET begins to conduct current. When

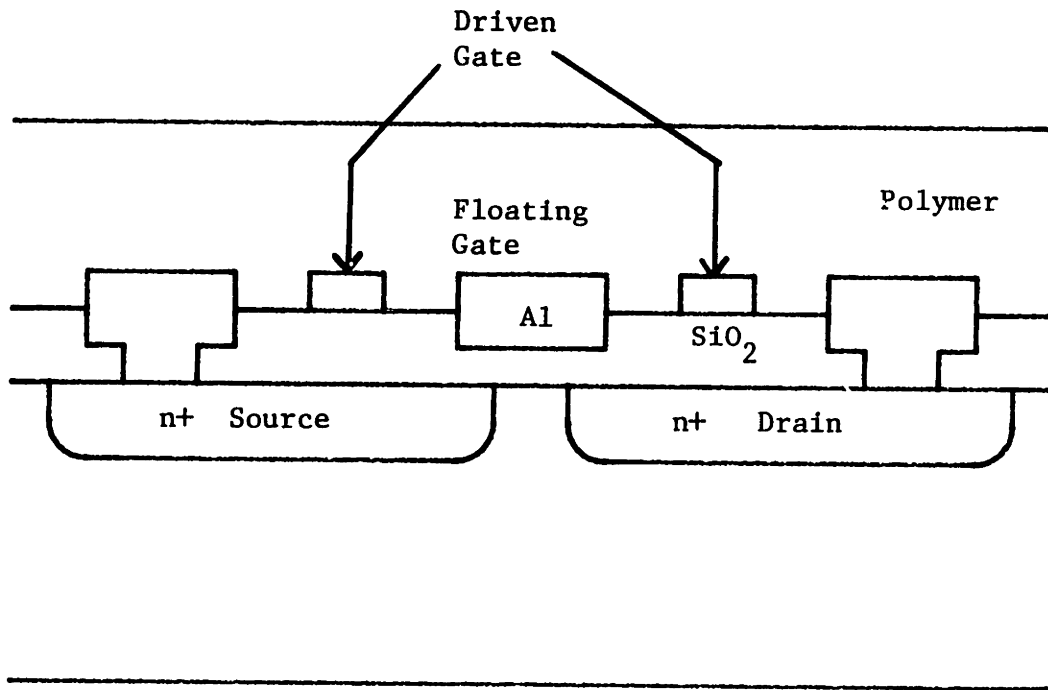


Figure 2A) Cross section of floating-gate CFT

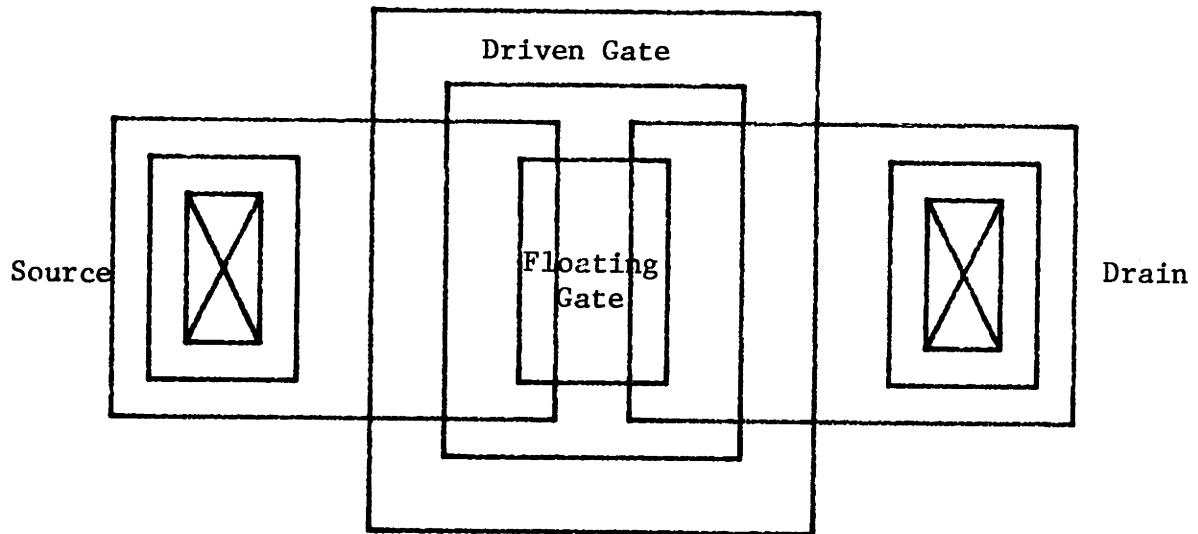


Figure 2B) Top view of floating-gate CFT

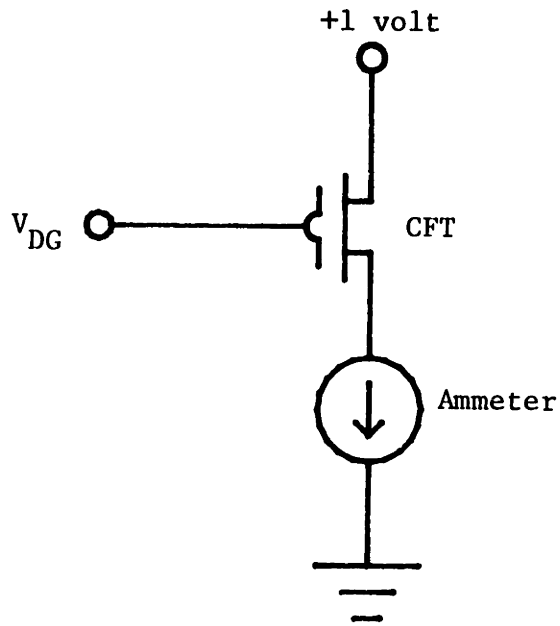


Figure 3A) Schematic Representation of Turn-on Measurement Technique

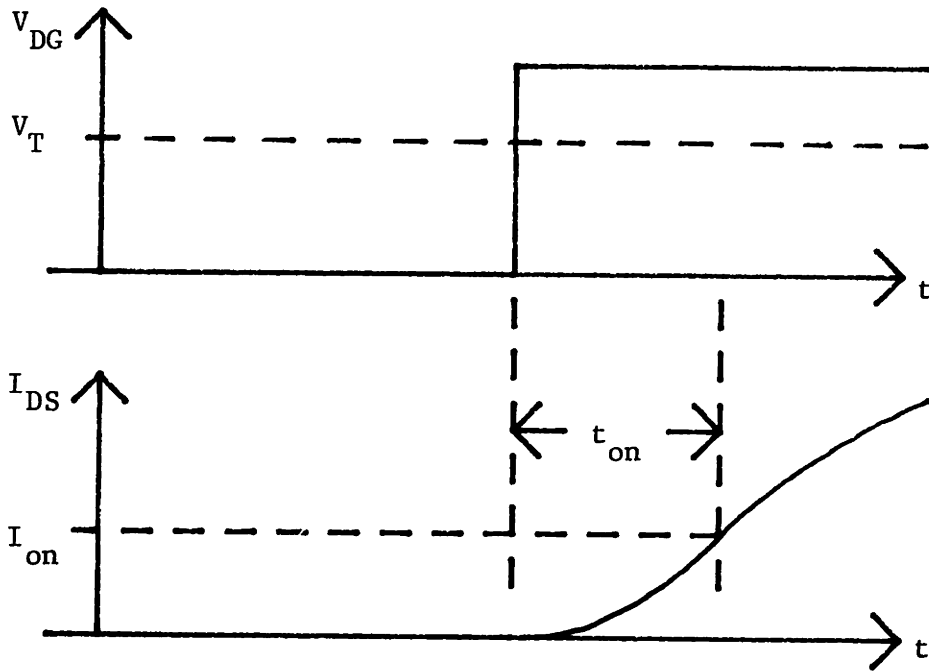


Figure 3B) Illustration of Turn-on Waveforms

FET current reaches the predefined level  $I_{on}$  (typically 1 microampere), the device is said to have turned on. The turn-on delay  $t_{on}$  is heavily dependent upon the sheet resistance of the thin film.

While this time-delay measurement scheme does give a reflection of the value of the sheet resistance, it is very hard to determine this value from the turn-on data. The primary difficulties are attributable to the variation of threshold from device to device, and the uncertainty of charge distribution in the thin film prior to application of the voltage step. The A.C. measurement technique presented in this paper represents a major improvement over CFT turn-on time for the determination of sheet resistance.

The CFT has also been applied recently to the problem of resin cure monitoring (5). Initial measurements in these studies were made using the turn-on time technique. However, in this case, an A.C. measurement technique that employed the CFT was developed, and shown to be more suitable (9).

In the A.C. method, a D.C. bias greater than threshold is applied to the driven gate, upon which an A.C. signal is superimposed. The effective FET is in this way biased into its linear region of operation, and the channel conductance is modulated by the sinusoid. This channel modulation is measured and compared to the applied sinusoid. The result is expressed in terms of the gain and phase of the ratio of the two sinusoids. Given the proper model, the conductivity and dielectric constant of the device medium can presumably be computed from the gain-phase data.

To date, this model has consisted of a capacitively-loaded RC transmission line (8) (Figure 4). The model assumes negligible contact

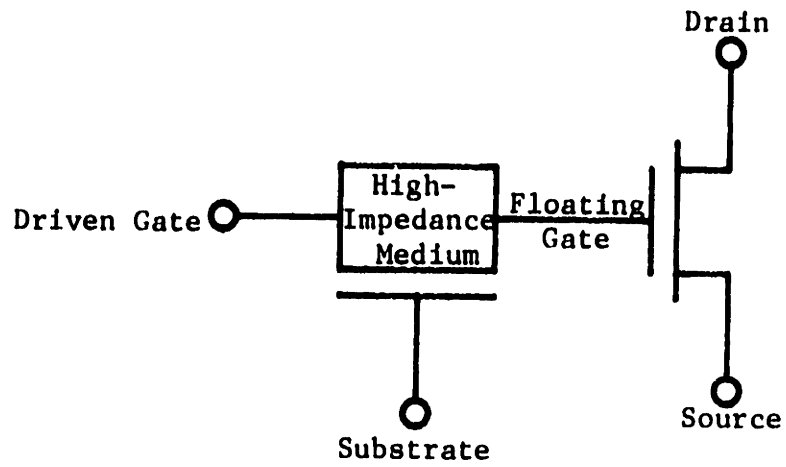


Figure 4A) Transmission Line Model of CFT

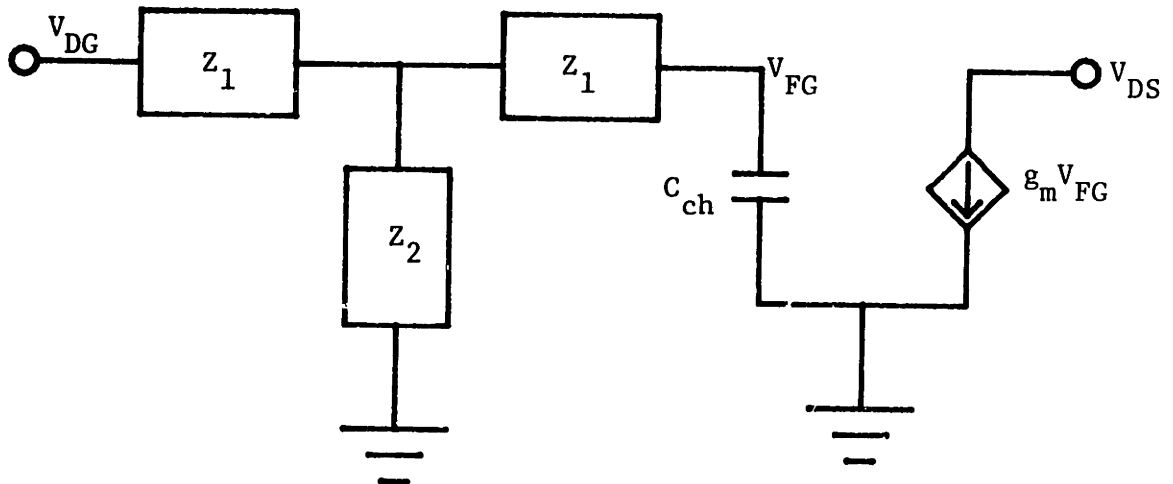


Figure 4B) Incremental CFT Model

impedances, and lumps the two-dimensional distributed effects into a one-dimensional transmission line. The transmission line may be represented incrementally as a two-port network, with parameters  $Z_1$  and  $Z_2$  that are functions of device geometry and the electrical properties of the resin. The FET is biased such that it operates in its "linear" regime, and is represented incrementally as a capacitor and a voltage-controlled current source. A similar model will be shown to apply to the device developed here.

The major problem with the A.C. method is keeping the device biased properly. Not only may it be difficult to establish the initial bias voltage, but as the properties of the medium change, so may the bias voltage on the floating gate. This effect has caused device to turn off during the course of epoxy resin cure. One driving force behind the effort to make depletion-mode charge-flow transistors for the project reported here is to remove the D.C. bias as an issue in such measurements.

CHAPTER 3: THE NEW METHOD FOR  
A.C. MEASUREMENT OF DIELECTRIC PROPERTIES

A. THE NEW DEVICE

Theory of Operation. A new device has been designed and fabricated which takes advantage of the best properties of the CFT and the lock and key (Figure 5), and in addition, operates with zero D.C. bias. The device consists of a depletion-mode n-channel FET and a lock and key, combined into a single structure. One electrode of the lock and key is driven externally, while the other electrode ties directly to the gate of the FET. The source and drain of the FET are available externally, just as with the CFT. In a sense, the new structure is simply a modified version of the floating-gate CFT, the differences being that the FET is depletion-mode, and the gate structure is interdigitated, rather than simply ringed.

As compared to the simple lock and key, the new structure has the primary advantage that the lock and key current is buffered by an on-chip amplifier: the FET. In addition, a secondary advantage is gained by the uninterrupted guarding of the floating electrode by the driving electrode.

The new structure has three main advantages over previous CFT's for making A.C. measurements. The first is that the transistor is depletion-mode, and may therefore be operated with zero D.C. gate voltage bias. Secondly, the floating-gate electrode has been shaped into the form of a lock and key, primarily for ease of modeling, while remaining entirely guarded by the driving electrode. An additional advantage of this adaptation is the averaging of process variations. The third key improvement is that the high-impedance path between electrodes, as well

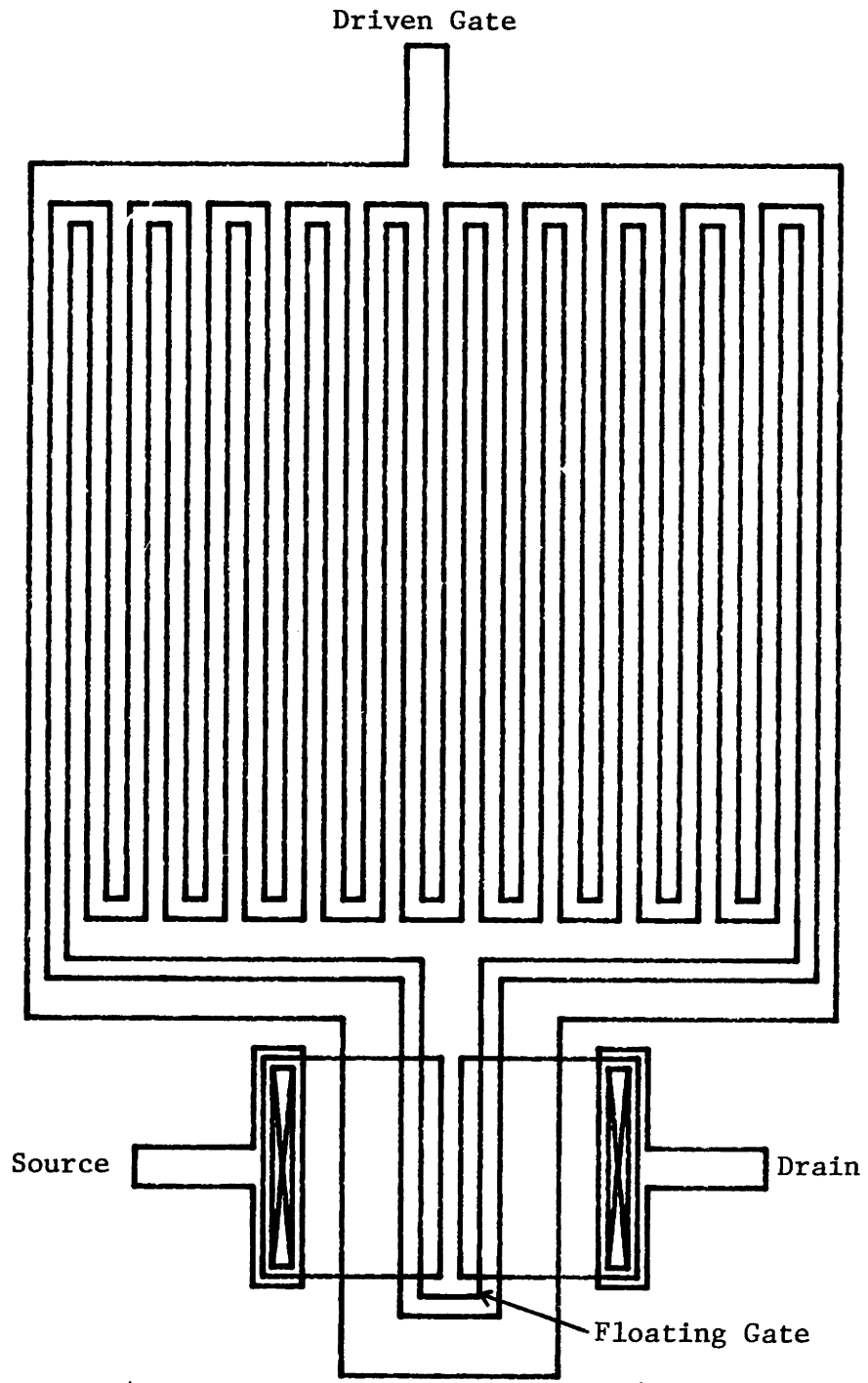


Figure 5) Top View of Fingered-Gate CFT



as the floating electrode is now fabricated over the relatively thick field oxide. This leads to a lessening of the capacitive loading to the substrate.

The advantage of this third improvement can be illustrated by estimating the voltage divider ratio of the FET gate capacitor and the lock and key interelectrode capacitance, for the uncoated device (an infinite-medium system of air). The existing model of the lock and key structure will be employed in making this estimate (10).

The interelectrode capacitance of the lock and key is approximated by

$$C_{lk} \approx \frac{9NL}{\pi^2} \left( \epsilon_m + \epsilon_{sub} + \frac{t_{ox}}{2W} \epsilon_{ox} \right),$$

where  $\epsilon_m$ ,  $\epsilon_{sub}$ , and  $\epsilon_{ox}$  are the dielectric permittivity of the medium (air in this example), the substrate, and silicon dioxide. The oxide thickness is  $t_{ox}$ , and the lock and key is described by  $N$ ,  $L$ , and  $W$ , the number of inner-electrode fingers, and the length and width of each one (assuming the finger width and the interelectrode spacing are equal). The new device has a lock and key with  $N=10$ ,  $L=37.5$  mils, and  $W=.5$  mils.

In this case, the silicon substrate is at a constant potential, and resembles a ground plane. If it is assumed that the field lines in the medium are not drastically affected by the effective ground plane, the interelectrode capacitance can be approximated as

$$C_{lk} \approx NL\epsilon_0.$$

The channel capacitor  $C_{ch}$  can be approximated by

$$C_{ch} \approx \frac{NWL\epsilon_{ox}}{t_{ox}},$$

so the voltage divider ratio becomes

$$\frac{V_{FG}}{V_{DG}} = \frac{C_{lk}}{C_{lk} + C_{ch}} \approx \frac{C_{lk}}{C_{ch}} \approx \frac{t_{ox}}{W} \frac{\epsilon_0}{\epsilon_{ox}},$$

where  $t_{ox}$  is the oxide thickness over which the floating electrode is fabricated. This illustrates that the fingered-gate structure will not have a greater response than the floating-gate structure simply due to the added electrode area. However, because the floating electrode of the fingered-gate structure is fabricated over field oxide, whereas it is over channel oxide for the ringed structure, an improvement of about a factor of ten is achieved. Using a  $t_{ox}$  of one micron, and a  $W$  of 12.5 microns, the formula estimates that the new structure should have a voltage divider relation of about 1/50 for the uncoated device (this approximation, of course, neglects the effect of the ground plane).

The existing CFT model must be modified to account for this interelectrode capacitance (Figure 6). When this new model is applied to a thin-film system in which conductance is predominately across the surface, the elements represent the following: 1)  $R_a$  and  $C_a$  are the parallel conductance and capacitance across the thin film, and may model bulk conduction as well as surface conduction; 2)  $C_1$  is the capacitance of the floating electrode to substrate; 3)  $C_t$  is the distributed capacitance from the (surface of the) thin film to substrate; and 4)  $C_x$  is the interelectrode capacitance, as determined above. It is assumed that contact impedances are negligible, and that electrical properties are not dispersive, i.e., not functions of frequency in the range of interest.

If sinusoidal steady state is assumed, the transfer function from driven electrode to floating electrode may be solved exactly

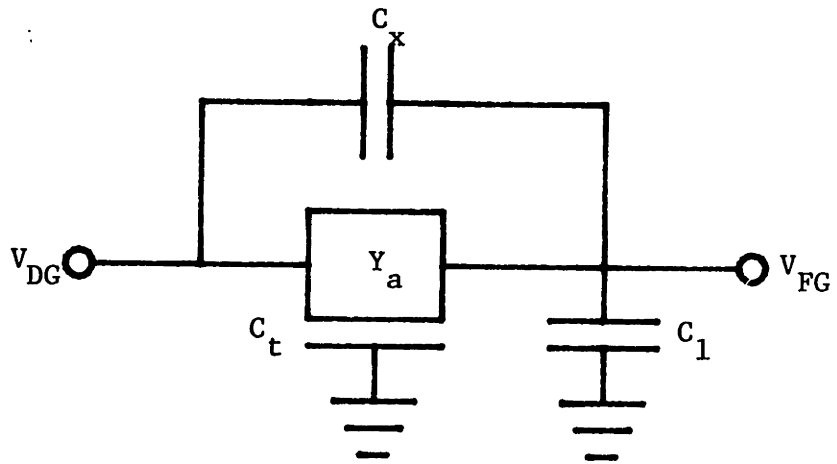


Figure 6A) Transmission Line Model of CFT with Addition of Stray Capacitance

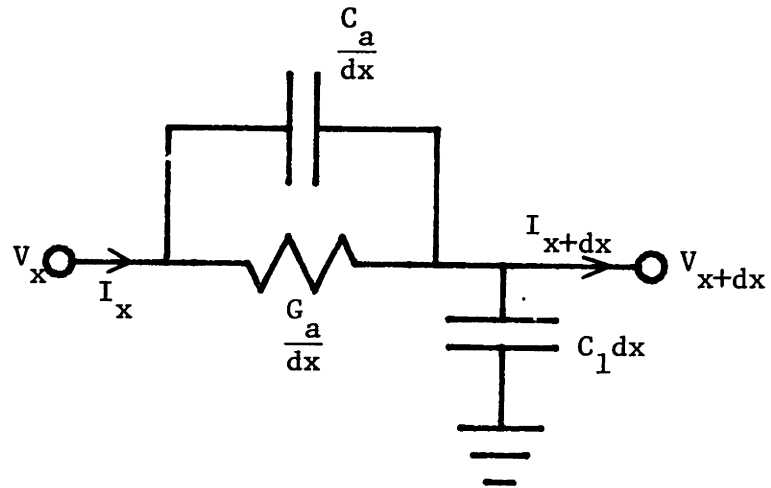


Figure 6B) Incremental Section of Transmission Line

(Appendix B). The solution contains essentially four parameters:

$C_1/C_t$ ,  $C_t/C_a$ ,  $C_x/C_t$ , and  $\gamma = 1/(R_a C_a \omega)$ . It is important to note that sheet resistance and frequency appear in only one place in the solution, and they scale with each other (11). This fact will be used to great advantage in using the model in experimental contexts (Chapter 4).

Device Fabrication. The basic steps of device fabrication are depicted in Figure 7. For a detailed step-by-step process description, refer to Appendix C. The process is an adaptation of the aluminum-gate p-channel process currently in use at the MIT Microelectronics Laboratory. It is not intended that this process be the ultimate in processing technology, but rather the simplest process with which the device objectives may be obtained.

The substrate is a <100> p-type silicon wafer, with a relatively low resistivity. As in the PMOS process, the first step is the growth of a thick field oxide. This oxide will be approximately one micron thick; oxides of greater thickness require extremely long growth times, even in steam. A masking step is then performed in which holes are etched through the oxide to the silicon in the regions of the wafer where source or drain regions are desired.

An implant is now used to introduce the n-type dopant, arsenic, into the exposed regions of the silicon. Arsenic was chosen because of its low diffusivity as compared to phosphorous at the temperature of gate oxide growth (1100 degrees centigrade).

A layer of oxide 2500 Angstroms thick is then grown over the arsenic-doped regions. A masking step follows in which holes are etched through the oxide to the silicon in the gate and contact hole areas of the wafer. A gate oxide of approximately 1000 Angstroms is then

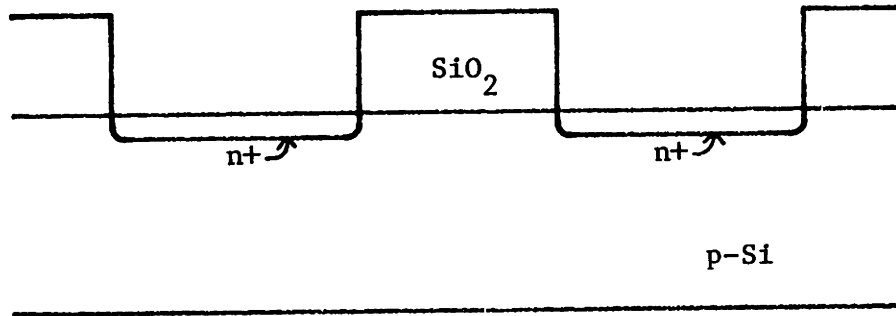


Figure 7A) Wafer cross section following arsenic implant

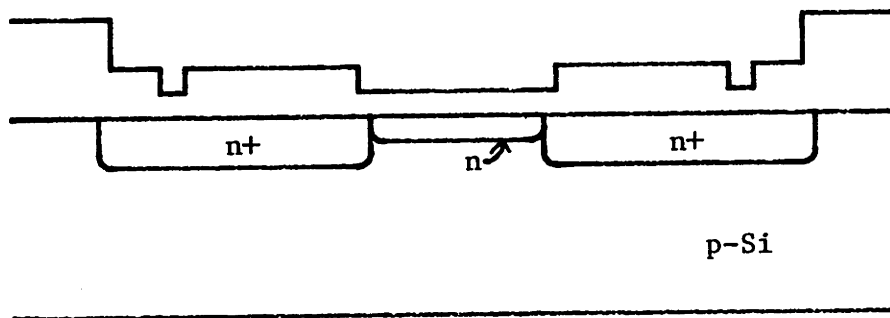


Figure 7B) Wafer cross section following phosphorous implant

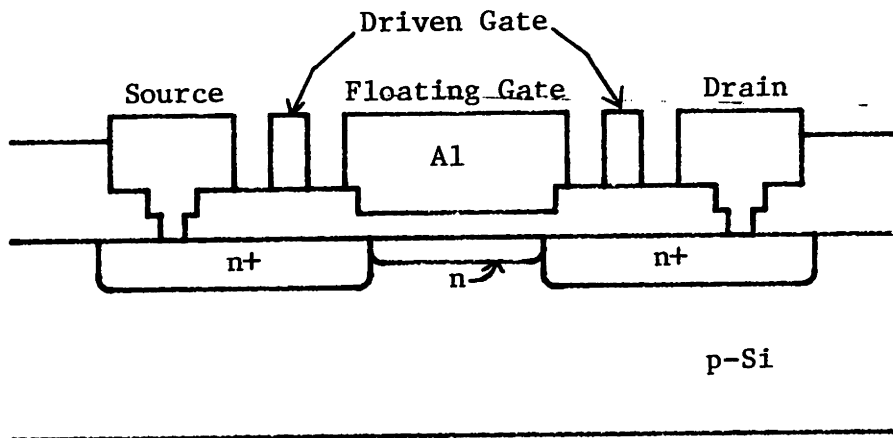


Figure 7C) Wafer cross section of completed device

grown over these regions.

A second ion implantation is now done, this time with phosphorous as the dopant. The implant strength is such that only the regions of the wafer under the thin gate oxide receive any impurities. This implant dopes the channel regions n-type, forming the depletion-mode devices.

A masking step in which the contact holes are opened to the silicon now takes place. The entire wafer is then coated with a layer of aluminum by evaporation. The aluminum is patterned in a final masking step to form the gates, electrodes, bonding pads, and interconnections for the devices.

The proposed processing sequence was simulated on the device fabrication computer simulation program SUPREM (12) (Appendix D).

A mask set was designed which included both a fingered-gate and ringed-gate CFT (Appendix E). In addition, a standard FET is included in the mask design. This FET will serve as a reference in the measurement scheme to be described in the next section.

Mask sets were produced from hand-cut rbylith at 100x, using the mask-making facilities at the MIT Center for Materials Science and Engineering. Masks have been produced that will yield a 12 x 12 matrix of square dies, each die being 75 mils per side.

Wafers of p-type <100> silicon were selected for fabrication. Wafer resistivity was .1-.4 ohm-cm, low enough to prevent unwanted inversion under the field oxide. Devices were fabricated in the MIT Microelectronics Laboratory over a period of about two weeks.

The first processing run produced very satisfactory devices, with a yield excluding wafer edges of better than 90%. Typical FET I-V curves are presented in Figures 8 and 9, and a comparison between predicted and

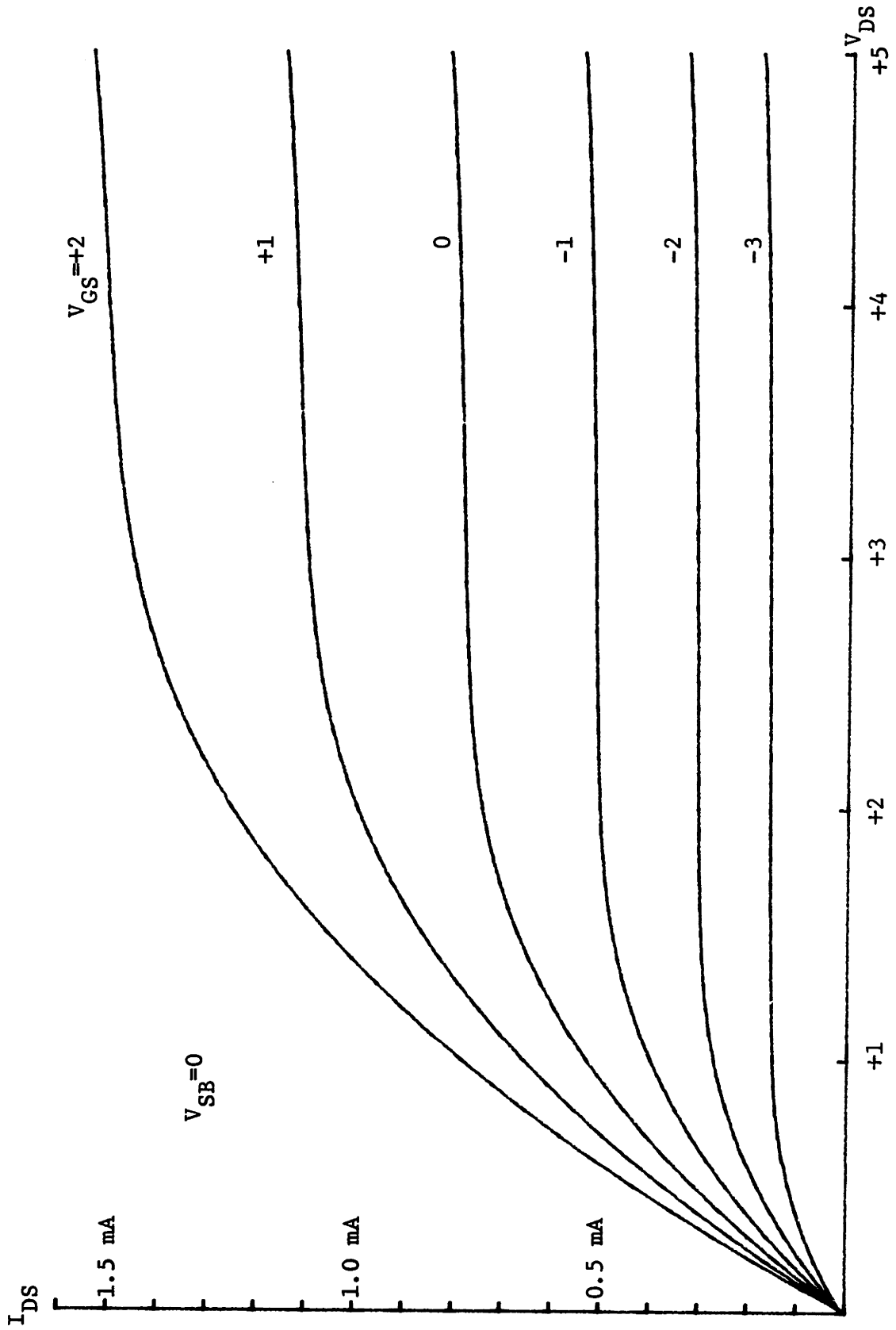


Figure 8) Typical FET I-V Curve for Constant Substrate Bias

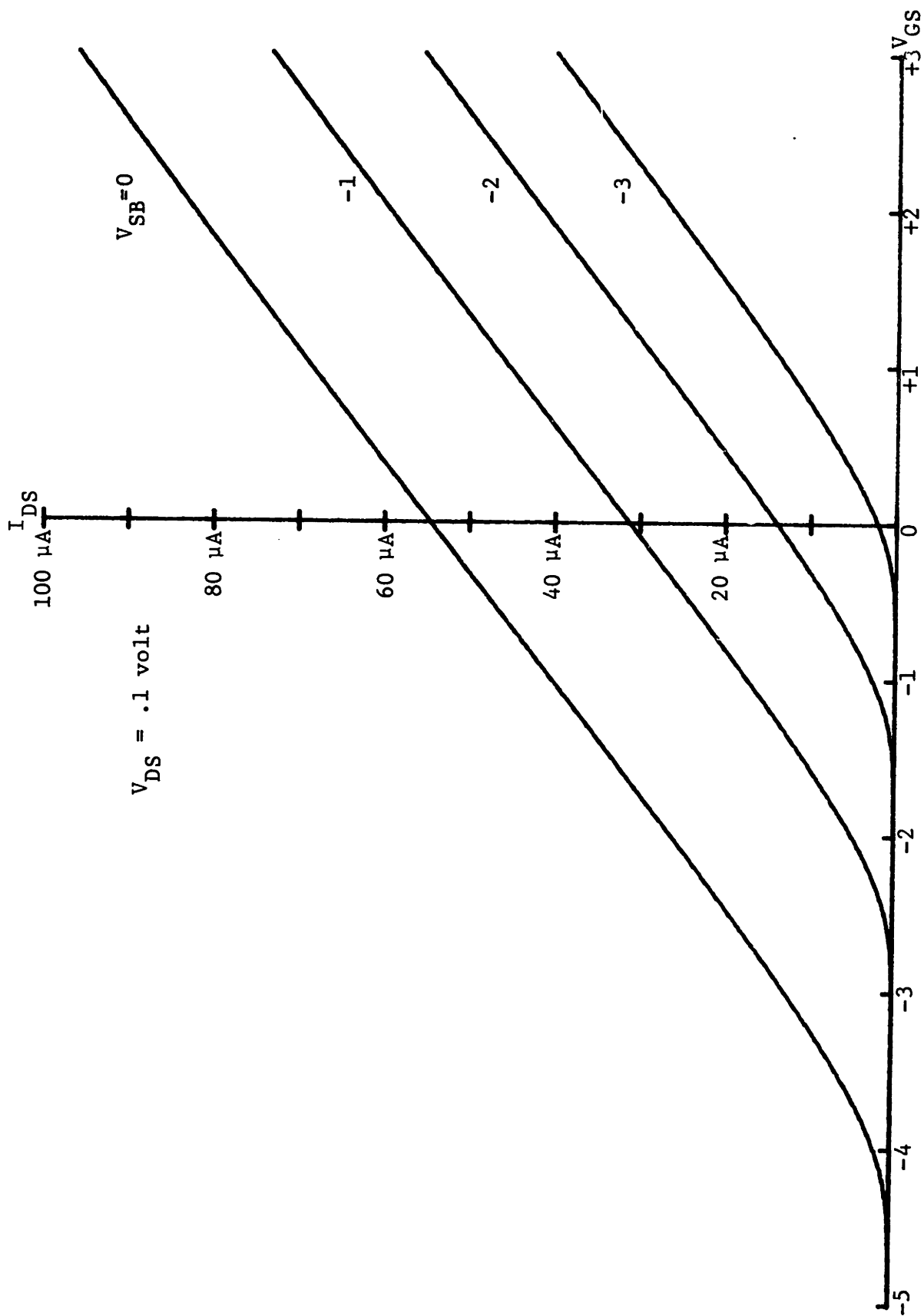


Figure 9) Typical FET I-V Curve for Constant Drain Voltage



experimental results may be found in Table 1. These curves were generated and data analysis was performed with the aid of the computer-based MOS Characterization System at the MIT Microelectronics Laboratory.

In general, there was good agreement between predicted and experimental results. Perhaps the widest discrepancy is in the prediction of the gain factor,  $k$ . This is due to a lower than expected carrier mobility, probably resulting from the larger than typical surface state density present in our process. This is partially made up for by the extremely low mobility degradation exhibited by the devices. It should be noted that a surface state density of  $2.5 \times 10^{11}$  was used in predicting threshold, rather than the typical  $1 \times 10^{11}$  for <100> silicon. The value  $2.5 \times 10^{11}$  has proven to best account for thresholds obtained in our PMOS process.

#### B. THE MEASUREMENT TECHNIQUE

In the past, A.C. measurements with CFT's have consisted of measuring the incremental drain current as compared to the sinusoid applied to the driven gate (9). Several parameters such as device gain and stray resistances interfere with the interpretation of such data. It would be more desirable to make an indirect reading of the floating-gate voltage. A measurement scheme built around the new device accomplishes this goal.

The block diagram of the measurement scheme is presented in Figure 10. The technique employs a CFT, a matched FET, and external circuitry. The circuit consists of two major feedback loops: a primary loop which forces FET current equal to that of the CFT, and a secondary loop which maintains the D.C. operating point of the CFT.

The drain of the CFT and matched FET are connected to a variable

TABLE 1

	PREDICTED	MEASURED (average)
Oxide Thickness		
Field	.91 $\mu\text{m}$	--
Source/Drain	.28 $\mu\text{m}$	.25 $\mu\text{m}$
Channel	840 Angstroms	1050 Angstroms
Sheet Resistance of		
Source/Drain Implant	18.5 $\Omega/\square$	12.1 $\Omega/\square$
Threshold Voltage		
Field	16.7 v	15.0 v
Channel	-4.3 v	-4.5 v
Source to Substrate		
Breakdown Voltage	--	18.0 v
Gain (k)	117 $\mu\text{mhos/v}$ *	75 $\mu\text{mhos/v}$
Body Effect Factor (m)	2.92 $\sqrt{\text{v}}$	3.85 $\sqrt{\text{v}}$
Mobility Degradation ( $\theta$ )	--	1%

\*This value was predicted using an expected value of electron channel mobility of 570  $\text{cm}^2/\text{v-sec}$  (13).

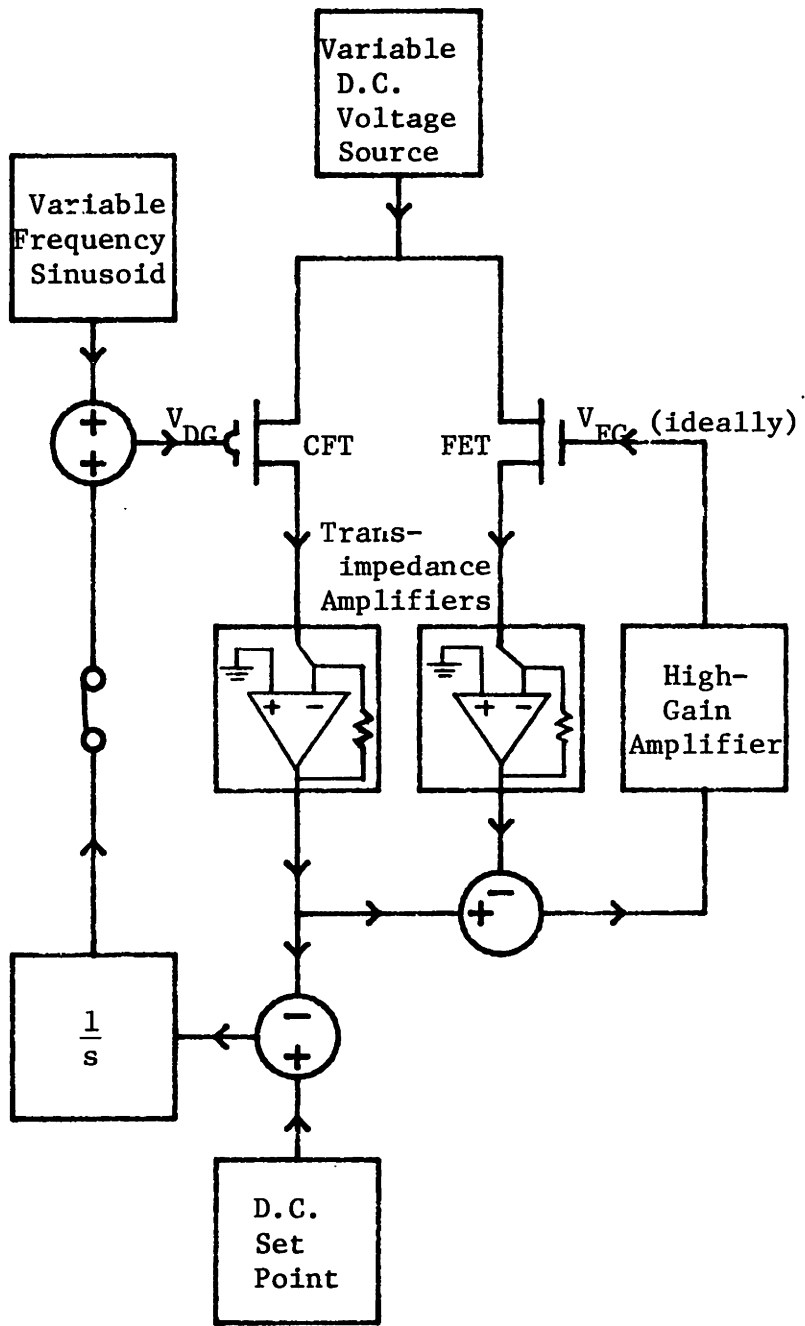


Figure 10) Block Diagram of Measurement Technique

D.C. voltage source. The sources of the two transistors are connected to the inputs of transimpedance current amplifiers, and are thus at virtual ground. In the primary loop, the outputs of the current amplifiers are compared, and the difference is amplified by a high-gain differential amplifier. The output of this differential amplifier drives the gate of the FET, forcing both A.C. and D.C. components of the FET current to be equal to those of the CFT.

The secondary loop takes the CFT transimpedance amplifier output, and adds it to a user-selected D.C. set point. The result is integrated, and added to a variable-frequency sinusoid to provide gate drive for the CFT. This loop serves to maintain CFT D.C. current at the user-selected set point. This feature is optional, and does not function when the D.C. Level Control Switch is opened.

Given that the drain, source, and substrate voltages are the same for both the CFT and the FET, and since the drain to source currents are forced to be the same as well, the gate voltage of the FET must be equal to the floating-gate voltage of the CFT. Thus, the floating-gate voltage of the CFT can be determined indirectly simply by measuring the FET gate voltage which is supplied by the external circuitry.

As long as the CFT and FET have well matched transistor properties, the circuit will successfully subtract out all common-mode properties, and output a signal that reflects only the desired property: the voltage of the floating gate as compared to the driven gate. It may be argued that the same result may be accomplished more simply by constructing a differential pair by grounding both sources, and loading the drains with a resistor. However, if this technique was employed, the drain voltage would no longer be a constant. This complicates the

analysis of the data.

The detailed circuit diagram is presented in Figure 11. The circuit employs six operational amplifiers, four of which are user-compensatable for improved high-frequency response. The circuit was initially tested using bipolar devices to model the as yet unfabricated FET's, and compensation was adjusted accordingly. On completion of device fabrication, circuit performance was retested by inserting FET's in both the FET and CFT slots. For frequencies up to 4 kHz, the circuit responded with less than one degree of phase error. This limiting frequency is less than hoped for, and could presumably be improved by adjusting the compensation to match the lower than expected device gain. However, because we are interested primarily in the low-frequency response, no effort has been made to correct this at this time.

As a final check, uncoated CFT's were tested for frequency response at room humidity, using the experimental set-up depicted in Figure 12. The devices behaved as expected. For low frequencies, the presence of  $\text{SiO}_2$  surface conduction could be observed by a relatively high gain, and a negative phase shift. As frequency was increased, gain decreased, and eventually levelled off, while the phase returned to zero. This high-frequency response is due to the interelectrode capacitance.

For the fingered-gate devices, this response was  $-49 \pm 1$  decibels, or  $1/280$ . This is more than a factor of 5 down from the estimate of  $1/50$ . Part of this error in the estimate can be attributed to the fact that the channel capacitance is not negligible, and actually contributes about  $1/3$  of the total capacitance. The rest of the error should be attributable to the effects of the ground plane.

Gain-Phase Meter  
Channel A

Gain-Phase Meter  
Channel B

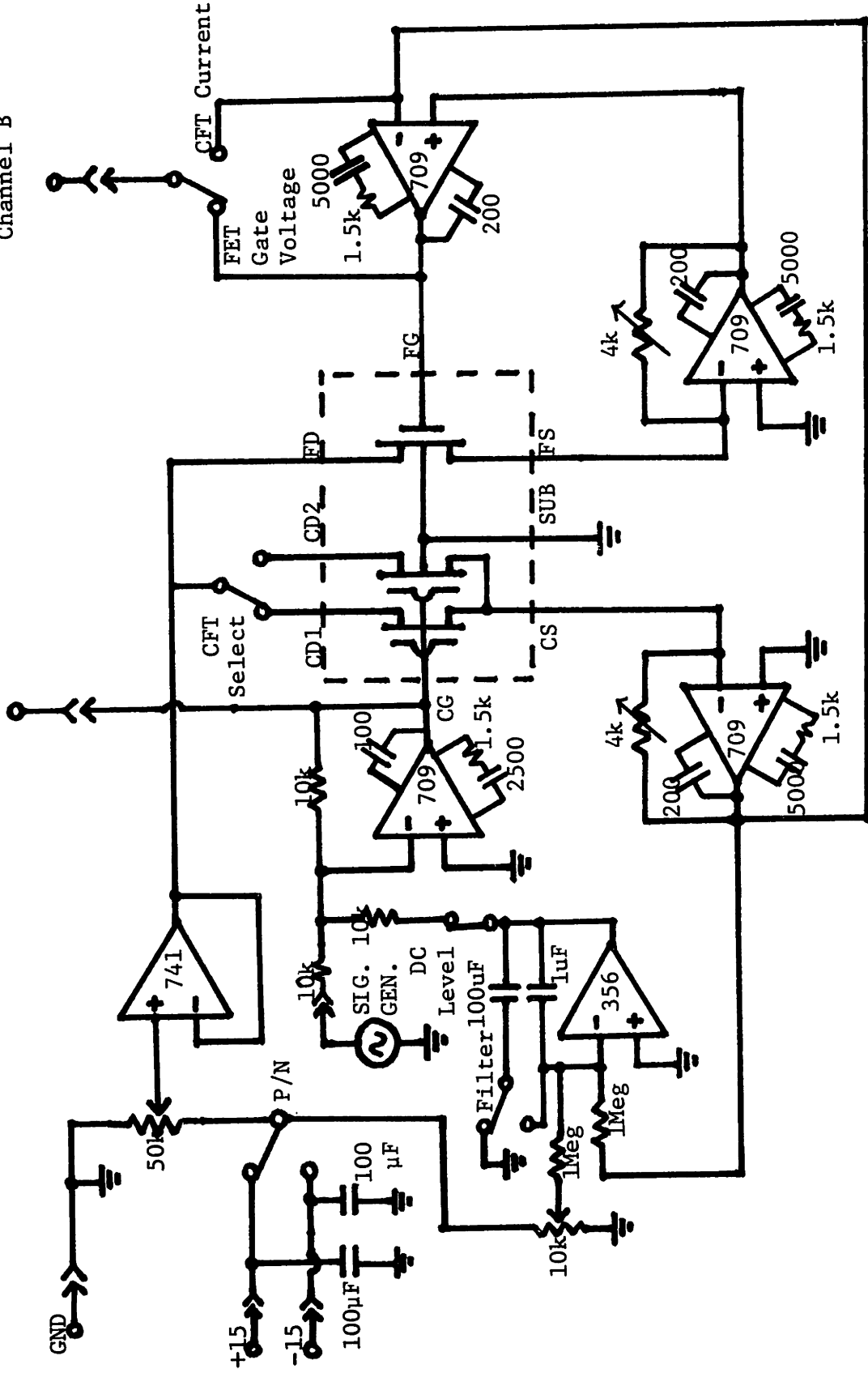


Figure 11) Measurement Circuit Schematic

The ringed structure has a typical gain of -60 decibels in the high-frequency limit, or 1/1000. This is one half the estimated value. There is approximately a factor of four difference between the high-frequency gain of the two devices.

#### CHAPTER 4: ANALYSIS OF A THIN-FILM SYSTEM: POLY ETHYLENE OXIDE

In order to establish the usefulness of the measurement scheme, the moisture-sensitive polymer poly ethylene oxide was examined. Prior to dicing, wafer slices were coated with a thin film of the polymer by coating the slice with a dilute aqueous solution of the polymer, and then spinning at 4000 RPM for 4 minutes. The slices were then carefully diced, and mounted on headers using non-conducting epoxy (since the polymer cannot stand the 120 degrees centigrade heat used to cure our conducting epoxy). The devices were then wire bonded, and tested for basic functionality.

Packaged devices were placed in our humidity-controlled flow system (Figure 12), and response was measured versus frequency and moisture content of the device ambient at room temperature. Studies were made on six samples, with three of the samples having been aged approximately one month. One of the aged samples failed. Data presented below were taken from the five remaining samples, two of which had been aged.

Measurements were taken in as near identical fashion as allowable by our flow system. The response of each sample was measured at ten different dew points, although the exact dew points varied from one device to the next, due to the inability to accurately tune the flow system. Measurements were taken at room temperature, which was observed to fluctuate between 22.5 and 25.0 degrees centigrade. Frequency of measurement was varied from 1 Hz to 2 kHz, taken with two points per decade. The D.C. Level Control Switch was left off for these measurements, and drain voltage was adjusted to one volt. Data was collected by hand, then entered into the HP-9835A calculator for aid in analysis (Appendix F).



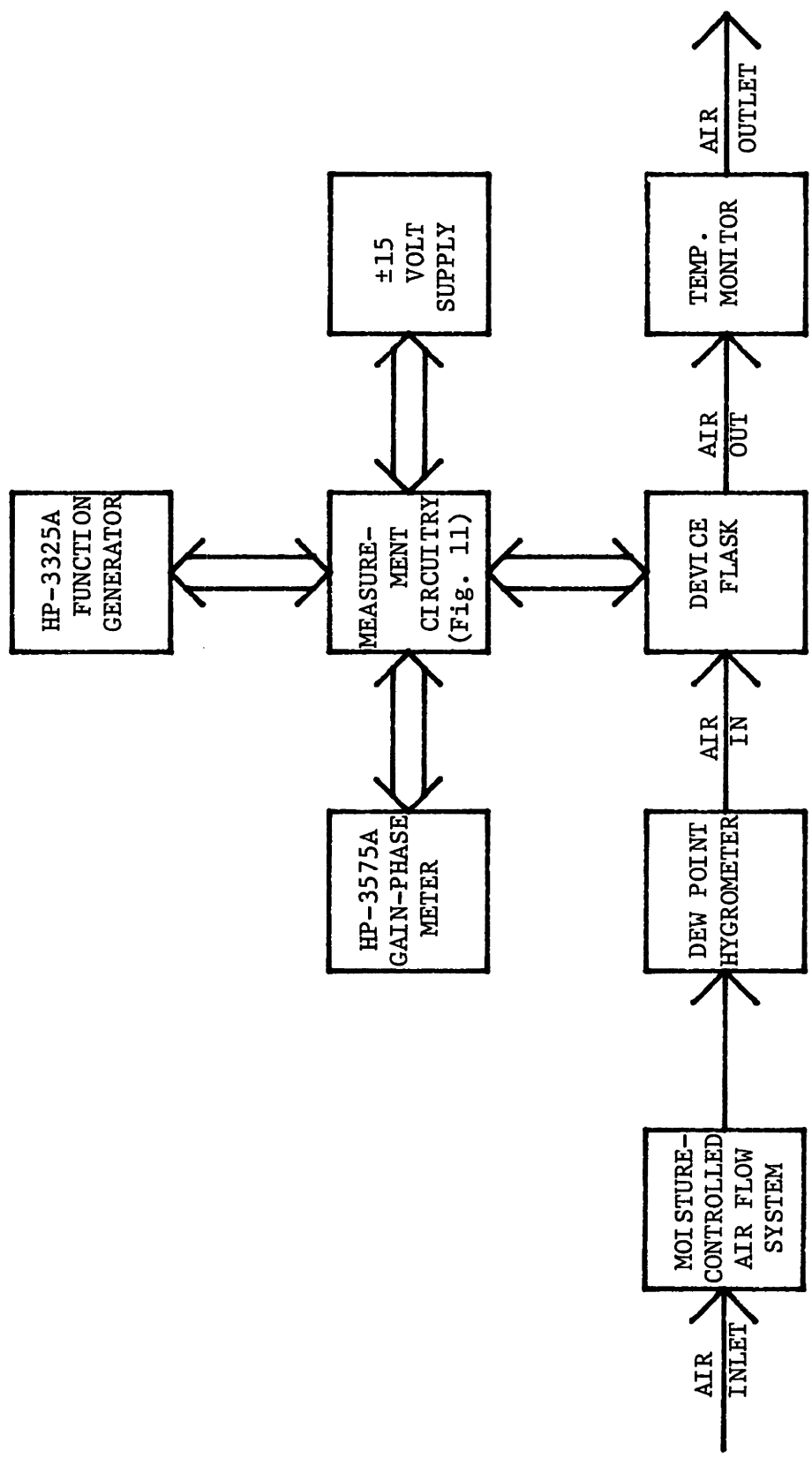


Figure 12) Block Diagram of Experimental Arrangement

Figure 13 shows typical data from these experiments plotted on axes of gain vs. phase. This particular data is for the fingered-gate device; similar results were observed with the ringed-gate device. Data is seen to behave qualitatively as expected: 1) for low frequency and high dew point (low sheet resistance) the transfer function  $V_{FG}/V_{DG}$  was approximately unity (zero dB gain and zero degrees of phase shift); 2) as dew point decreases (increasing sheet resistance) or frequency increases, the gain decreases and the phase falls because the system resembles an RC filter; 3) for low enough dew point or high enough frequency, the gain levels off and phases approaches zero because of the capacitive coupling between electrodes. Not surprisingly, this high-frequency gain was the same -49 decibels that had been observed with the uncoated devices.

The first step in calibration of the devices was taken at this point. As mentioned, at high dew point and low frequency, the gain approaches unity (0 dB) and the phase nears zero. However, this maximum gain varied from sample to sample, with values ranging from -1.2 to 1.6 decibels. This offset is primarily due to the mismatch in gain of the two transistors, and possibly partially due to a slight mismatch in gain of the two transimpedance current amplifiers. It is assumed that this gain offset is independent of frequency and dew point. The first step in processing the data is to subtract this gain offset, as determined for each device, from all measurements.

An attempt was now made to match the data of the fingered-gate devices to the model of Figure 4 and Appendix B. To reiterate, if the three capacitive ratios of the model are independent of both frequency and dew point, there remains but the parameter  $\gamma$  which accounts for both frequency and dew point variations. This means that in gain-phase

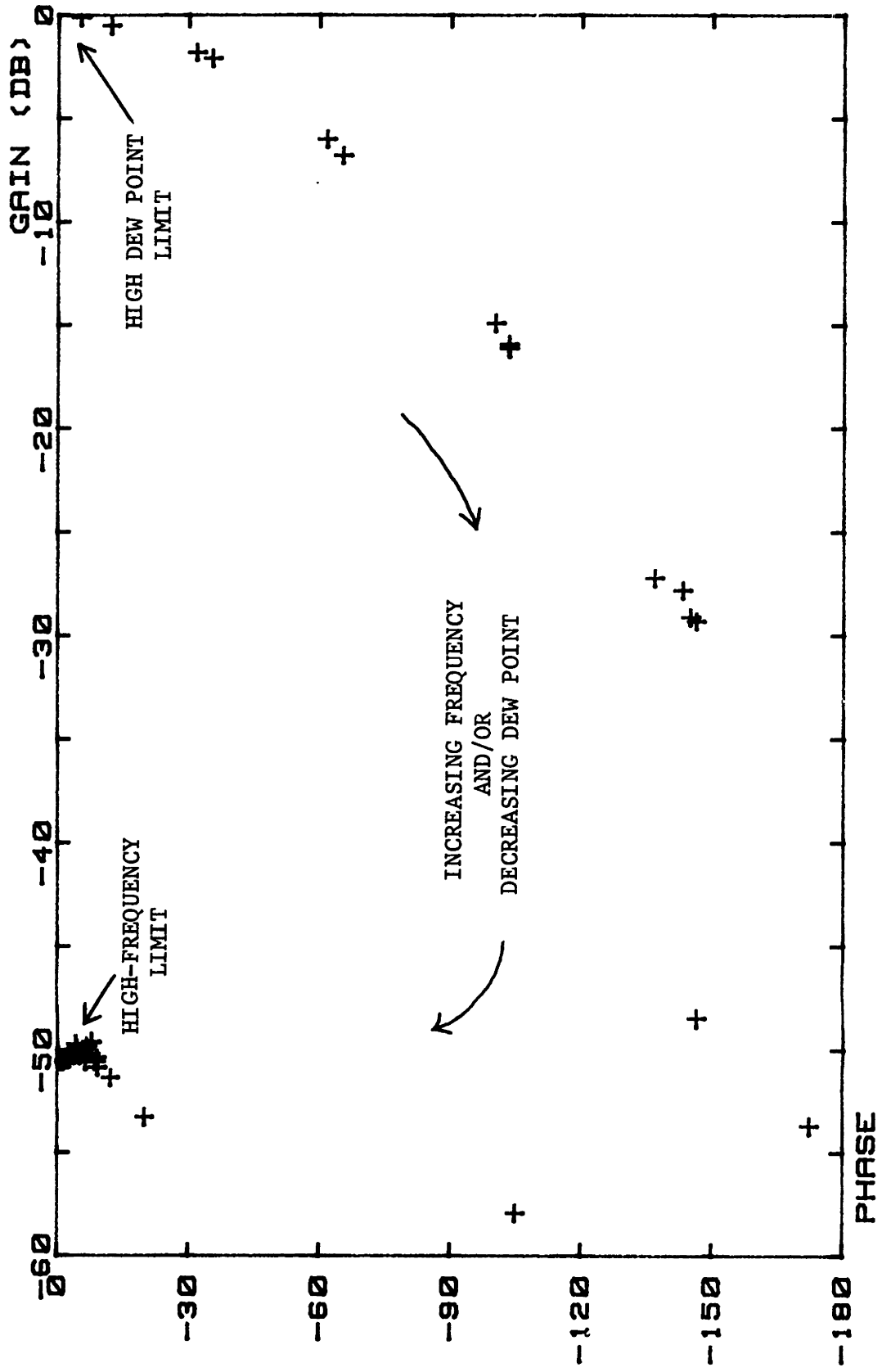


Figure 13) Data for Various Dew Points and Frequencies for an Aged Sample

space, points of both varying sheet resistance and varying frequency will lie on a single smooth curve. For both of the aged samples, the data, for the most part, did in fact behave in this manner (Figure 13). However, this was not the case for the three freshly-coated devices (Figure 14).

The next step was to compute, when possible, the model parameters from device geometry. The parameter  $\gamma$  cannot be computed, since it depends on sheet resistance, the quantity of interest. The parameters  $C_x/C_t$  and  $C_t/C_a$  are also not calculable from device geometry. However, the final parameter,  $C_1/C_t$ , may be computed.

The values of  $C_1$  and  $C_t$  were first computed separately by measuring the area of each capacitor over each oxide thickness. Areas were determined from the mask layout (Table 2). The field, source/drain, and channel oxides were assumed to be 1, .25, and .1 microns thick. The transmission line capacitor was assumed to lie entirely over field oxide plus .2 micron thick polymer. The polymer dielectric constant was equated to that of silicon dioxide (3.9). The capacitor  $C_1$  was computed to be 4.3 pF. This value compares very favorably to a measured value of 4.35 pF. The ratio  $C_1/C_t$  was computed to be 1.1.

In addition, we know from the model that given  $C_1/C_t$ , the high-frequency gain is determined uniquely by the two parameters  $C_x/C_t$  and  $C_t/C_a$ . From the low-dew-point, high-frequency measurements we know the value of the high-frequency gain for all devices to be  $-49 \pm 1$  decibels. On this basis, it was assumed that this high-frequency gain of  $-49$  dB is a device constant. Given a value of  $C_t/C_a$  (and  $C_1/C_t$ ), the value of  $C_x/C_t$  that is required for a high-frequency model gain of  $-49$  dB may be determined.

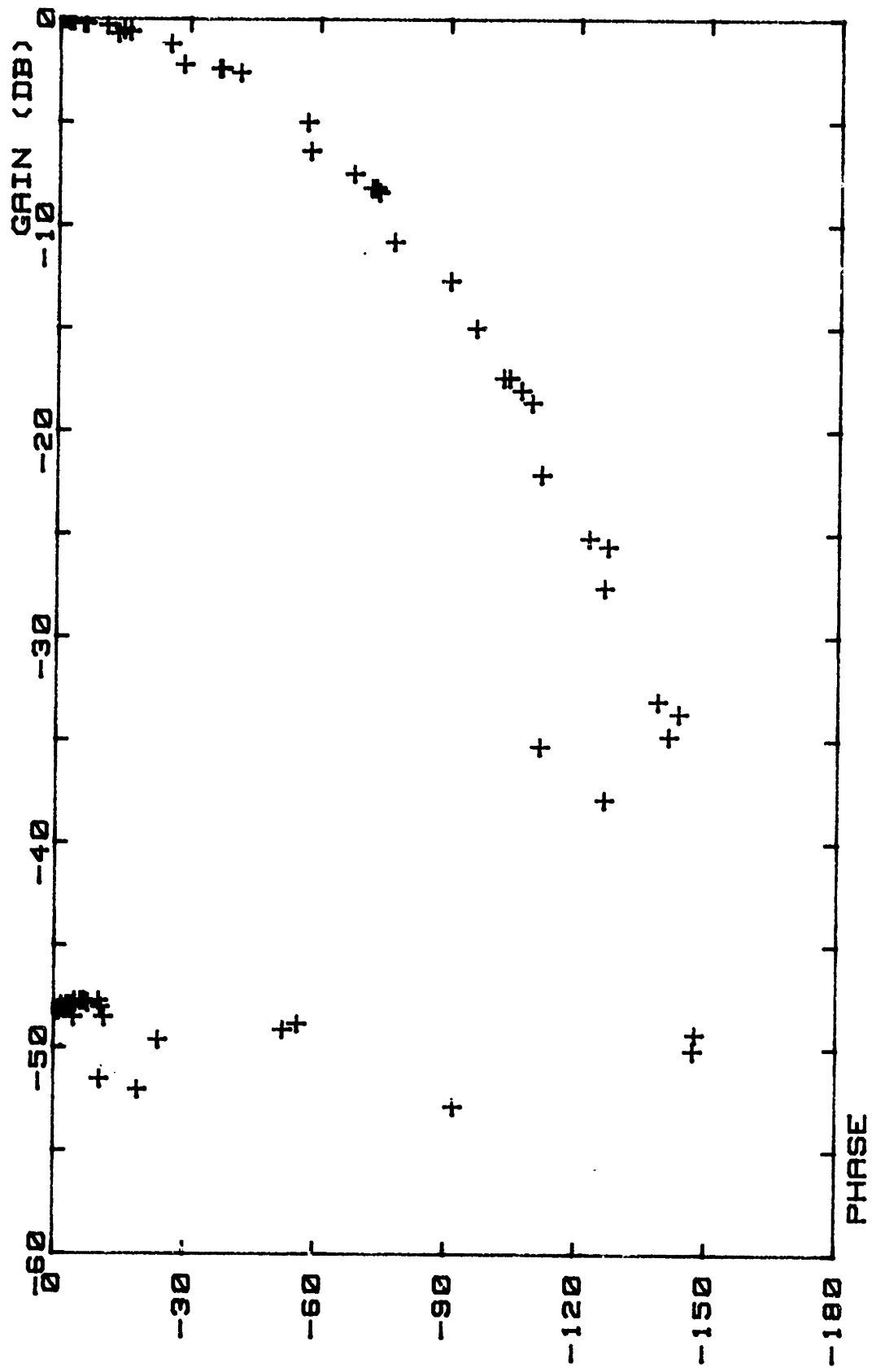


Figure 14) Data for Various Dew Points and Frequencies for a Freshly-Coated Sample

TABLE 2

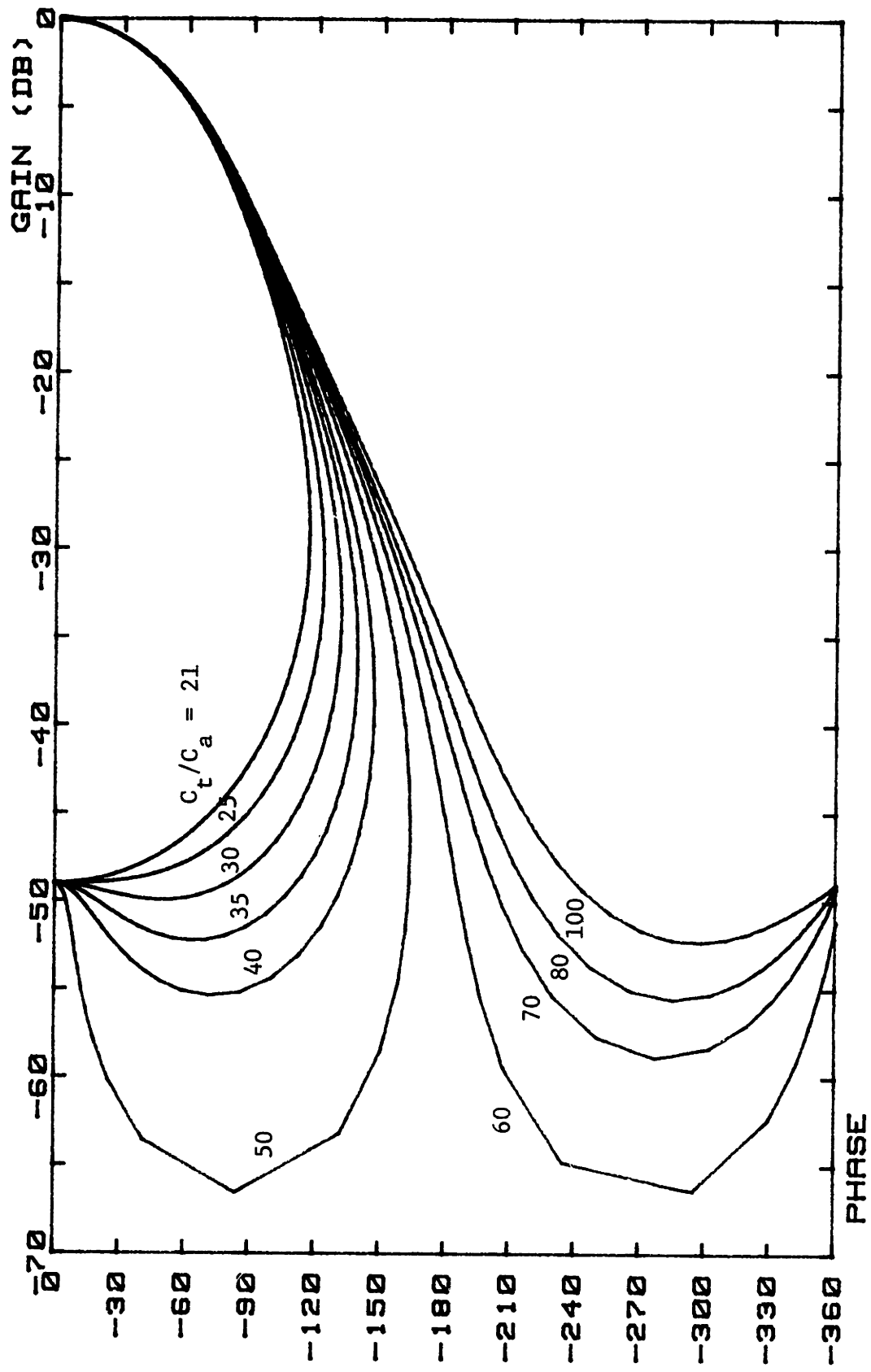
DIELECTRIC	AREA (mil <sup>2</sup> )		THICKNESS ( $\mu$ m)	DIELECTRIC PERMITIVITY
	C <sub>1</sub>	C <sub>t</sub>		
Field oxide	129.0	--	1.0	3.9
Source/Drain Oxide	3.5	--	0.25	3.9
Channel Oxide	5.0		0.10	3.9
Field Oxide and Polymer	--	203	1.2	3.9
CAPACITANCE (pF)	4.30	3.77		

Thus, of the four model parameters, two may be treated as device constants:  $C_1/C_t$  and high-frequency gain. These two may be considered as independent of frequency and of dew point. The remaining two parameters may be expressed as a family of curves in gain-phase space (Figure 15). These curves were generated by first selecting a value for  $C_t/C_a$ , and then computing the value for  $C_x/C_t$  necessary to maintain the high-frequency gain of -49 dB. The parameter  $\gamma$  was then varied logarithmically from very low to very high, each value yielding a gain and phase which was subsequently plotted as a continuous curve. The ratio of  $C_t/C_a$  is limited to a minimum of approximately 21 by the high-frequency gain restriction, but has no such restriction as far as maximum value.

In general, the effect of increasing  $C_t/C_a$  is to increase the bowing of the curve in gain-phase space. If  $C_t/C_a$  is large enough, phase will fall to -360 degrees and settle there, rather than returning to zero. This phenomenon has been observed on some samples (14).

The measured data can be plotted in gain-phase space and compared to the model curves. For the two aged samples, most of the data lie on one curve, for a value of  $C_t/C_a$  of 44 (Figure 16). For the freshly-coated samples, the data are seen to fall between the curves for which  $C_t/C_a$  has values 21 and 45 (Figure 17).

An effort was made to determine why the data for freshly-coated samples did not fall on a single curve. Data were plotted for constant frequency (Figure 18) and for constant dew point (Figure 19) in the gain-phase space. For both constant frequency and constant dew point, the data do fall on a single, smooth curve. However, in neither case do these curves exhibit a unique value for  $C_t/C_a$ . This indicates that  $C_t/C_a$ , or perhaps some other component of the model, is a weak function of



Figures 15) Model curves for  $C_1/C_t = 1.1$ , High-Frequency Gain = -49dB, and varying  $C_t/C_a$



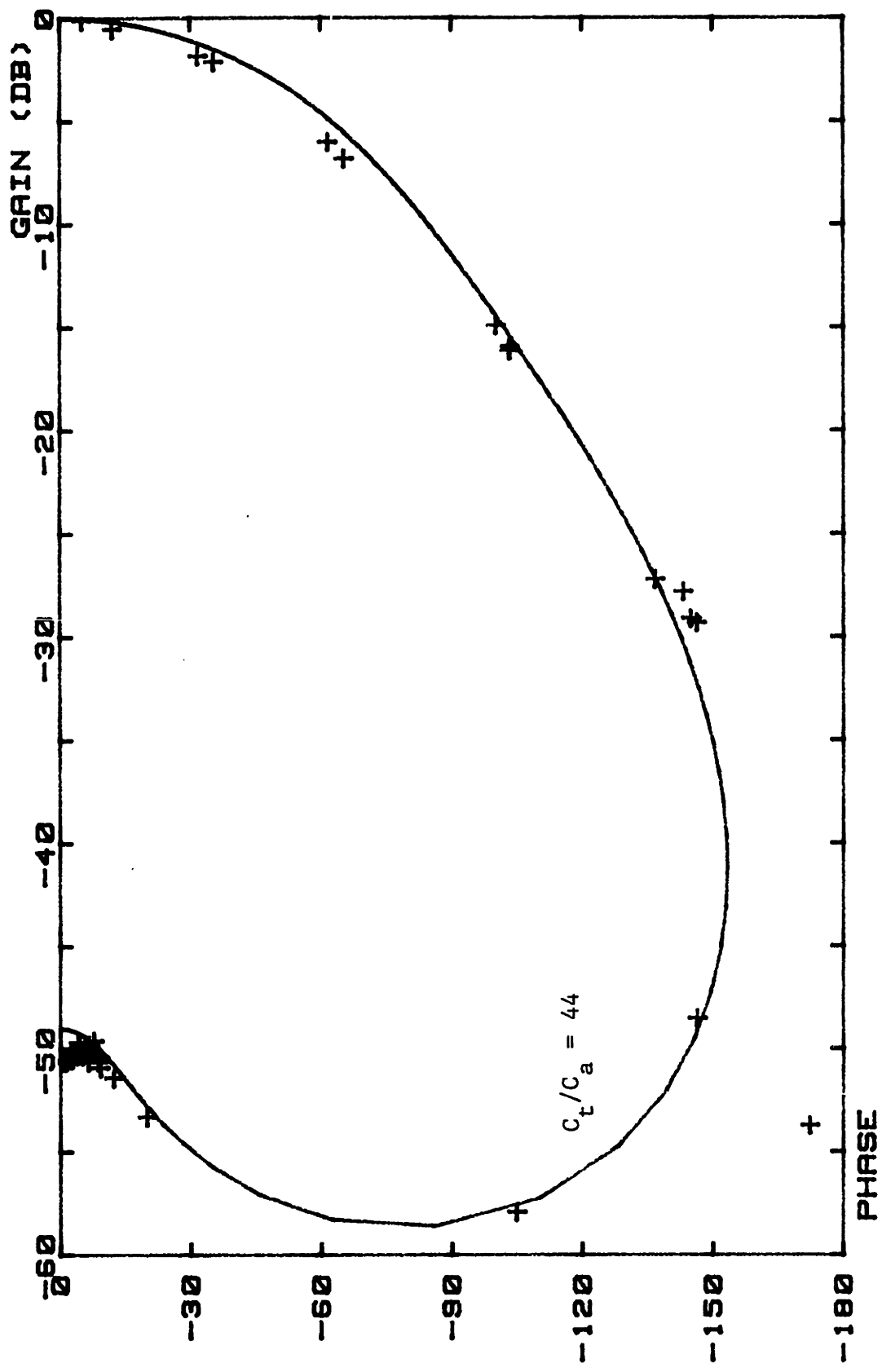


Figure 16) Model Curve Plotted with Data for all Frequencies and Dew Points for an Aged Sample

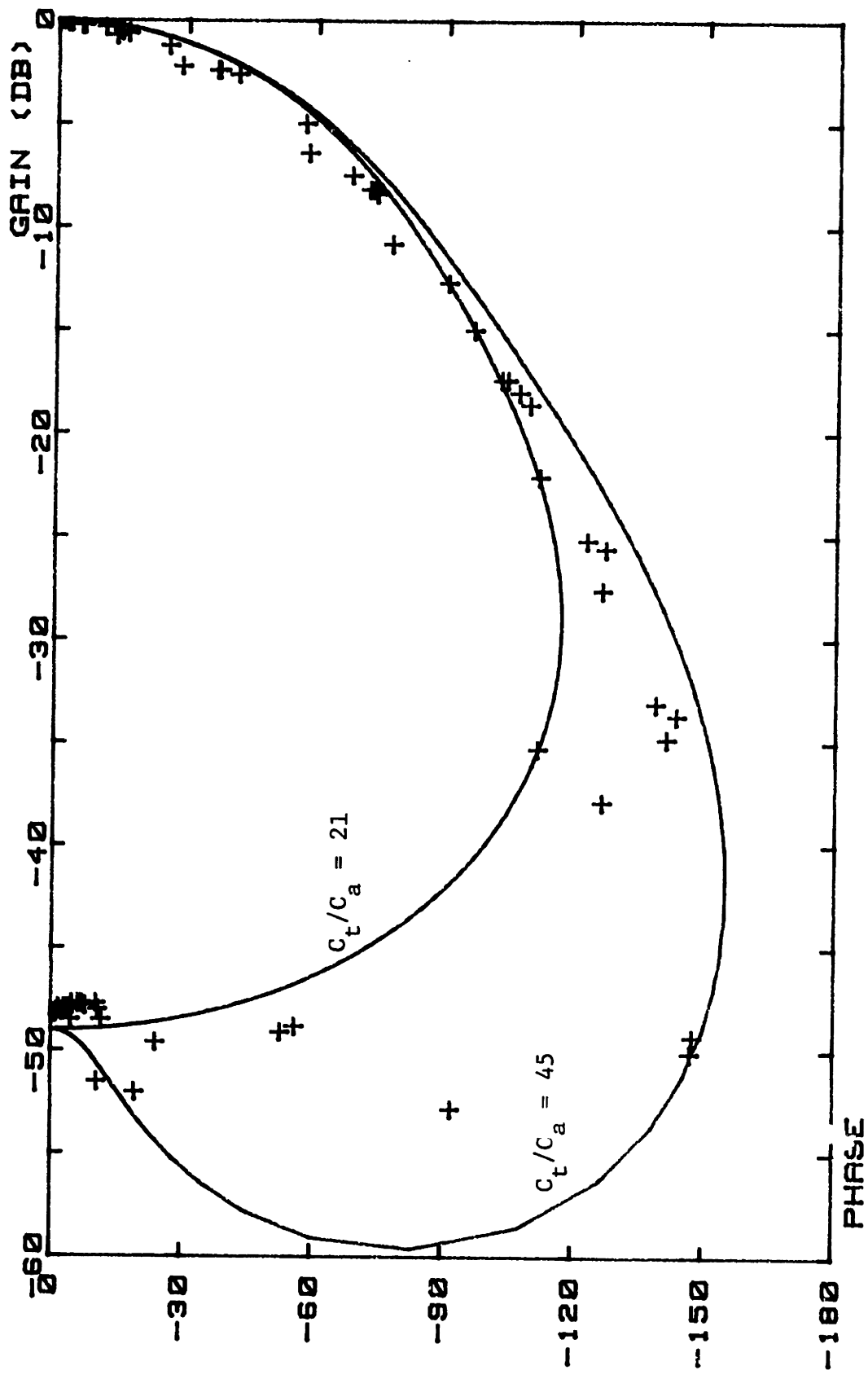


Figure 17) Model Curves Plotted with Data for all Frequencies and Dew Points for a Freshly-Coated Sample

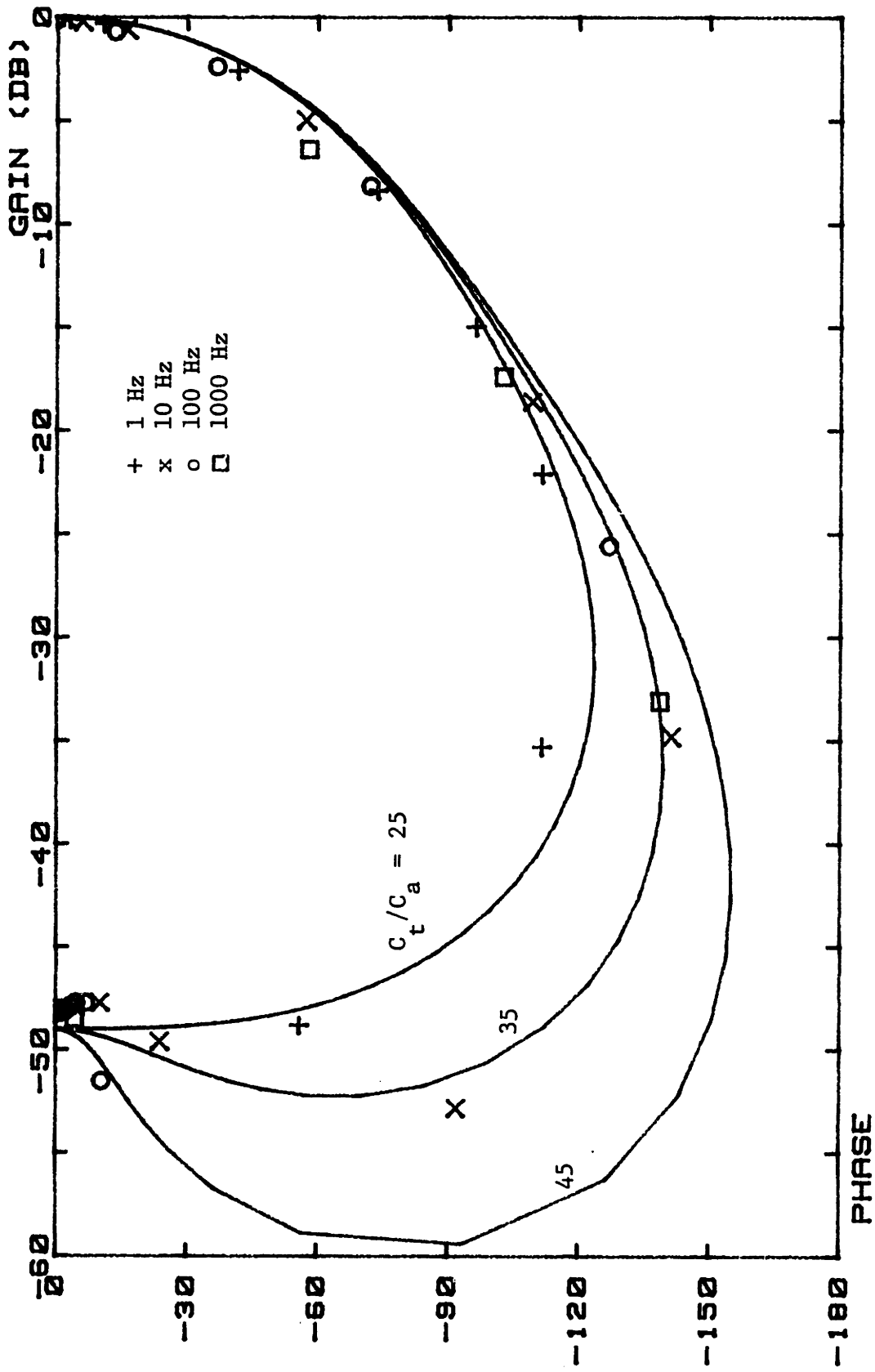


Figure 18) Comparison of Model Curves to Data of Constant Frequency for a Freshly-Coated Sample

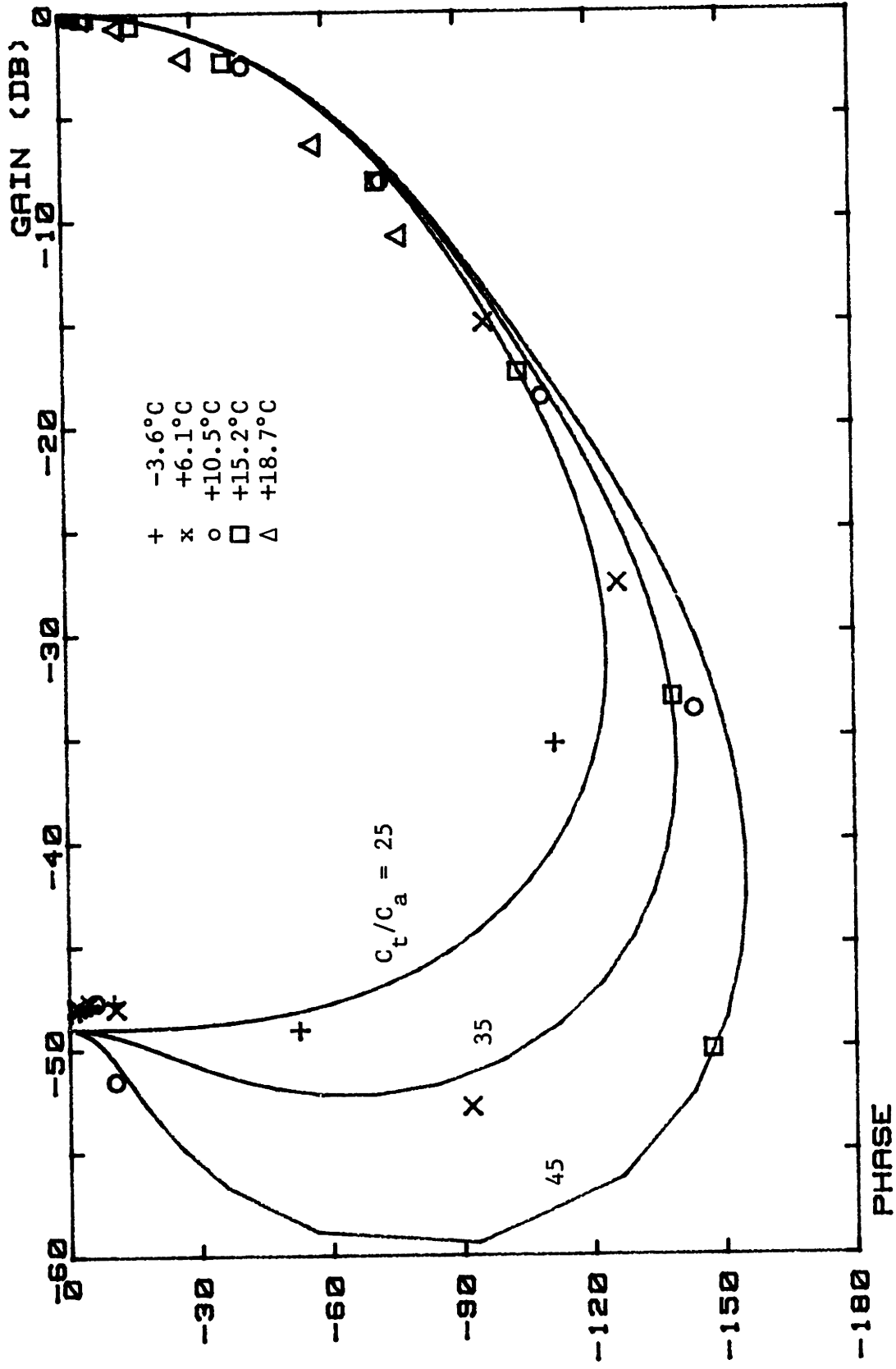


Figure 19) Comparison of Model Curves to Data of Constant Dew Point for a Freshly-Coated Sample

frequency and/or dew point. In general, for both the case of constant frequency and of constant dew point, the ratio  $C_t/C_a$  appears to increase as gain decreases. Perhaps, the portion of the interelectrode capacitance which interacts with the thin film conductance decreases for decreasing gain, or maybe an element, such as contact admittance, must be added to the model. This phenomenon has not as yet been explained satisfactorily.

The final unknown to be extracted from the data is sheet resistance,  $\rho$ . This may be done with relatively little effort, since  $R_a$  and frequency scale with one another.

For each dew point, the measured data are plotted on two sets of axes: gain vs. frequency, and phase vs. frequency. An arbitrary value for the product  $R_a C_a$  is selected. A model curve is plotted for this value of  $R_a C_a$ , using the extracted  $C_t/C_a$  and the computed  $C_1/C_t$  and  $C_x/C_t$ . When  $R_a C_a$  is varied, the model curves simply shift along the frequency axis. The value of  $R_a C_a$  is selected which results in best agreement between the model and the data for the particular dew point. The value of the sheet resistor for that dew point is then determined from the formula

$$R_a = \frac{R_a C_a}{C_1} \frac{C_1}{C_t} \frac{C_t}{C_a}$$

The sheet resistance in ohms per square is then computed by dividing by the number of interelectrode squares--in this case, 1/812.

The value of sheet resistance was extracted in this way for the two aged samples, using a value of 45 for the ratio  $C_t/C_a$ . After extraction of this final unknown, data is replotted versus model curves for several dew points (Figure 20). Agreement between the model and

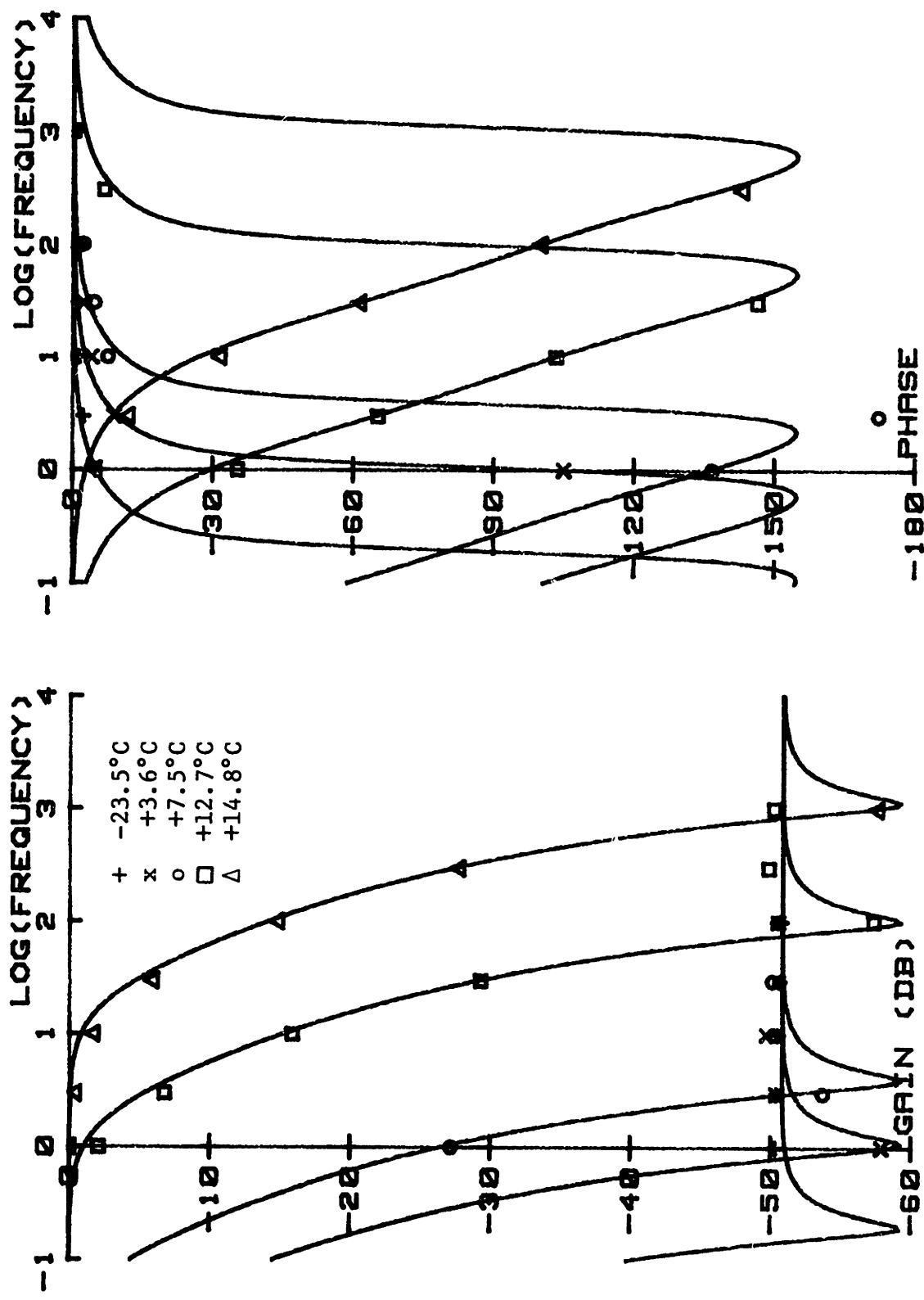


Figure 20) Model Curves Plotted with Data for Various Dew Points for an Aged Sample

the data is excellent.

For the freshly-coated devices, this extraction was performed using three values for  $C_t/C_a$ : the limiting case values of 21 and 45, as well as an intermediate value of 35. Agreement between the three cases is very good (Table 3)--only at very high sheet resistances was there noticeable discrepancy. This is due to the fact that the extraction concentrates on the data at the high-gain end of the spectrum, where variations in  $C_t/C_a$  are unimportant. For the high sheet resistances, however, the 1 Hz minimum frequency limitation of our measurements, forced extraction from the low-gain data.

Because of the relative insensitivity to the ratio  $C_t/C_a$ , all further extractions of sheet resistance were done with  $C_t/C_a = 45$ . The resulting comparison of experimental data and model for a freshly-coated sample is presented in Figure 21. Agreement is again quite good.

The extracted values of sheet resistance for all five samples are plotted versus dew point in Figure 22. For dew point values greater than approximately +5 degrees centigrade, reproducibility between the samples is good. The existing variation from device to device appears to be an offset in temperature, more than one of sheet resistance. This temperature offset is at most 4 degrees centigrade, slightly greater than the temperature fluctuation observed during the measurement period.

At low dew points, the sheet resistance saturates at some high value. This saturation value varies from one sample to the next by a maximum of about an order of magnitude, the two highest values being those measured on the aged samples. It is suggested that this high-frequency value of sheet resistance is determined by the bulk conduction

TABLE 3

DEW POINT (°C)	SHEET RESISTANCE ( $\Omega/\square$ )			% VARIATION	
	$C_t/C_a = 21$	$C_t/C_a = 35$	$C_t/C_a = 45$	Linear	Log
-26.6	$1.71 \times 10^{15}$	$1.30 \times 10^{15}$	$1.14 \times 10^{15}$	33.3	1.16
-3.6	$5.26 \times 10^{14}$	$4.86 \times 10^{14}$	$4.81 \times 10^{14}$	8.8	.27
+3.6	$2.10 \times 10^{14}$	$1.93 \times 10^{14}$	$1.91 \times 10^{14}$	9.0	.29
+6.1	$1.07 \times 10^{14}$	$1.07 \times 10^{14}$	$1.09 \times 10^{14}$	1.8	.06
+8.2	$5.07 \times 10^{13}$	$4.91 \times 10^{13}$	$4.95 \times 10^{13}$	3.2	.10
+10.5	$1.60 \times 10^{13}$	$1.56 \times 10^{13}$	$1.57 \times 10^{13}$	2.5	.08
+13.0	$2.88 \times 10^{12}$	$2.91 \times 10^{12}$	$2.94 \times 10^{12}$	1.0	.07
+15.2	$4.70 \times 10^{11}$	$4.60 \times 10^{11}$	$4.63 \times 10^{11}$	2.1	.08
+17.2	$1.40 \times 10^{11}$	$1.42 \times 10^{11}$	$1.44 \times 10^{11}$	2.8	.11
+18.7	$3.73 \times 10^{10}$	$3.80 \times 10^{10}$	$3.83 \times 10^{10}$	2.6	.11



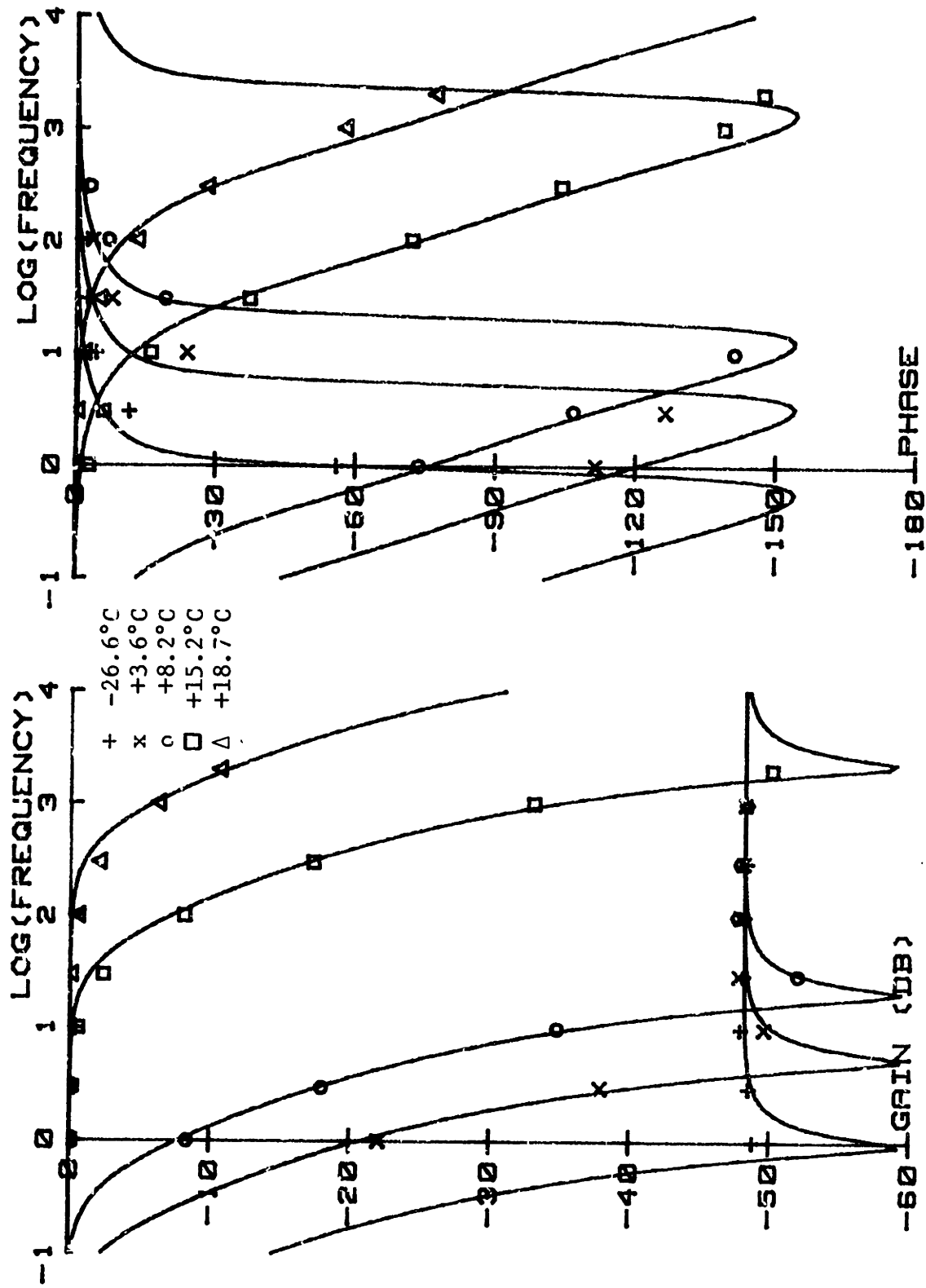


Figure 21) Model Curves Plotted with Data for Various Dew Points for a Freshly Coated Sample

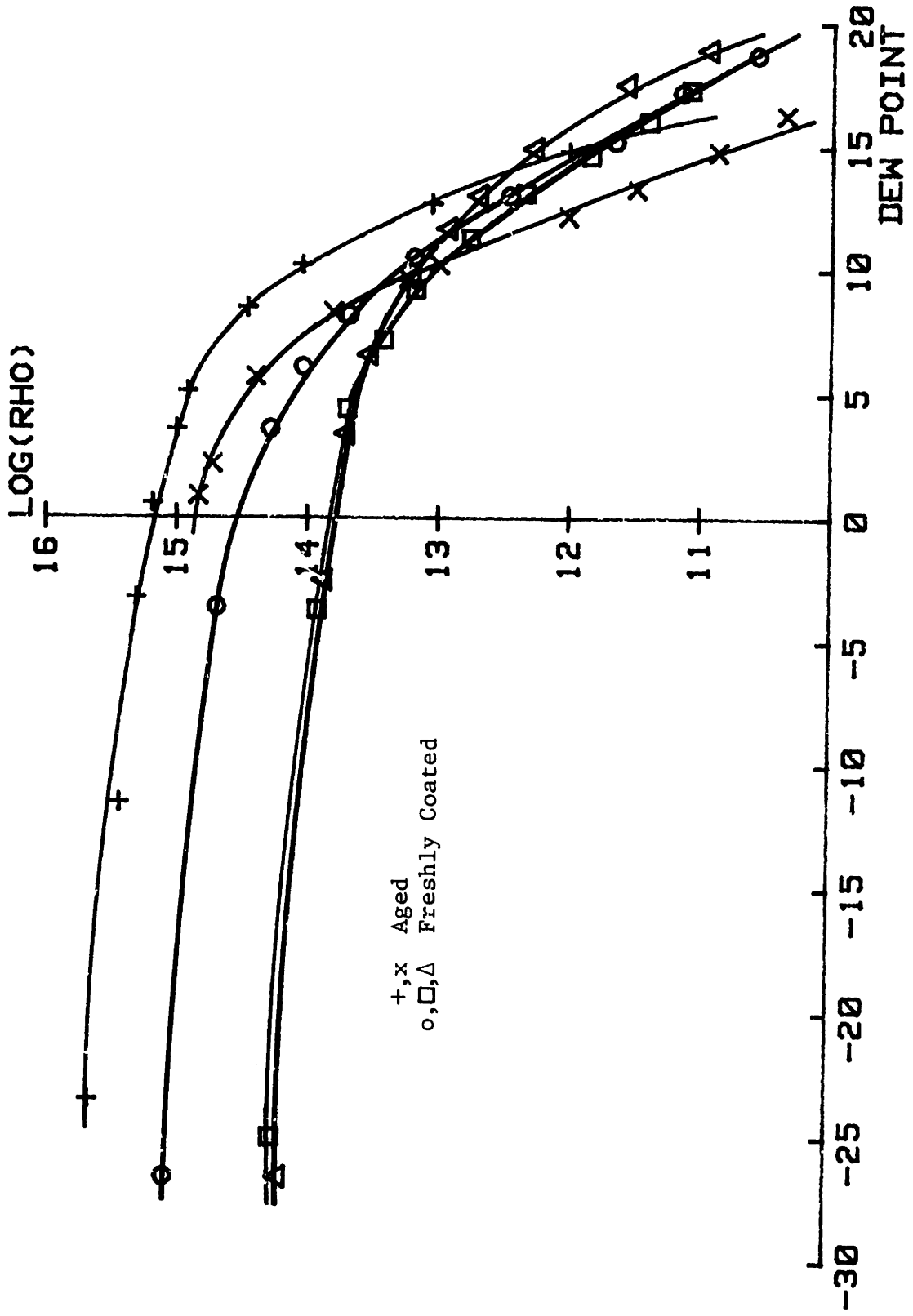


Figure 22) Plot of Extracted Sheet Resistance vs. Dew Point for All Samples

through the polymer, and that the bulk conduction for freshly-coated samples is greater than for aged samples, perhaps due to incomplet removal of the solvent (water) from the freshly cast films. For higher dew points, surface conduction dominates, independent of polymer age, and bulk conductivity variations from device to device are unimportant.

## CHAPTER 5: LIMITATIONS OF THE NEW TECHNIQUE

Thus far, the fingered-gate device has been used to measure sheet resistances in the range  $10^{10}$  to  $10^{16}$  ohms per square. At the high end of this range, there has been no information in the gain of the measured transfer function--extraction relied entirely on the information contained in the phase. For sheet resistances higher than approximately  $10^{16}$  ohms per square, even information in the phase of the response is lost.

This, however, does not arise from a fundamental limitation of the device or measurement technique, but from the frequency limitation of the equipment employed. Presumably, for any value of sheet resistance, there is a frequency of measurement at which any portion of the transfer function curve may be measured. From the theory, this is seen from the important fact that frequency and sheet resistance scale. This arises physically due to the fact that all impedances in the system are capacitive, other than the sheet resistance itself.

The low-frequency limitation of 1 Hz is contributed by the gain-phase measuring instrument. The high-frequency limitation of 3 kHz is attributable to the operational amplifiers in the measurement circuitry. Both of these could be extended. Reasonable measurement times prevent the use of frequencies less than about .1 Hz, however.

In addition, device geometry may be modified to adjust the range of sensitivity, given a restricted frequency range. Effects of device geometry variations may be estimated by making a simplified model of the system (Figure 23). In this model, the capacitors  $C_a$  and  $C_x$  have been lumped together to form a single capacitor,  $C_x'$ . Likewise,  $C_1$  and  $C_t$  have been joined to form a single load capacitor,  $C_1'$ . The transfer

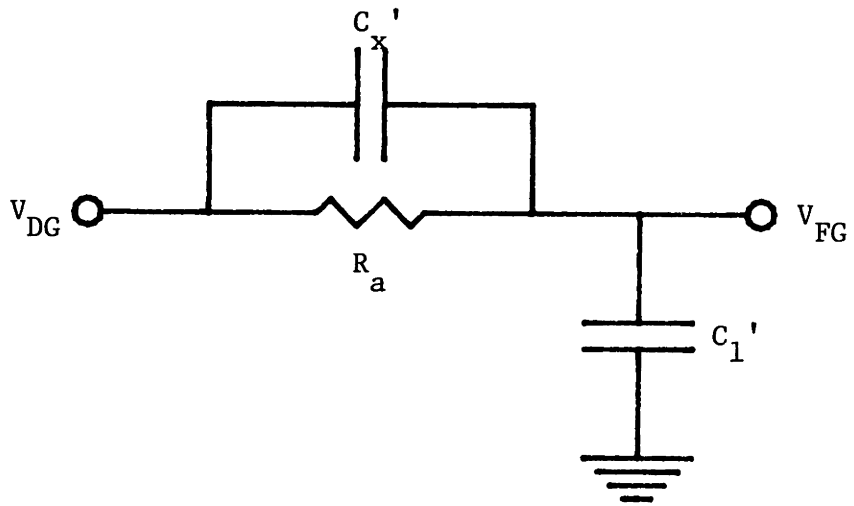


Figure 23) Simplified CFT Mo. 21

function  $V_{FG}/V_{DG}$  for this model is

$$\frac{V_{FG}}{V_{DG}} = \frac{R_a C_x' \omega j + 1}{R_a (C_x' + C_1') \omega j + 1} .$$

The values of the three elements are estimated as before:

$$R_a = \frac{\rho W}{2NL} ,$$

$$C_1' = 3NWL \frac{\epsilon_{ox}}{t_{ox}} ,$$

$$C_x' = NL\epsilon_0 .$$

At high sheet resistances, the imaginary terms of the transfer function dominate. To retain sensitivity,

$$R_a C_x' = \omega \rho \epsilon_0 \frac{W}{2} \gtrsim 10 .$$

Therefore, the maximum sheet resistance that may be measured is

$$\rho_{max} = \frac{20}{\omega_{min} \epsilon_0 W} .$$

The formula says that the maximum measurable sheet resistance is indirectly proportional to the electrode spacing and minimum frequency.

For the current device dimensions, the formula predicts a  $\rho_{max} = 3 \times 10^{16}$  ohms per square for 1 Hz measurements. If devices were made with lock and keys having 1 micron spaces, an increase of  $\rho_{max}$  to  $4 \times 10^{17}$  ohms per square is predicted.

At low sheet resistances, the real terms of the transfer function dominate. To retain sensitivity,

$$R_a (C_x' + C_1') \omega \cong R_a C_1' \omega = \frac{3}{2} \frac{\epsilon_{ox}}{t_{ox}} \rho W^2 \gtrsim .1 .$$

Therefore,

$$\rho_{\min} = \frac{.2}{3} \frac{t_{\text{ox}}}{\epsilon_{\text{ox}}} \frac{1}{\omega_{\max} W^2} .$$

This formula indicates that minimum measurable sheet resistance is indirectly proportional to oxide thickness, and proportional to the square of the interelectrode spacing. For a maximum frequency of 3 kHz, and current device dimensions, the formula predicts

$$\rho_{\min} = 6 \times 10^8 .$$

This value is not unreasonable, since during the course of the PEO experiments, this minimum sheet resistance limit was not pushed.

In summary, the present technique is applicable over a wide range of sheet resistance. The range of sensitivity may be improved by either extending the range of frequency of measurement, or by modifying the device geometry.

## APPENDIX A. SYMBOL DEFINITIONS

$C_a$	Horizontal capacitive component of transmission line model
$C_{ch}$	Channel capacitance
$C_l$	Load capacitor of transmission line model
$C_{lk}$	Interelectrode capacitance of the lock and key
$C_t$	Vertical capacitive component of transmission line model
$C_x$	Stray capacitor in the transmission line model
$G_a$	Horizontal conductance of transmission line model, $1/R_a$
$g_m$	FET transconductance
$I$	Complex current variable
$k$	FET gain
$L$	Length of lock and key fingers
$m$	Body-effect factor
$N$	Number of lock and key fingers
$R_a$	Interelectrode resistance of the transmission line model, $1/G_a$
$s_p$	Natural frequency of the transmission line model
$t$	Time
$t_{ox}$	Oxide thickness
$V$	Complex voltage variable
$V_{DG}$	Driven-gate voltage
$V_{DS}$	Drain to source voltage
$V_{FG}$	Floating-gate voltage
$V_{GS}$	Gate to source voltage
$V_{SB}$	Source to substrate voltage
$W$	Width of lock and key finger (and gap)
$x$	Spacial variable in the transmission line model
$Y$	Complex admittance
$Z$	Complex impedance
$\epsilon_m$	Dielectric permitivitty of sensing medium
$\epsilon_{ox}$	Dielectric permitivitty of silicon dioxide
$\epsilon_{sub}$	Dielectric permitivitty of substrate
$\omega$	Radial frequency
$\rho$	Sheet resistance in ohms/square
$\theta$	Mobility degradation parameter
$\gamma$	Transmission line model parameter, $1/(R_a C_a \omega)$



## APPENDIX B. SOLUTION TO TRANSMISSION LINE MODEL

Refer to Figure 12. Voltage on the transmission line varies both with time  $t$  and position  $x$ . The driven gate is at position  $x = 0$ , and the floating gate is at  $x = W$ . The variation with time is assumed to be sinusoidal, and complex notation is employed:

$$V(x,t) = V(x) e^{j\omega t} .$$

All elements are also converted to complex notation, for example,

$$Y_a = G_a + C_a \omega j .$$

The voltage and current variation along the line may be described by the following two equations:

$$I_x = (V_x - V_{x+dx}) Y_a (W/dx) = -WY_a \frac{dV}{dx} ;$$

$$V_{x+dx} Y_t (dx/W) = I_x - I_{x+dx} , \text{ or } V_{x+dx} = - \frac{W}{Y_t} \frac{dI}{dx} .$$

The variable  $I(x)$  may be eliminated from the above equations, to yield a single expression for the voltage distribution:

$$\frac{d^2 V}{dx^2} = \frac{Y_t}{Y_a W^2} V(x) .$$

The general form of the solution is

$$V(x) = A \sinh s_0 x + B \cosh s_0 x ,$$

where  $s_0 = \frac{1}{W} (Y_t / Y_a)^{1/2}$ . The values of the constants  $A$  and  $B$  may be determined by application of the appropriate boundary conditions:

$$1) V(x=0) = V_0$$

$$2) I(x=W) = -WY_a \frac{dV}{dx}(x=W) = Y_1 V(x=W) + Y_x (V(x=W) - V(x=0)) .$$

The first boundary condition yields  $B = V_0$ . The second boundary condition is expressed as the following equation:

$$-\alpha Y_a (A \cosh \alpha + B \sinh \alpha) = (Y_x + Y_1)(A \sinh \alpha + B \cosh \alpha) - Y_x B,$$

where  $\alpha = s_0 W = (Y_t / Y_a)^{1/2}$ .

This expression may be solved for the constant A yielding

$$A = \frac{-V_0 (\alpha Y_a \sinh \alpha + (Y_1 + Y_x) \cosh \alpha - Y_x)}{(\alpha Y_a \cosh \alpha + (Y_1 + Y_x) \sinh \alpha)}.$$

The transfer function from driven gate to floating gate is expressed as

$$\frac{V_{FG}}{V_{DG}} = \frac{V(x=W)}{V(x=0)} = \frac{A}{V_0} \sinh \alpha + \cosh \alpha.$$

The result may be expressed as

$$\frac{V_{FG}}{V_{DG}} = \frac{\alpha Y_a + Y_x \sinh \alpha}{\alpha Y_a \cosh \alpha + (Y_1 + Y_x) \sinh \alpha}$$

by taking advantage of the identity  $\cosh^2 \alpha - \sinh^2 \alpha = 1$ .

By dividing this expression by  $\alpha Y_a$ , and reconverting from complex admittances to conductances and capacitances, the solution may be expressed as

$$\frac{V_{FG}}{V_{DG}} = \frac{1 + (C_x / C_t) \alpha \sinh \alpha}{\cosh \alpha + (C_1 / C_t + C_x / C_t) \alpha \sinh \alpha}.$$

Note that  $\alpha$  may be expressed as

$$\alpha = \frac{(C_t / C_a)^{1/2} j}{1 / R_a C_a \omega + j}.$$

Expressed in this form, the model has essentially four parameters:

$$C_1 / C_t, C_x / C_t, C_t / C_a, \text{ and } \gamma = 1 / (R_a C_a \omega).$$

## APPENDIX C. DEVICE FABRICATION PROCEDURE

1. Wafer Characterization--use a <100>, p-type silicon wafer, .1-.4 ohm-cm
  - a. Hot probe check for wafer carrier type
  - b. 4-point probe measurement of sheet resistance
  - c. Wafer thickness measurement with the micrometer
2. Field Oxidation
  - a. I-Clean
  - b. 15 minutes in dry O<sub>2</sub> @ 1100°C  
120 minutes in wet O<sub>2</sub> @ 1100°C  
10 minutes in dry O<sub>2</sub> @ 1100°C
3. Source/Drain Photolithography
  - a. Apply KTRF
  - b. Expose wafer for 5 seconds using Source/Drain Mask
  - c. Develop and postbake KTRF
  - d. 10 minute etch in buffered etch, rinse in DH<sub>2</sub>O, and blow dry (N<sub>2</sub>)
  - e. Strip KTRF
4. Source/Drain Implant
  - a. Element--Arsenic
  - b. Dose--8 x 10<sup>15</sup>
  - c. Energy--100 keV
5. Source/Drain Anneal and Oxidation
  - a. G-Clean
  - b. 20 minutes in wet O<sub>2</sub> @ 1000°C
6. Thin Oxide Photolithography
  - a. Apply KTRF
  - b. Expose wafer for 5 seconds using Thin Oxide Mask
  - c. Develop and postbake KTRF
  - d. 10 minute etch in buffered etch, rinse in DH<sub>2</sub>O, and blow dry (N<sub>2</sub>)
  - e. Strip KTRF
7. Gate Oxidation
  - a. G-Clean
  - b. 40 minutes in dry O<sub>2</sub> @ 1100°C  
10 minutes in N<sub>2</sub> @ 1100°C

8. Channel Implant Photolithography
  - a. Apply Shipley B photoresist
  - b. Expose wafer for 5 seconds using Contact Mask
  - c. Develop and postbake Shipley B photoresist
9. Channel Implant
  - a. Element--Phosphorous
  - b. Dose-- $2.5 \times 10^{12}$
  - c. Energy--90 keV
10. Channel Implant Activation and Anneal
  - a. Strip Shipley B photoresist
  - b. G-Clean
  - c. 20 minutes in  $N_2$  @  $950^\circ C$
11. Contact Photolithography
  - a. Apply KTRF
  - b. Expose wafer for 5 seconds using Contact Mask
  - c. Develop and postbake KTRF
  - d. Etch for 2 minutes in buffered etch, rinse in  $DH_2O$ , blow dry ( $N_2$ )
  - e. Strip KTRF
12. Clean Metal Aluminization--as per instructions (15)
13. Metallization Photolithography
  - a. Apply Shipley B photoresist
  - b. Expose wafer for 5 seconds using Metallization Mask
  - c. Develop and postbake Shipley B photoresist
  - d. Etch in PAN etch for approximately 5 minutes (do by inspection),  
rinse in  $DH_2O$ , blow dry ( $N_2$ )
  - e. Strip Shipley B photoresist
14. Alloying
  - a. Rinse wafers in Trico, acetone,  $DH_2O$ , and blow dry ( $N_2$ )
  - b. Alloy in  $N_2$  @  $450^\circ C$  for 5 minutes, leave in tube end for  
5 additional minutes

I-Clean

- a. 10 minutes in #3 stripping solution @ 90°C
- b. 1 minute rinse in  $\text{DH}_2\text{O}$
- c. 15 seconds in concentrated HF
- d. 1 minute rinse in  $\text{DH}_2\text{O}$
- e. 10 minutes in nitric acid @ 90°C
- f. 3 minute rinse in  $\text{DH}_2\text{O}$ , blow dry ( $\text{N}_2$ )

G-Clean

- a. 10 minutes in #3 stripping solution @ 90°C
- b. 1 minute rinse in  $\text{DH}_2\text{O}$
- c. 15 seconds in 10:1 HF
- d. 1 minute rinse in  $\text{DH}_2\text{O}$
- e. 10 minutes in nitric acid @ 90°C
- f. 3 minute rinse in  $\text{DH}_2\text{O}$ , blow dry ( $\text{N}_2$ )

Procedure for Application of KTFR

- a. Spin on resist for 15 seconds @ 6000 RPM
- b. Pre-bake for 20 minutes @ 90 degrees centigrade

Procedure for Application of Shipley B photoresist

- a. Spin on resist for 15 seconds @ 3000 RPM
- b. Pre-bake for 2-1/2 minutes @ 90°C
- c. Repeat steps a. and b.

Procedure for the Developing and Postbaking of KTFR

- a. Develop by spraying with KTFR developer for 60 seconds
- b. Postbake for 30 minutes @ 180°C

Procedure for the Developing and Postbaking of Shipley B photoresist

- a. Develop by immersion in beaker of Az Developer for 25 seconds
- b. Postbake for 30 minutes @ 180°C

Procedure for Stripping Photoresist (KTFR or Shipley B)

- a. Strip resist for 5 minutes in A-20 @ 90°C
- b. Rinse in warm  $\text{DH}_2\text{O}$ , cool  $\text{DH}_2\text{O}$ , and blow dry ( $\text{N}_2$ )

## APPENDIX D. SUPREM SIMULATION OF DEVICE FABRICATION

The device fabrication procedure was designed with the aid of the computer simulation program SUPREM (Stanford University Process Engineering Models Program), executed on the MIT CMS system. The program output is presented in condensed form in the following pages. Simulation was performed over three areas of the device: the field, the source/drain, and the channel regions.

\*\*\* STANFORD UNIVERSITY PROCESS ENGINEERING MODELS PROGRAM \*\*\*

\*\*\* VERSION O-03A \*\*\*

```
1....TITLE FIELD REGION
2....GRID DYS1=.01,DPTH=1.0,YMAX=3
3....SUBS ORNT=100,ELEM=B,CONC=6.3E16
4....MODEL NAME=SPM1,GATE=AL,QSSQ=2.5E11,CBLK=0
5....STEP TYPE=OXID,TEMP=1100,TIME=15,MODL=DRYO
6....STEP TYPE=OXID,TEMP=1100,TIME=120,MODL=WETO
7....STEP TYPE=OXID,TEMP=1100,TIME=10,MODL=DRYO
8....STEP TYPE=OXID,TEMP=1000,TIME=20,MODL=WETO
9....STEP TYPE=OXID,TEMP=1100,TIME=40,MODL=DRYO
10....PRINT HEAD=Y
11....PLOT TOTL=Y,CMIN=14,NDEC=7,WIND=3,IDIV=Y
12....STEP TYPE=OXID,TEMP=1100,TIME=10,MODL=NITO,MODL=SPM1
13....END
```

\*\*\* STANFORD UNIVERSITY PROCESS ENGINEERING MODELS PROGRAM \*\*\*

\*\*\* VERSION O-03A \*\*\*

```
1....TITLE MODEL OF ARSENIC-DOPED REGIONS
2....GRID DYS1=.001,DPTH=.5,YMAX=4
3....SUBS ORNT=100,ELEM=B,CONC=6.3E16
4....STEP TYPE=IMPL,ELEM=AS,DOSE=8E15,AKEV=100
5....STEP TYPE=OXID,TEMP=1000,TIME=20,MODL=WETO
6....STEP TYPE=OXID,TEMP=1100,TIME=40,MODL=DRYO
7....PRINT HEAD=Y
8....PLOT TOTL=Y,CMIN=14,NDEC=7,WIND=2
9....STEP TYPE=OXID,TEMP=1100,TIME=10,MODL=NITO
10....END
```

\*\*\* STANFORD UNIVERSITY PROCESS ENGINEERING MODELS PROGRAM \*\*\*

\*\*\* VERSION O-03A \*\*\*

```
1....TITLE CHANNEL REGION
2....GRID DYS1=.01,DPTH=.5,YMAX=2
3....SUBS ORNT=100,ELEM=B,CONC=6.3E16
4....MODEL NAME=SPM1,CBLK=0,QSSQ=2.5E11,GATE=AL
5....STEP TYPE=OXID,TIME=40,TEMP=1100,MODL=DRYO
6....STEP TYPE=OXID,TIME=10,TEMP=1100,MODL=NITO
7....STEP TYPE=IMPL,DOSE=2.5E12,AKEV=90,ELEM=P
8....PRINT HEAD=Y
9....PLOT TOTL=Y,IDIV=N,CMIN=14,NDEC=7,WIND=.5
10....STEP TYPE=OXID,TIME=20,TEMP=950,MODL=NITO,MODL=SPM1
11....END
```

FIELD REGION

STEP # 6

NEUTRAL AMBIENT DRIVE-IN

TOTAL STEP TIME = 10.0 MINUTES  
 INITIAL TEMPERATURE = 1100.00 DEGREES C.  
 OXIDE THICKNESS = .9131 MICRONS

	I OXIDE	I SILICON	I	I SURFACE	I
	I DIFFUSION	I DIFFUSION	I SEGREGATION	I TRANSPORT	
	I COEFFICIENT	I COEFFICIENT	I COEFFICIENT	I COEFFICIENT	I
BORON	I 2.0972E-07	I 8.9033E-04	I .66145	I 1.3113E-02	I

SURFACE CONCENTRATION = 4.04126E+16 ATOMS/CM<sup>3</sup>

GATE MATERIAL = ALUMINUM SILICON UNDER GATE = P - TYPE  
 OXIDE THICKNESS = 9131.4 ANG. CAPACITANCE/AREA = 3.78E-05 PF/UM<sup>2</sup>  
 INTERFACE CHARGES = 2.50E+11 CM-2 INTF CHARGE VOLT. = -10.596 VOLTS  
 FLATBAND VOLTAGE = -11.652 VOLTS  
 /VSB/ 0.0 0.50 1.00 1.50 2.00 3.00 4.00 5.00 6.00 7:00 10.00 15.00  
 VTHR 16.68 24.46 30.85 36.42 41.44 50.35 58.20 65.31 71.87 78.00 94.52 117.97  
 XDPL 0.16 0.21 0.24 0.27 0.30 0.34 0.38 0.42 0.45 0.48 0.55 0.65

JUNCTION DEPTH	I	SHEET RESISTANCE
	I	1114.77 OHMS/SQUARE

NET ACTIVE CONCENTRATION

OXIDE CHARGE = 3.69384E+12 IS 19.7 % OF TOTAL  
 SILICON CHARGE = 1.50836E+13 IS 80.3 % OF TOTAL  
 TOTAL CHARGE = 1.87774E+13 IS 100. % OF INITIAL  
 INITIAL CHARGE = 1.87772E+13

CHEMICAL CONCENTRATION OF BORON

OXIDE CHARGE = 3.69384E+12 IS 19.7 % OF TOTAL  
 SILICON CHARGE = 1.50836E+13 IS 80.3 % OF TOTAL  
 TOTAL CHARGE = 1.87774E+13 IS 100. % OF INITIAL  
 INITIAL CHARGE = 1.87772E+13



FIELD REGION

I STEP = 6      TIME = 10.0 MINUTES.

DEPTH (UM)	CONCENTRATION (LOG ATOMS/CC)							
	14	15	16	17	18	19	20	21
-0.91	I	I	I	*	I	I	I	I
	I	I	I	*	I	I	I	I
	I	I	I	*	I	I	I	I
	I	I	I	*	I	I	I	I
	I	I	I	*	I	I	I	I
	I	I	I	*	I	I	I	I
	I	I	I	*	I	I	I	I
	I	I	I	*	I	I	I	I
0.0	I	I	I	*	I	I	I	I
	I	I	I	*	I	I	I	I
	I	I	I	*	I	I	I	I
	I	I	I	*	I	I	I	I
	I	I	I	*	I	I	I	I
	I	I	I	*	I	I	I	I
	I	I	I	*	I	I	I	I
	I	I	I	*	I	I	I	I
1.00	I	I	I	*	I	I	I	I
	I	I	I	*	I	I	I	I
	I	I	I	*	I	I	I	I
	I	I	I	*	I	I	I	I
	I	I	I	*	I	I	I	I
	I	I	I	*	I	I	I	I
	I	I	I	*	I	I	I	I
	I	I	I	*	I	I	I	I
2.00	I	I	I	*	I	I	I	I
	I	I	I	*	I	I	I	I
	I	I	I	*	I	I	I	I
	I	I	I	*	I	I	I	I
	I	I	I	*	I	I	I	I
	I	I	I	*	I	I	I	I
	I	I	I	*	I	I	I	I
	I	I	I	*	I	I	I	I
3.00	I	I	I	I	I	I	I	I
	I	I	I	I	I	I	I	I
	I	I	I	I	I	I	I	I
	I	I	I	I	I	I	I	I
	I	I	I	I	I	I	I	I
	I	I	I	I	I	I	I	I
	I	I	I	I	I	I	I	I
	I	I	I	I	I	I	I	I
4.00	I	I	I	I	I	I	I	I

1  
MODEL OF ARSENIC-DOPED REGIONS

STEP # 4

NEUTRAL AMBIENT DRIVE-IN

TOTAL STEP TIME = 10.0 MINUTES  
 INITIAL TEMPERATURE = 1100.00 DEGREES C.  
 OXIDE THICKNESS = .2936 MICRONS

	I OXIDE I DIFFUSION I COEFFICIENT	I SILICON I DIFFUSION I COEFFICIENT	I SEGREGATION I COEFFICIENT	I SURFACE I TRANSPORT I COEFFICIENT
BORON	I 2.0972E-07	I 8.9033E-04	I .66145	I 1.3113E-02
ARSENIC	I 1.1840E-08	I 1.2294E-04	I 10.000	I 4.4701E-02

SURFACE CONCENTRATION = -1.06986E+20 ATOMS/CM<sup>3</sup>

JUNCTION DEPTH	I	SHEET RESISTANCE
.774699 MICRONS	I 18.4962	OHMS/SQUARE
	I 884.844	OHMS/SQUARE

NET ACTIVE CONCENTRATION

OXIDE CHARGE = 3.12483E+15 IS 39.9 % OF TOTAL  
 SILICON CHARGE = 4.70315E+15 IS 60.1 % OF TOTAL  
 TOTAL CHARGE = 7.82799E+15 IS 100. % OF INITIAL  
 INITIAL CHARGE = 7.81584E+15

CHEMICAL CONCENTRATION OF BORON

OXIDE CHARGE = 1.04950E+12 IS 4.17 % OF TOTAL  
 SILICON CHARGE = 2.41363E+13 IS 95.8 % OF TOTAL  
 TOTAL CHARGE = 2.51858E+13 IS 100. % OF INITIAL  
 INITIAL CHARGE = 2.51837E+13

CHEMICAL CONCENTRATION OF ARSENIC

OXIDE CHARGE = 3.30221E+15 IS 41.1 % OF TOTAL  
 SILICON CHARGE = 4.73577E+15 IS 58.9 % OF TOTAL  
 TOTAL CHARGE = 8.03798E+15 IS 100. % OF INITIAL  
 INITIAL CHARGE = 8.03770E+15

1

MODEL OF ARSENIC-DOPED REGIONS

I STEP = 4      TIME = 10.0 MINUTES.

DEPTH (UM)	14	15	16	17	18	19	20	21
-0.29	I	I	I	I	I	*I	I	I
	I	I	I	I	I	I	*	I
	I	I	I	I	I	I	I*	I
	I	I	I	I	I	I	I*	I
	I	I	I	I	I	I	I*	I
	I	I	I	I	I	I	I*	I
	I	I	I	I	I	I	I*	I
	I	I	I	I	I	I	I*	I
0.0	I	I	I	I	I	I	*	I
	I	I	I	I	I	I	*	I
	I	I	I	I	I	I	*	I
	I	I	I	I	I	I	*	I
	I	I	I	I	I	I	*	I
	I	I	I	I	I	I	*I	I
	I	I	I	I	I	I	*I	I
	I	I	I	I	I	I	*I	I
0.50	I	I	I	I	I	I	*	I
	I	I	I	I	I	I	*	I
	I	I	I	I	I	I	*	I
	I	I	I	I	I*	I	I	I
	I	I	I	*	I	I	I	I
	I	I	I	*	I	I	I	I
	I	I	I	*	I	I	I	I
	I	I	I	*	I	I	I	I
1.00	I	I	I	*	I	I	I	I
	I	I	I	*	I	I	I	I
	I	I	I	*	I	I	I	I
	I	I	I	*	I	I	I	I
	I	I	I	*	I	I	I	I
	I	I	I	*	I	I	I	I
	I	I	I	*	I	I	I	I
	I	I	I	*	I	I	I	I
1.50	I	I	I	*	I	I	I	I
	I	I	I	*	I	I	I	I
	I	I	I	*	I	I	I	I
	I	I	I	*	I	I	I	I
	I	I	I	*	I	I	I	I
	I	I	I	*	I	I	I	I
	I	I	I	*	I	I	I	I
	I	I	I	*	I	I	I	I
2.00	I	I	I	*	I	I	I	I

1 SUPREM END.

1  
CHANNEL REGION

STEP # 4

NEUTRAL AMBIENT DRIVE-IN

TOTAL STEP TIME = 20.0 MINUTES  
 INITIAL TEMPERATURE = 950.000 DEGREES C.  
 OXIDE THICKNESS = 8.407E-02 MICRONS

	I	OXIDE	I	SILICON	I	SEGREGATION	I	SURFACE	I
	I	DIFFUSION	I	DIFFUSION	I	COEFFICIENT	I	TRANSPORT	I
	I	COEFFICIENT	I	COEFFICIENT	I	COEFFICIENT	I	COEFFICIENT	I
BORON	I	5.4047E-09	I	2.5566E-05	I	.24457	I	1.0023E-03	I
PHOSPHORUS	I	1.7279E-07	I	1.9182E-05	I	10.000	I	5.6835E-03	I

SURFACE CONCENTRATION = -2.28879E+17 ATOMS/CM<sup>3</sup>

GATE MATERIAL = ALUMINUM SILICON UNDER GATE = N - TYPE  
 OXIDE THICKNESS = 840.7 ANG. CAPACITANCE/AREA = 4.11E-04 PF/UM2  
 INTERFACE CHARGES = 2.50E+11 CM-2 INTF CHARGE VOLT. = -0.976 VOLTS  
 FLATBAND VOLTAGE = -2.031 VOLTS  
 /VSB/ 0.0 0.50 1.00 1.50 2.00 3.00 4.00 5.00 6.00 7.00 10.00 15.00  
 VTHR -4.28 -3.55 -2.95 -2.43 -2.81 -1.16 -0.45 0.21 0.83 1.41 3.00 5.26  
 XDPL 0.22 0.25 0.27 0.30 0.31 0.35 0.38 0.41 0.44 0.46 0.54 0.62

JUNCTION DEPTH	I	SHEET RESISTANCE
.100110	I	8625.84 OHMS/SQUARE
	I	1496.56 OHMS/SQUARE

NET ACTIVE CONCENTRATION

OXIDE CHARGE = 5.43101E+11 IS 4.15 % OF TOTAL  
 SILICON CHARGE = 1.25525E+13 IS 95.9 % OF TOTAL  
 TOTAL CHARGE = 1.30956E+13 IS 99.7 % OF INITIAL  
 INITIAL CHARGE = 1.31320E+13

CHEMICAL CONCENTRATION OF BORON

OXIDE CHARGE = 5.45771E+11 IS 4.36 % OF TOTAL  
 SILICON CHARGE = 1.19650E+13 IS 95.6 % OF TOTAL  
 TOTAL CHARGE = 1.25108E+13 IS 100. % OF INITIAL  
 INITIAL CHARGE = 1.25109E+13

CHEMICAL CONCENTRATION OF PHOSPHORUS

OXIDE CHARGE = 6.77489E+11 IS 27.1 % OF TOTAL  
 SILICON CHARGE = 1.82289E+12 IS 72.9 % OF TOTAL  
 TOTAL CHARGE = 2.50038E+12 IS 100. % OF INITIAL  
 INITIAL CHARGE = 2.50086E+12

1

CHANNEL REGION

I STEP = 4 TIME = 20.0 MINUTES.

DEPTH (UM)	CONCENTRATION (LOG ATOMS/CC)							
	14	15	16	17	18	19	20	21
-0.08	I	I	I *	I	I	I	I	I
	I	I	I *	I	I	I	I	I
	I	I	I *	I	I	I	I	I
	I	I	I *	I	I	I	I	I
	I	I	I *	I	I	I	I	I
	I	I	I *	I	I	I	I	I
	I	I	I *	I	I	I	I	I
	I	I	I *	I	I	I	I	I
	I	I	I *	I	I	I	I	I
0.0	I	I	I *	I	I	I	I	I
	I	I	I *	I	I	I	I	I
	I	I	I *	I	I	I	I	I
	I	I	I *	I	I	I	I	I
	I *	I	I *	I	I	I	I	I
	I	I	I *	I	I	I	I	I
	I	I	I *	I	I	I	I	I
	I	I	I *	I	I	I	I	I
	I	I	I *	I	I	I	I	I
0.20	I	I	I *	I	I	I	I	I
	I	I	I *	I	I	I	I	I
	I	I	I *	I	I	I	I	I
	I	I	I *	I	I	I	I	I
	I	I	I *	I	I	I	I	I
	I	I	I *	I	I	I	I	I
	I	I	I *	I	I	I	I	I
	I	I	I *	I	I	I	I	I
	I	I	I *	I	I	I	I	I
0.40	I	I	I *	I	I	I	I	I
	I	I	I *	I	I	I	I	I
	I	I	I *	I	I	I	I	I
	I	I	I *	I	I	I	I	I
	I	I	I *	I	I	I	I	I
	I	I	I *	I	I	I	I	I
	I	I	I *	I	I	I	I	I
	I	I	I *	I	I	I	I	I
	I	I	I *	I	I	I	I	I
0.60	I	I	I *	I	I	I	I	I
	I	I	I *	I	I	I	I	I
	I	I	I *	I	I	I	I	I
	I	I	I *	I	I	I	I	I
	I	I	I *	I	I	I	I	I
	I	I	I *	I	I	I	I	I
	I	I	I *	I	I	I	I	I
	I	I	I *	I	I	I	I	I
	I	I	I *	I	I	I	I	I
0.80	I	I	I *	I	I	I	I	I

1 SUPREM END.

## APPENDIX E. DETAILED MASK LAYOUT

The device fabrication procedure as detailed in Appendix C employs four photomasks: 1) Source/Drain, 2) Thin Oxide, 3) Contact, and 4) Metalization. In addition, a fifth mask for overglass passivation was designed and fabricated, but not as yet used in device fabrication. The following pages include an overlay of the four utilized masks, followed by an individual presentation of each of the five masks (Figures E1-6).

The layout contains a fingered-gate CFT, a floating-gate CFT, and a standard FET. The devices are surrounded by eight bonding pads, labeled as follows:

- FD: the FET drain;
- FG: the FET gate;
- FS: the FET source;
- CG: the driven gate for both CFT's;
- CD1: the drain of the floating-gate CFT;
- CS: the source of both CFT's;
- CD2: the drain of the fingered-gate CFT;
- SUB: the substrate contact.

The interdigitated portion of the inner electrode has 10 fingers, each finger being .5 mils wide and 37.5 mils long. The interelectrode gap is a constant .5 mils. The circumference of the inner electrode is 406 mils.

The FET's have a channel length of .5 mils, and a channel width of 5 mils. Bonding pads are 10 mils to the side, and separated by 20 mils. The unusually large bonding pads are required for the flip-chip packaging scheme described in Appendix G.

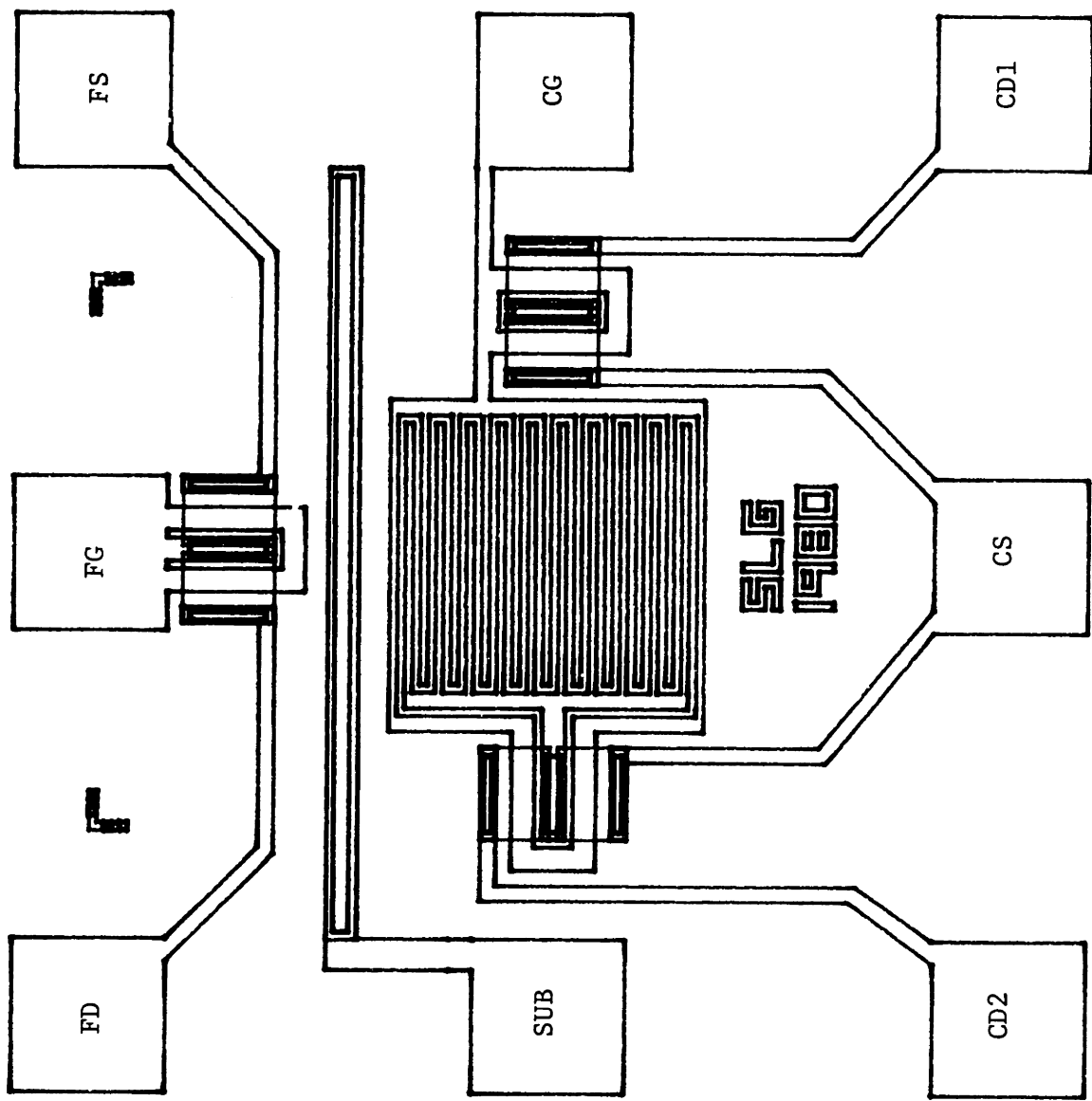


Figure E1) 4-Mask Overlay

□

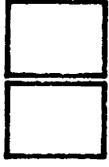
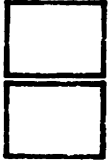


Figure E2) Source/Drain Mask at Approx. 80x



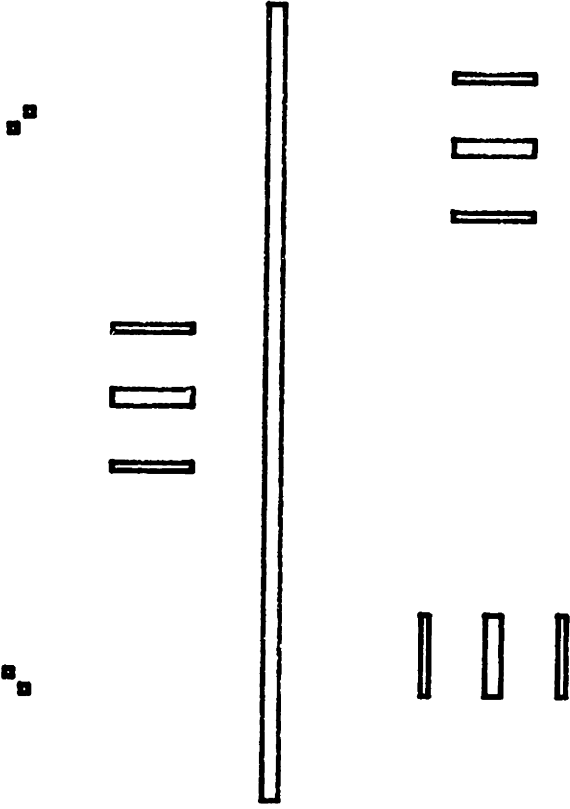


Figure E3) Thin Oxide Mask at Approx. 80x

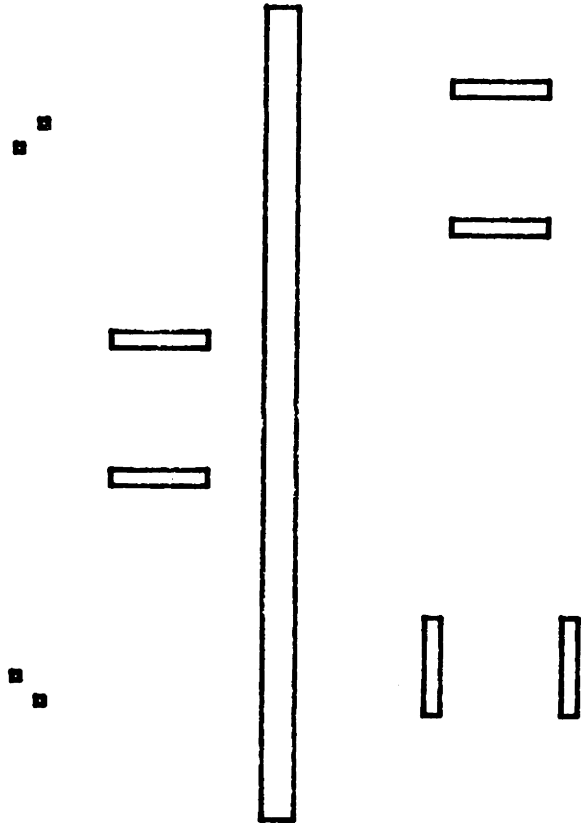


Figure E4) Contact Mask at Approx. 80x

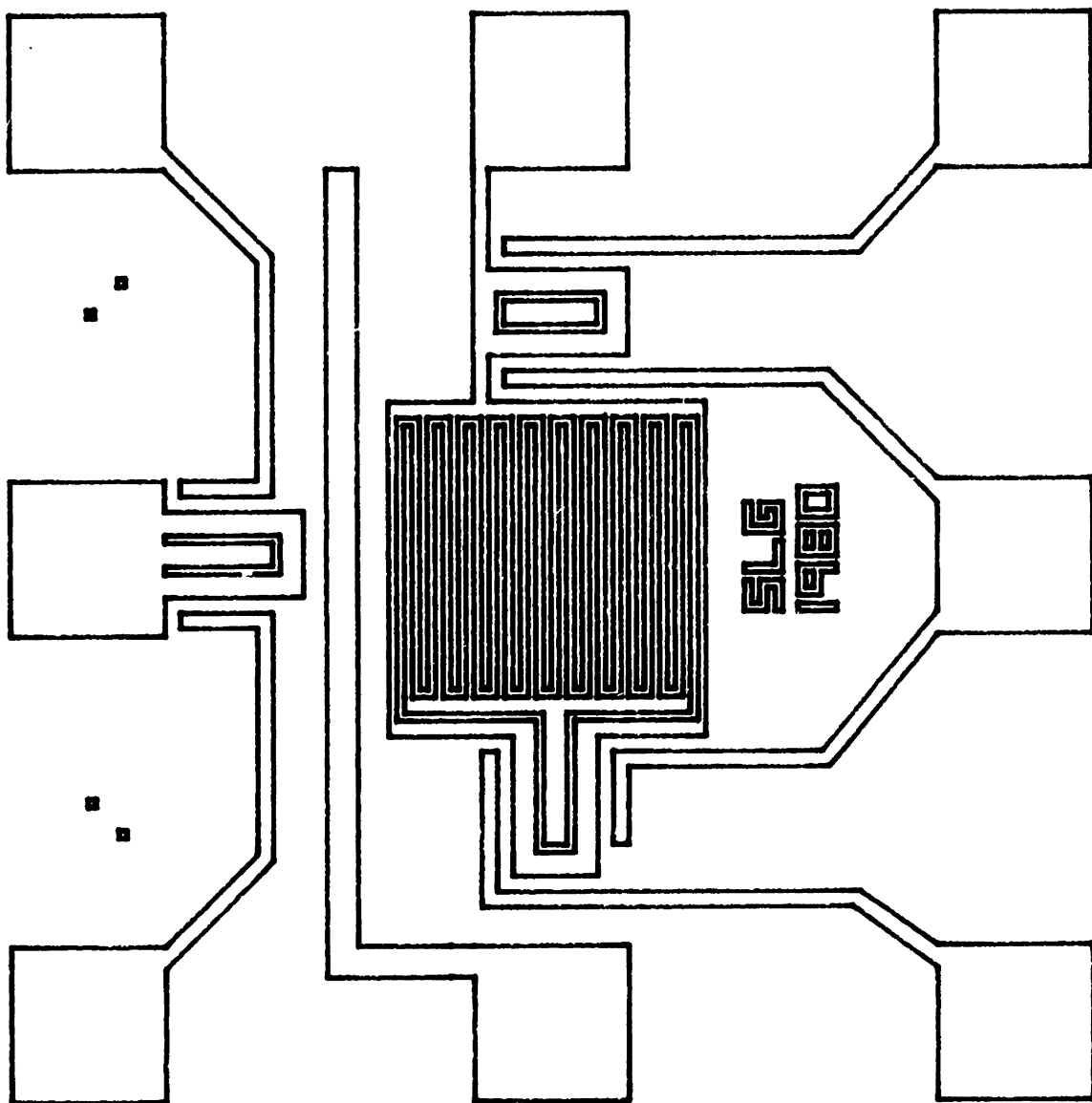


Figure E5) Metallization Mask at Approx. 80x

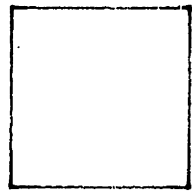
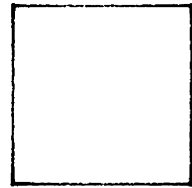
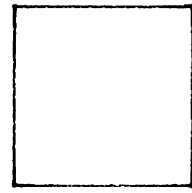
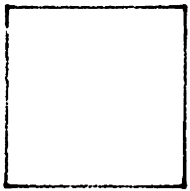
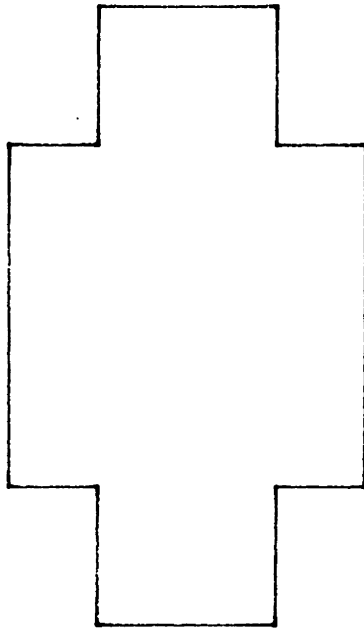
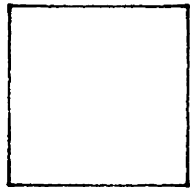
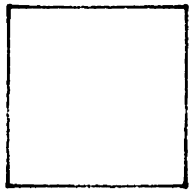
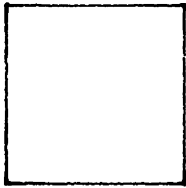
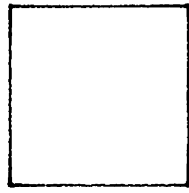


Figure E6) Overglass Mask at Approx. 80x

## APPENDIX F. DESCRIPTION OF THE COMPUTER PROGRAM DEWPNT

To aid in the analysis of the moisture-sensing data, the computer program DEWPNT was written on the MIT Microelectronics Laboratory HP-9835A calculator. The program is written in BASIC, and employs the HP-2631A line printer and the HP-7225A plotter. The user controls the flow of the program with the twelve Special Function Keys, number zero through eleven (SFK#0-11).

Keys SFK#0-2 initiate the data handling routines within the program. Data files managed by the program consist of a collection of data points. Each data point in the file consists of four numbers: 1) dew point, 2) frequency, 3) gain, and 4) phase. SFK#0 is used to create new data files, SFK#1 is used to edit existing files, and SFK#2 is used to load existing files from the cassette tape on which they are stored.

Keys SFK#3-4 are used to create the plots of gain vs. phase. SFK#3 initiates the plot (draws the axes, does the labeling, etc.) and allows the user to plot data in the gain-phase space. Data of selected dew point values, or all data, may be plotted.

SFK#4 is used to plot model curves in the gain-phase space. When this key is pressed the user is asked to enter values for  $C_1/C_t$ , measured high-frequency gain (Mhfg), and  $C_t/C_a$ . The parameter  $\gamma$  (Gamma) is varied logarithmically from negligibly small, to very large. At each Gamma, the value of the transfer function  $V_{FG}/V_{DG}$  is computed using the solution of Appendix B, and subsequently plotted as a smooth curve in gain-phase space.

Pressing SFK#5 initiates the sheet resistance extraction routine.

For each dew point, this routine determines the value of the product  $R_a C_a$  which results in the best fit of model to data. Most recently entered model parameters are used in the extraction, and in addition the user is asked to enter the value of two more quantities: the load capacitor  $C_1$  (in pF), and the reciprocal number of interelectrode squares (Nsq).

The first step in the extraction algorithm is to generate an array of values for gain and phase, calculated from the model with a wide range of values for the parameter Gamma. This step consumes the bulk of the computing time (about 1 minute). Next, the high-frequency gain (Hfg) as predicted by the model is computed. Then, for each value of dew point contained in the data file, the following is done:

- (1) the data file is searched for all data points of the particular dew point, and a new list of these points only is formed;
- (2) the data point list is searched for points that have gain less than -3 dB but greater than Hfg+3 dB. If one or more such points exist, the routine continues with a gain-based extraction. If no such points exist, then a phase-based extraction is employed;
- (3) the value of  $R_a C_a$  (Raca), and the computed value of sheet resistance are printed on the line printer. Sheet resistance is computed from extracted Raca using the relation

$$= R_a C_a \frac{C_t}{C_a} \frac{C_1}{C_t} \frac{Nsq}{C_1} .$$

The gain-based extraction begins by finding the value of Gamma for each of the selected data points. These values of Gamma are determined by searching the array of model points for the two surrounding values of gain, and interpolating. The product Raca is then computed for each data point using the relation

$$\text{Raca} = \text{Gamma}/\omega ,$$

where  $\omega$  is the frequency in radians of the data point.

These values of Raca are then averaged with a weighting factor of Gslope, the slope of the gain curve. In other words, data points that are located near the flat portion of the gain curve receive a small weighting factor, while the data points on the steep portion of the gain curve are heavily weighted. The weighted average of Raca is returned as the extracted value.

When it is determined that the gain of the data points contain little information, a phase-based extraction is attempted. The list of data points is searched for the point with minimum phase. If this minimum phase is greater than -5 degrees, the routine returns a value of Raca=0, to indicate the lack of sufficient information in the data. Otherwise, the value of Raca that best fits the minimum phase data point is determined by the method discussed above, and is returned as the extracted value.

The keys SFK#6-7 are used to generate gain and phase vs. frequency plots. Pressing SFK#6 initiates the plot. When SFK#7 is pressed, the user may have data for selected dew points plotted on the gain and phase vs. frequency axes. Each set of dew point data is accompanied by a smooth curve as calculated from the model using the extracted values of Raca.

Pressing SFK#8 activates a routine that plots sheet resistance vs. dew point and relative humidity. The user must enter the value of R.H. for each dew point.

SFK#9, 10, and 11 are used respectively to modify plotter limits, enter values for the model parameters, and display the SFK menu. Included

with the plotter parameters is Perdec, which sets the number of model points per decade that will be calculated by all routines within the program. Included with the model parameters is Goffset, which is the gain offset of the data, as determined experimentally as a first step in calibration. The SFK menu includes the following information:

1) a short description of the function that each SFK performs, 2) current values of the plotter limits, and 3) current values of the model parameters. The SFK menu is normally redisplayed after returning from each of the subroutines.

Following, is a listing of the computer program DEWPNT.



THE ORIGINAL PRINT ON THE FOLLOWING PAGES IS ILLEGIBLE

```

10 ! PROGRAM TO AID IN THE ANALYSIS OF MOISTURE SENSING DATA
20 OPTION BASE 1
30 SHORT Results(200,4),Dewmat(25),Values(20,3),Devmat(25)
40 SHORT Racsamat(25),Anglemat(200),Gainmat(200),Ramat(25),Prh(25)
50 SHORT Dewmat,Freq,Gain,Phase
60 INTEGER Dewmark(25)
70 COM Fmin,Fmax,Gmin,Gmax,Pmin,Pmax
80 COM Clt,Cxt,Cta,Gta,Gxa,Gla
90 OVERLAP
100 Datalimit=Dewlimit=Goffset=Gmax=Pmax=Gta=Gxa=Gla=0
110 Fmin=.1
120 Fmax=10000
130 Gmin=-70
140 Pmin=-180
150 Clt=1
160 Cxt=.01
170 Cta=20
180 Perdec=10
190 ON KEY #0 GOSUB Newfile
200 ON KEY #1 GOSUB Loaddata
210 ON KEY #2 GOSUB Editloop
220 ON KEY #3 GOSUB Gvspoltinit
230 ON KEY #4 GOSUB Eandn
240 ON KEY #5 GOSUB Extract
250 ON KEY #6 GOSUB Gopltinit
260 ON KEY #7 GOSUB Goolot
270 ON KEY #8 GOSUB Rhooolt
280 ON KEY #9 GOSUB Plotlimits
290 ON KEY #10 GOSUB Getoaram
300 ON KEY #11 GOSUB Menu
310 GOSUB Menu
320 Mainloop: GOTO Mainloop
321 ! SUBROUTINE TO DISPLAY INSTRUCTIONS, CURRENT PARAMETER VALUES
330 Menu: PRINTER IS 16
340 PRINT PAGE,"CFK# ":"FUNCTION"
350 PRINT 0;" CREATE NEW DATA FILE"
360 PRINT 1;" LOAD EXISTING DATA FILE"
370 PRINT 2;" EDIT MOISTURE DATA (THAT EXISTS IN CORE MEMORY)"
380 PRINT 3;" INITIALIZE GAIN VS. PHASE PLOT, AND PLOT MOISTURE DATA"
390 PRINT 4;" ENTER PARAMETER VALUES, AND PLOT MODEL CURVE IN GAIN/PHASE SPACE"
400 PRINT 5;" DO SHEET RESISTANCE EXTRACTION, BASED ON CURRENT PARAMETER VALUES"
410 PRINT 6;" INITIALIZE GAIN AND PHASE VS. FREQUENCY PLOT"
420 PRINT 7;" GAIN AND PHASE VS. FREQUENCY PLOT, MODEL AND DATA, FOR ONE DEWPOINT"
430 PRINT 8;" PLOT OF SHEET RESISTANCE VS. DEW POINT, AND RELATIVE HUMIDITY"
440 PRINT 9;" CHANGE PLOTTER LIMITS"
450 PRINT 10;" ENTER MODEL PARAMETERS"
460 PRINT LIN(1),"LIST OF CURRENT PARAMETER VALUES:"
470 PRINT USING "3X,12A,12A,12A,12A,12A,12A";"CL/CT";"CT/CA";"CX/CT";"GT/GA";"GX/GA";"GL/GA"
480 PRINT USING "5D,2D,4X,5D,2D,4X,D,DDE,4X,D,DDE,4X,D,DDE,4X,D,DDE";Clt,Cta,Cxt,Gta,Gxa,Gla
490 PRINT "LIST OF CURRENT PLOTTER PARAMETERS:"
500 PRINT USING "4X,12A,12A,12A,12A,12A,12A";"GMIN";"GMAX";"PMIN";"PMAX";"FMIN";"FMAX"
510 PRINT USING "8D,12D,12D,12D,4X,D,DDE,4X,D,DDE";Gmin;Gmax;Pmin;Pmax;Fmin;Fmax
520 PRINT "GAIN OFFSET: ";Goffset
530 BEEP
540 RETURN
541 ! SUBROUTINE TO ENTER PLOTTER LIMITS FROM KEYBOARD
550 Plotlimits: INPUT "ENTER FREQUENCY MINIMUM,MAXIMUM FOR PLOTTER",Fmin,Fmax
560 INPUT "ENTER GAIN MINIMUM,MAXIMUM FOR PLOTTER",Gmin,Gmax
570 INPUT "ENTER PHASE MINIMUM,MAXIMUM FOR PLOTTER",Pmin,Pmax
580 INPUT "ENTER NUMBER OF POINTS PER DECADE",Perdec
590 GOSUB Menu
600 RETURN
601 ! SUBROUTINE TO ENTER MODEL PARAMETER VALUES FROM KEYBOARD
610 Getoaram: INPUT "ENTER VALUE OF CL/CT",Clt

```

```

620 INPUT "ENTER VALUE OF CX/CT",Cxt
630 INPUT "ENTER VALUE OF CT/CA",Cta
640 INPUT "ENTER VALUE OF GT/GA",Gta
650 INPUT "ENTER VALUE OF GX/GA",Gxa
660 INPUT "ENTER VALUE OF GL/GA",Gla
670 INPUT "ENTER GAIN OFFSET OF DEVICE",Goffset
680 GOTO Menu
681 ! SUBROUTINE TO INITIALIZE GAIN AND PHASE VS. FREQUENCY PLOT
690 Gopltinit: PLOTTER IS 7,5,"9872A"
700 CSIZE 2.5,.8
710 LOCATE 20,70,15,90
720 SCALE LGT(Fmin),LGT(Fmax),Gmin,Gmax
730 AXES 1,10,0,0
740 LORG 4
750 FOR I=INT(LGT(Fmin)) TO INT(LGT(Fmax))
760 MOVE I,.02*(Gmax-Gmin)
770 LABEL I
780 NEXT I
790 LORG 7
800 MOVE LGT(Fmax),Gmax+.05*(Gmax-Gmin)
810 LABEL "LOG(FREQUENCY)"
820 LORG 8
830 FOR I=INT(Gmin/10) TO INT(Gmax/10)
840 MOVE 0,I*10
850 LABEL I*10
860 NEXT I
870 MOVE .03*(LGT(Fmax)-LGT(Fmin)),Gmin
880 LORG 1
890 LABEL "GAIN (DB)"
900 LOCATE 80,130,15,91
910 SCALE LGT(Fmin),LGT(Fmax),Pmin,Pmax
920 AXES 1,30,0,0
930 LORG 4
940 FOR I=INT(LGT(Fmin)) TO INT(LGT(Fmax))
950 MOVE I,.02*(Pmax-Pmin)
960 LABEL I
970 NEXT I
980 MOVE LGT(Fmax),Pmax+.05*(Pmax-Pmin)
990 LORG 7
1000 LABEL "LOG(FREQUENCY)"
1010 LORG 8
1020 FOR I=INT(Pmin/30) TO INT(Pmax/30)
1030 MOVE 0,I*30
1040 LABEL I*30
1050 NEXT I
1060 LORG 1
1070 MOVE .03*(LGT(Fmax)-LGT(Fmin)),Pmin
1080 LABEL "PHASE"
1090 GOSUB Menu
1100 RETURN
1101 ! SUBROUTINE TO OVERSEE EXTRACTION OF SHEET RESISTANCE
1110 Extract:INPUT "ENTER NUMBER OF SQUARES FOR SHEET RESISTANCE",Nsq
1120 INPUT "ENTER VALUE OF CL (IN PF)",Clpf
1130 GOSUB Tablegen
1140 BEEP
1150 Capf=Clpf/Clt/Cta
1160 PRINTER IS 7,2,WIDTH(160)
1170 FOR Dctr=1 TO Dewlimit
1180 Dewont=Dewmat(Dctr)
1190 GOSUB Getraca
1200 Ramat(Dctr)=10^12*Raca*Nsq/Capf
1210 PRINT USING "K,SDD.D,K,D.DDE,K,D.DDE"; " DEWPOINT: ",Dewont, " RACA: ",Raca, " SHEET RESISTA

```

```

NCE:  ,Ramat(Dctr)
1220 NEXT Dctr
1230 GOSUB Menu
1240 RETURN
1241 ! SUBROUTINE TO PLOT DATA AND MODEL CURVE ON GAIN AND PHASE VS. FREQUENCY AXES
1250 Goplot:PRINTER IS 16
1260 PRINT PAGE,"J.D.", "DEW POINT"
1270 FOR I=1 TO Dewlimit
1280 PRINT I,Dewmat(I)
1290 NEXT I
1300 Dewnum=0
1310 INPUT "ENTER DEW POINT NUMBER TO BE PLOTTED, OR HIT CONTINUE",Dewnum
1320 IF Dewnum=0 THEN GOTO Menu
1330 INPUT "ENTER TYPE FOR DATA PLOT (+,X,O,B,D)",T$
1340 Glast=1/(Ramat(Dewnum)/Nsq*Capf/1E12*2*PI*Fmin)
1350 Gfirst=1/(Ramat(Dewnum)/Nsa*Capf/1E12*2*PI*Fmax)
1360 Mult=10^(1/Perdec)
1370 CALL Modelplot(Gainmat(*),Anglemat(*),Npoints,Gfirst,Glast,Mult)
1380 LOCATE 20,70,15,90
1390 SCALE LGT(Fmin),LGT(Fmax),Gain,Gmax
1400 PENUP
1410 W=2*PI*Fmax
1420 FOR I=1 TO Npoints
1430 PLOT LGT(W/(2*PI)),Gainmat(I)
1440 W=W/Mult
1450 NEXT I
1460 PENUP
1470 W=2*PI*Fmax
1480 LOCATE 20,130,15,90
1490 SCALE LGT(Fmin),LGT(Fmax),Pmin,Pmax
1500 Lastangle=0
1510 FOR I=1 TO Npoints
1520 PLOT LGT(W/(2*PI)),Anglemat(I)
1530 W=W/Mult
1540 NEXT I
1550 PENUP
1560 Dewont=Dewmat(Dewnum)
1570 GOSUB Gpdataplot
1580 GOTO Goplot
1581 ! SUBROUTINE TO PLOT SHEET RESISTANCE VS. DEW POINT AND RELATIVE HUMIDITY
1590 Rhoplot:PRINTER IS 7,2,WIDTH(160)
1600 PRINT LIN(2)
1610 PLOTTER IS 7,5,"9872A"
1620 LOCATE 20,70,15,85
1630 Ramin=1E80
1640 Ramax=0
1650 Dewmin=100
1660 Dewmax=-100
1670 FOR I=1 TO Dewlimit
1680 IF (Ramat(I)<Ramax) AND (Ramat(I)<1E20) THEN Ramax=Ramat(I)
1690 IF (Ramat(I)<Ramin) AND (Ramat(I)<>0) THEN Ramin=Ramat(I)
1700 IF Dewmat(I)>Dewmax THEN Dewmax=Dewmat(I)
1710 IF Dewmat(I)<Dewmin THEN Dewmin=Dewmat(I)
1720 NEXT I
1730 Ymin=INT(LGT(Ramin))
1740 Ymax=1+INT(LGT(Ramax))
1750 Xmin=5*INT(Dewmin/5)
1760 Xmax=5*(1+INT(Dewmax/5))
1770 Xint=.01*(Xmax-Xmin)
1780 Yint=.01*(Ymax-Ymin)
1790 SCALE Xmin,Xmax,Ymin,Ymax
1800 AXES 5,1,0,Ymin
1810 MOVE 0,Ymax+.02*(Ymax-Ymin)

```

```

1820 LOG 1
1830 LABEL "LOG(RHO)"
1840 MOVE Xmax,Ymin-.06*(Ymax-Ymin)
1850 LOG 9
1860 LABEL "DEW POINT"
1870 FOR I=Ymin+1 TO Ymax
1880 MOVE 0,I
1890 LOG 8
1900 LABEL 1
1910 NEXT I
1920 FOR I=INT(Xmin/5) TO INT(Xmax/5)
1930 MOVE 5*I,Ymin-.02*(Ymax-Ymin)
1940 LOG 6
1950 LABEL 5*I
1960 NEXT I
1970 PENUP
1980 FOR I=1 TO Dewlimit
1990 IF (Rammat(1)=0) OR (Rammat(I))>Ramax) THEN GOTO 2050
2000 MOVE Dewmat(I)-Xint,LGT(Rammat(I))
2010 DRAW Dewmat(I)+Xint,LGT(Rammat(I))
2020 MOVE Dewmat(I),LGT(Rammat(I))-Yint
2030 DRAW Dewmat(I),LGT(Rammat(I))+Yint
2040 PENUP
2050 NEXT I
2060 PENUP
2070 LOCATE 80,130,15,85
2080 SCALE 0,100,Ymin,Ymax
2090 AXES 10,1,0,Ymin
2100 MOVE 0,Ymax+.02*(Ymax-Ymin)
2110 LOG 1
2120 LABEL "LOG(RHO)"
2130 MOVE 100,Ymin-.06*(Ymax-Ymin)
2140 LOG 9
2150 LABEL "% RH"
2160 FOR I=0 TO 100 STEP 20
2170 MOVE I,Ymin-.02*(Ymax-Ymin)
2180 LOG 6
2190 LABEL I
2200 NEXT I
2210 FOR I=Ymin TO Ymax
2220 MOVE 0,I
2230 LOG 8
2240 LABEL I
2250 NEXT I
2260 FOR I=1 TO Dewlimit
2270 PRINTER IS 16
2280 PRINT PAGE,LIN(15),"ENTER RELATIVE HUMIDITY FOR DEWPOINT ":Dewmat(I)
2290 BEEP
2300 INPUT "ENTER % RH",Prh(I)
2310 NEXT I
2320 PRINTER IS 7,2,WIDTH(160)
2330 PRINT LIN(2),"DEW POINT","RELATIVE HUMIDITY"
2340 FOR I=1 TO Dewlimit
2350 PRINT Dewmat(I),Prh(I)
2360 NEXT I
2370 PENUP
2380 FOR I=1 TO Dewlimit
2390 IF (Rammat(I)=0) OR (Rammat(I))>Ramax) THEN GOTO 2450
2400 MOVE Prh(I)-1,LGT(Rammat(I))
2410 DRAW Prh(I)+1,LGT(Rammat(I))

```

```

2420 MOVE Prh(I),LGT(Ramat(I))-Yint
2430 DRAW Prh(I),LGT(Ramat(I))+Yint
2440 PENUP
2450 NEXT I
2460 PENUP
2470 GOSUB Menu
2480 RETURN
2490 Dewfound:Dewnum=Dewnum+1
2500 FOR I=1 TO 3
2510 Values(Dewnum,I)=Results(Datactr,I+1)
2520 NEXT I
2530 RETURN
2540 Lsq:N=N+1
2550 Currentx=LGT(Values(Dewctr,1))
2560 X1=X1+Currentx
2570 Y1=Y1+Values(Dewctr,Ytype)
2580 X2=X2+Currentx*Currentx
2590 Z=Z+Values(Dewctr,Ytype)*Currentx
2600 RETURN
2601 ! SUBROUTINE TO EXTRACT RaCa FOR A GIVEN DEWPOINT
2610 Getraca:Dewnum=0
2620 Hfalpha=SQR(Cta)
2630 CALL Cosh(Hfalpha,0,Cr,Ci)
2640 CALL Sinh(Hfalpha,0,Sr,Si)
2650 Hfg=20*LGT((1+Cxt*Hfalpha*Sr)/(Cr+(Clt+Cxt)*Hfalpha*Sr))
2660 FOR Datactr=1 TO Datalimit
2670 IF Results(Datactr,1)=Dewont THEN GOSUB Dewfound
2680 NEXT Datactr
2690 FOR Dewctr=1 TO Dewnum
2700 IF (Values(Dewctr,2)-Goffset(-3) AND (Values(Dewctr,2)-Goffset)Hfg+3) THEN GOTO Gainextract
2710 NEXT Dewctr
2711 ! PHASE-BASED EXTRACTION ROUTINE
2720 Phaseextract:Pminimum=1E10
2730 FOR Dewctr=1 TO Dewnum
2740 IF Values(Dewctr,3)<Pminimum THEN GOSUB Pminfound
2750 NEXT Dewctr
2760 Raca=0
2770 IF Pminimum<-5 THEN RETURN
2780 IF (Values(Marker,2)-Goffset(-3) OR (Anglemat(1)<(-180) THEN GOTO Highend
2790 Lowend:FOR I=1 TO Npoints
2800 IF Anglemat(I)<Pminimum THEN GOTO Lowfound
2810 NEXT I
2820 Lowfound:Imark=I-(Values(Marker,3)-Anglemat(I))/(Anglemat(I-1)-Anglemat(I))
2830 Gamma=Gfirst*10^((Imark-1)/Perdec)
2840 Raca=1/(Gamma*Values(Marker,1)*2*PI)
2850 RETURN
2860 Highend:FOR I=Npoints TO 1 STEP -1
2870 IF Anglemat(I)<Pminimum THEN GOTO Highfound
2880 NEXT I
2890 Highfound:Imark=I+(Values(Marker,3)-Anglemat(I))/(Anglemat(I+1)-Anglemat(I))
2900 Gamma=Gfirst*10^((Imark-1)/Perdec)
2910 Raca=1/(Gamma*Values(Marker,1)*2*PI)
2920 RETURN
2921 ! GAIN-BASED EXTRACTION ROUTINE
2930 Gainextract:N=Racasum=0
2940 FOR Dewctr=1 TO Dewnum
2950 IF (Values(Dewctr,2)-Goffset(-3) OR (Values(Dewctr,2)-Goffset)Hfg+3) THEN Gainskip
2960 FOR I=Npoints TO 1 STEP -1
2970 IF Gainmat(I)<(Values(Dewctr,2)-Goffset) THEN GOTO Gainfound
2980 NEXT I
2990 Gainfound:Imark=I+(Values(Dewctr,2)-Gainmat(I))/(Gainmat(I+1)-Gainmat(I))
3000 Gamma=Gfirst*10^((Imark-1)/Perdec)
3010 N=N+(Gainmat(I+1)-Gainmat(I))

```

```

3020 Racasum=Racasum+LGT(1/(Gamma*Values(Dewctr,1)))*(Gainmat(I+1)-Gainmat(I))
3030 Gainskip:NEXT Dewctr
3040 Racasum=Racasum/N
3050 Raca=10^Racasum/(2*PI)
3060 RETURN
3070 Pminfound:Marker=Dewctr
3080 Pminimum=Values(Dewctr,3)
3090 RETURN
3091 ! SUBROUTINE TO PLOT DATA ON GAIN AND PHASE VS. FREQUENCY AXES
3100 Gpdataplot:PENUP
3110 Fint=.01*(LGT(Fmax)-LGT(Fmin))
3120 Gint=.01*(Gmax-Gmin)*2/3
3121 Pint=.01*(Pmax-Pmin)*2/3
3140 FOR Datactr=1 TO Datalimit
3150 IF Results(Datactr,1())Dewont THEN GOTO Sko
3160 Gain=Results(Datactr,3)-Goffset
3170 Phase=Results(Datactr,4)
3180 Freq=Results(Datactr,2)
3190 LOCATE 20,70,15,90
3210 SCALE LGT(Fmin),LGT(Fmax),Gmin,Gmax
3210 CALL Dataplot(LGT(Freq),Gain,Fint,Gint,T$)
3220 LOCATE 80,130,15,90
3230 SCALE LGT(Fmin),LGT(Fmax),Pmin,Pmax
3240 CALL Dataplot(LGT(Freq),Phase,Fint,Pint,T$)
3250 Skp:NEXT Datactr
3260 RETURN
3261 ! SUBROUTINE TO ENTER MODEL PARAMTER VALUES, AS A PREFACE TO PLOTTING GAIN/PHASE CURVE
3270 Eandn:Mhfg=1E10
3280 INPUT "ENTER MEASURED GAIN AT HIGH FREQUENCIES (DB) (HIT CONTINUE TO EXIT)",Mhfg
3290 IF Mhfg=1E10 THEN GOTO Menu
3300 INPUT "ENTER CT/CA RATIO",Cta
3310 INPUT "ENTER CL/CT RATIO",Clt
3320 INPUT "ENTER GT/GA RATIO",Gta
3330 INPUT "ENTER GX/GA RATIO",Gxa
3340 INPUT "ENTER GL/GA RATIO",Gla
3360 Cxt=FNGetext(Mhfg,Clt,Cta)
3370 PRINTER IS 16
3380 PRINT LIN(2)
3390 PRINT USING "#,K";" "
3400 PRINT USING "12A,12A,12A,12A,12A,12A";"CL/CT","CT/CA","CX/CT","GT/GA","GX/GA","GL/GA"
3410 PRINT USING "9D,2D,9D,2D,4X,D.DDE,4X,D.DDE,4X,D.DDE,4X,D.DDE";Clt,Cta,Cxt,Gta,Gxa,Gla
3420 GOTO Gvspmodplot
3421 ! SUBROUTINE TO INITIALIZE GAIN VS. PHASE PLOT
3430 Gvsppltinit:PLOTTER IS 7,5,"9872A"
3440 CSIZE 2.5,.8
3450 LOCATE 20,130,15,85
3460 SCALE Gmin,Gmax,Pmin,Pmax
3470 AXES 5,30,0,Pmax
3480 AXES 5,30,Gmin,Pmin
3490 LORG 4
3500 FOR I=INT(Gmin/10) TO 0
3510 MOVE 10*I,Pmax+.01*(Pmax-Pmin)
3520 LABEL 10*I
3530 NEXT I
3540 LORG 7
3550 MOVE -1,Pmax+.04*(Pmax-Pmin)
3560 LABEL "GAIN (DB)"
3570 LORG 8
3580 FOR I=INT(Pmin/30) TO INT(Pmax/30)
3590 MOVE Gmin,30*I
3600 LABEL 30*I
3610 NEXT I

```

```

3620 MOVE .97*Gain,Pmin-.02*(Pmax-Pmin)
3630 LORG 3
3640 LABEL "PHASE"
3650 GOTO Gvsodatanplot
3651 ! SUBROUTINE TO PLOT MODEL CURVE IN GAIN/PHASE SPACE
3660 Gvsmodplot:PENUP
3670 LOCATE 20,130,15,85
3680 SCALE Gmin,Gmax,Pmin,Pmax
3690 GOSUB Tablenen
3700 FOR I=i TO Npoints
3710 PLOT Gainmat(I),Anglemat(I)
3720 NEXT I
3730 PENUP
3740 GOTO Eandm
3741 ! SUBROUTINE TO PLOT DATA IN GAIN/PHASE SPACE
3750 Gvsodatanplot:PENUP
3760 LOCATE 20,130,15,85
3770 SCALE Gmin,Gmax,Pmin,Pmax
3790 Pint=.01*(Pmax-Pmin)
3791 Gint=.01*(Gmax-Gmin)*7/11
3810 GOSUB Getdewlimit
3820 PRINT PAGE,"LIST OF DEW POINT VALUES CONTAINED IN THIS FILE:"
3830 PRINT LIN(i),"I.D.", "DEW POINT"
3840 FOR I=i TO Dewlimit
3850 PRINT I,Dewmat(I)
3860 NEXT I
3870 Gvsploo:Dewctr=1E10
3880 INPUT "ENTER I.D. OF DATA TO BE PLOTTED, 0 FOR ALL, OR CONTINUE TO EXIT",Dewctr
3890 IF Dewctr=1E10 THEN GOTO Menu
3900 INPUT "ENTER TYPE FOR DATA PLOT (+,X,D,B,D)",T$
3910 FOR Datactr=1 TO Datalimit
3920 IF Dewctr=0 THEN GOTO 3931
3930 IF Results(Datactr,1)(>)Dewmat(Dewctr) THEN GOTO 3950
3931 Gain=Results(Datactr,3)-Goffset
3932 Phase=Results(Datactr,4)
3940 CALL Dataplot(Gain,Phase,Gint,Pint,T$)
3950 NEXT Datactr
3960 PENUP
3970 GOTO Gvsploo
3971 ! SUBROUTINE TO GENERATE AN ARRAY OF MODEL POINTS
3980 Tablenen:Mult=10^(1/Perdec)
3990 Glast=100*Cta
4000 IF Gta(>0) THEN Glast=100*MAX(i,Cta/Gta)
4010 Gfirst=.01
4020 IF Gta(>0) THEN G=.01*MIN(i,Cta/Gta)
4030 CALL Modelplot(Gainmat(*),Anglemat(*),Npoints,Gfirst,Glast,Mult)
4040 RETURN
4041 ! SUBROUTINE TO GENERATE LIST OF DEW POINTS VALUES CONTAINED IN A DATA FILE
4050 Getdewlimit:Dewlimit=0
4060 FOR Datactr=1 TO Datalimit
4070 FOR Doctr=1 TO Dewlimit
4080 IF Results(Datactr,1)=Dewmat(Doctr) THEN Dewskip
4090 NEXT Doctr
4100 Dewlimit=Dewlimit+1
4110 Dewmat(Dewlimit)=Results(Datactr,1)
4120 Dewskip:Datactr=Datactr+1
4130 NEXT Datactr
4140 RETURN
4141 ! SUBROUTINE TO PERFORM EDITING OF A DATA FILE
4150 Editloop:PRINT PAGE,"LIST OF DEW POINT VALUES CONTAINED IN THIS FILE:",LIN(2)
4160 GOSUB Getdewlimit
4170 PRINT "I.D.", "DEW POINT"
4180 FOR Dewctr=1 TO Dewlimit
4190 PRINT Dewctr,Dewmat(Dewctr)
4200 NEXT Dewctr
4210 Dewctr=1E10

```



```

4220 PRINT LIN(2),"ENTER DEW POINT I.D. TO SEE IT'S DATA LIST"
4230 PRINT LIN(1),"HIT CONTINUE TO ADD NEW DEW POINT, OR TO END EDITOR"
4240 INPUT " ",Dewctr
4250 IF Dewctr<>1E10 THEN GOTO Showdew
4260 Dewpnt=1E10
4270 INPUT "ENTER NEW DEW POINT VALUE, OR HIT CONTINUE TO END EDITING",Dewpnt
4280 IF Dewpnt=1E10 THEN GOTO Preclose
4290 GOTO Newdewpoint
4300 Showdew:PRINT PAGE,"DEW POINT: ";Dewmat(Dewctr),LIN(1)
4310 PRINT "I.D.", "FREQUENCY", "GAIN", "PHASE"
4320 Dewnum=0
4330 FOR Datactr=1 TO Datalimit
4340 IF Results(Datactr,1)=Dewmat(Dewctr) THEN GOSUB Dewfound2
4350 NEXT Datactr
4360 IF Dewnum=0 THEN GOTO Editloop
4370 PRINT LIN(1),"TO ADD DATA AT THIS DEWPOINT, ENTER THE NEW FREQUENCY"
4380 PRINT "TO DELETE A ROW OF DATA, ENTER IT'S I.D. NUMBER"
4390 PRINT "TO GOTO NEW DEW POINT, HIT CONTINUE"
4400 Freq=1E10
4410 INPUT " ",Freq
4420 IF Freq=1E10 THEN GOTO Editloop
4430 Gain=1E10
4440 INPUT "ENTER GAIN,PHASE (IF DELETING DATA HIT CONTINUE)",Gain,Phase
4450 IF Gain=1E10 THEN GOTO Dreedata
4460 Datalimit=Datalimit+1
4470 Results(Datalimit,1)=Dewmat(Dewctr)
4480 Results(Datalimit,2)=Freq
4490 Results(Datalimit,3)=Gain
4500 Results(Datalimit,4)=Phase
4510 GOTO Showdew
4520 Newdewpoint:Dewctr=Dewlimit=Dewlimit+1
4530 Dewmat(Dewlimit)=Dewpnt
4540 GOTO 4370
4550 Dreedata:Datalimit=Datalimit-1
4560 FOR Datactr=Location(Freq) TO Datalimit
4570 FOR I=j TO 4
4580 Results(Datactr,I)=Results(Datactr+1,I)
4590 NEXT I
4600 NEXT Datactr
4610 GOTO Showdew
4620 Dewfound2:Dewnum=Dewnum+1
4630 Location(Dewnum)=Datactr
4640 PRINT Dewnum,Results(Datactr,2),Results(Datactr,3),Results(Datactr,4)
4650 RETURN
4651 ! SUBROUTINE TO CREATE A NEW DATA FILE
4660 Newfile:Datalimit=0
4670 INPUT "ENTER GAIN OFFSET FOR THIS FILE",Goffset
4680 Newdew: PRINT PAGE
4690 Dewpnt=1E10
4700 INPUT "ENTER DEW POINT (HIT CONTINUE TO END DATA INPUT)",Dewpnt
4710 IF Dewpnt=1E10 THEN GOTO Preclose
4720 PRINT PAGE,LIN(12),"DEW POINT IS: ";Dewpnt
4730 Writeloop:Freq=0
4740 INPUT "ENTER FREQUENCY,GAIN,PHASE (HIT CONTINUE TO CHANGE DEW POINT)",Freq,Gain,Phase
4750 IF Freq=0 THEN GOTO Newdew
4760 Datalimit=Datalimit+1
4770 Results(Datalimit,1)=Dewpnt
4780 Results(Datalimit,2)=Freq
4790 Results(Datalimit,3)=Gain
4800 Results(Datalimit,4)=Phase
4810 GOTO Writeloop

```

```

4820 Preclose:GOSUB Getdewlimit
4830 Answer$="Y"
4840 INPUT "DO YOU WISH TO HAVE THIS FILE WRITTEN ONTO THE TAPE? (Y/N)",Answer$
4850 IF Answer$="N" THEN GOTO Menu
4860 GOTO Close
4861 ! SUBROUTINE TO LOAD EXISTING DATA FILE
4870 Loaddata:INPUT "ENTER INPUT DATA FILE NAME",File$
4880 INPUT "ENTER GAIN OFFSET FOR THIS FILE",Goffset
4890 Datalimit=0
4900 ASSIGN #1 TO File$
4910 ON END #1 GOTO Endload
4920 Dataloop:Datalimit=Datalimit+1
4930 FOR I=1 TO 4
4940 READ #1;Results(Datalimit,I)
4950 NEXT I
4960 GOTO Dataloop
4970 Endload:Datalimit=Datalimit-1
4980 ASSIGN #1 TO *
4990 GOSUB Getdewlimit
5000 GOSUB Menu
5010 RETURN
5020 Close:INPUT "ENTER OUTPUT FILE NAME",File$
5030 CREATE File$,1+INT(Datalimit/16)
5040 ASSIGN #1 TO File$
5050 FOR Datactr=i TO Datalimit
5060 FOR I=1 TO 4
5070 PRINT #1;Results(Datactr,I)
5080 NEXT I
5090 NEXT Datactr
5100 ASSIGN #1 TO *
5110 GOSUB Menu
5120 RETURN
5121 ! SUBPROGRAM TO MULTIPLY TWO COMPLEX NUMBERS
5130 SUB Multrans(A1,A2,B1,B2,C1,C2)
5140 C1=A1*B1-A2*B2
5150 C2=A2*B1+A1*B2
5160 SUBEND
5161 ! SUBPROGRAM TO DIVIDE COMPLEX NUMBERS
5170 SUB Divtrans(A1,A2,B1,B2,C1,C2)
5180 CALL Multrans(A1,A2,B1,-1*B2,C1,C2)
5190 Bsq=B1*B1+B2*B2
5200 C1=C1/Bsq
5210 C2=C2/Bsq
5220 SUBEND
5221 ! SUBPROGRAM TO COMPUTE HYPERBOLIC SINE OF A COMPLEX NUMBER
5230 SUB Sinh(A,B,C,D)
5240 RAD
5250 Expa=EXP(A)
5260 C=COS(B)*(Expa-1/Expa)/2
5270 D=SIN(B)*(Expa+1/Expa)/2
5280 SUBEND
5281 ! SUBPROGRAM TO COMPUTE HYPERBOLIC COSINE OF A COMPLEX NUMBER
5290 SUB Cosh(A,B,C,D)
5300 RAD
5310 Expa=EXP(A)
5320 C=COS(B)*(Expa+1/Expa)/2
5330 D=SIN(B)*(Expa-1/Expa)/2
5340 SUBEND
5341 ! SUBPROGRAM TO TAKE SQUARE ROOT OF A COMPLEX NUMBER
5350 SUB Cmplxsqr(A,B,C,D)
5360 Mag=SQR(A*A+B*B)
5370 Ang=ATN(B/A)
5380 Ang=Ang/2
5390 Mag=SQR(Mag)
5400 C=Mag*COS(Ang)
5410 D=Mag*SIN(Ang)

```

```

5420 SUREND
5421 ! SUBPROGRAM TO COMPUTE VALUE OF MODEL TRANSFER FUNCTION
5430 SUB Model(Gain,Phase,Gamma)
5440 COM Fmin,Fmax,Gmin,Gmax,Pmin,Pmax
5450 COM Clt,Cxt,Cta,Gta,Gxa,Gla
5460 CALL Divtrans(Gamma*Gta,Cta,Gamma,i,A2r,A2i)
5470 CALL Cmplxsqr(A2r,A2i,Ar,Ai)
5480 CALL Cosh(Ar,Ai,Cr,Ci)
5490 CALL Sinh(Ar,Ai,Sr,Si)
5500 CALL Multrans(Sr,Si,Ar,Ai,Spr,Spi)
5510 CALL Divtrans(Gamma*Gxa/Cta,Cxt,Gamma*Gta/Cta,i,Yxtr,Yxti)
5520 CALL Divtrans(Gamma*Gla/Cta,Clc,Gamma*Gta/Cta,i,Yltr,Ylti)
5530 CALL Multrans(Yxtr,Yxti,Spr,Spi,Npr,Npi)
5540 CALL Multrans(Yxtr+Yltr,Yxti+Ylti,Spr,Spi,Dpr,Dpi)
5550 CALL Divtrans(1+Npr,Npi,Cr+Dpr,Ci+Dpi,Re,Im)
5560 DEG
5570 Phase=ATN(Im/Re)
5580 IF Re<0 THEN Phase=Phase-180
5590 Gain=20*LGT(SQR(Re*Re+Im*Im))
5600 SUBEND
5601 ! SUBPROGRAM TO GENERATE ARRAY OF MODEL POINTS
5610 SUB Modelplot(SHORT Gainmat(*),Anglemat(*),REAL Npoints,Gfirst,Glast,Mult)
5620 Gamma=Gfirst
5630 Lastangle=0
5640 Npoints=0
5650 Repeat:Npoints=Npoints+1
5660 CALL Model(Gain,Thisangle,Gamma)
5670 Gainmat(Npoints)=Gain
5680 Anglemat(Npoints)=Thisangle
5690 Gamma=Gamma*Mult
5700 IF Gamma<Glast THEN GOTO Repeat
5710 Lastangle=0
5720 FOR I=Npoints TO 1 STEP -1
5730 Thisangle=Anglemat(I)
5740 Back:IF ABS(Thisangle-Lastangle)>180 THEN GOTO Anglecorrect
5750 Anglemat(I)=Thisangle
5760 Lastangle=Thisangle
5770 NEXT I
5780 SUBEXIT
5790 Anglecorrect:IF Thisangle>Lastangle THEN GOTO Anglefix
5800 Thisangle=Thisangle+360
5810 GOTO Back
5820 Anglefix:Thisangle=Thisangle-360
5830 GOTO Back
5840 SUREND
5841 ! FUNCTION TO COMPUTE Ct/Ca FROM HIGH-FREQUENCY GAIN AND Cl/Ct (ASSUMES Cx/Ct IS ZERO)
5850 DEF FNGctct(Hfg,Clc)
5860 X=1
5870 L1:Xlast=X
5880 X=LOG(10)*(-1*Hfg/20+LGT(2)-LGT(1+Clc*X))
5890 IF ABS((X-Xlast)/X)>.01 THEN GOTO L1
5900 Z=EXP(X)
5910 Ctaloo2:Zlast=Z
5920 A=1+Clc*LOG(Z)
5930 B=-2*10^(-1*Hfg/20)
5940 C=1-Clc*LOG(Z)
5950 Z=(-1*B+SQR(B*B-4*A*C))/(2*A)
5960 IF ABS((Z-Zlast)/Z)>.01 THEN GOTO Ctaloo2
5970 RETURN LOG(Z)^2
5971 ! SUBPROGRAM TO COMPUTE Cx/Ct FROM HIGH-FREQUENCY GAIN, Ct/Ct, AND Ct/Ca
5980 DEF FNGctct(Hfg,Clc,Cta)
5990 Alpha=SQR(Cta)
6000 G=10^(Hfg/20)
6010 CALL Sinh(Alpha,0,S,Xx)

```

```

6020 CALL Cash(Alpha,0,C,Xx)
6030 RETURN (G*(C+Alpha*Clr*S)-1)/((1-G)*Alpha*S)
6031 ! SUBPROGRAM TO PLOT DATA USING VARIOUS SYMBOLS
6040 SUB Dataplot(SHORT X,Y,REAL Deltax,Deltay,T$)
6050 IF T$="+" THEN Plus
6060 IF T$="X" THEN Cross
6070 IF T$="O" THEN Circle
6080 IF T$="B" THEN Box
6090 IF T$="D" THEN Del
6100 SUBEXIT
6110 Plus:MOVE X-Deltax,Y
6120 DRAW X+Deltax,Y
6130 MOVE X,Y-Deltay
6140 DRAW X,Y+Deltay
6150 PENUP
6160 SUBEXIT
6170 Cross:MOVE X-Deltax,Y-Deltay
6180 DRAW X+Deltax,Y+Deltay
6190 MOVE X-Deltax,Y+Deltay
6200 DRAW X+Deltax,Y-Deltay
6210 PENUP
6220 SUBEXIT
6230 Circle:DEG
6240 PENUP
6250 FOR Angle=0 TO 360 STEP 30
6260 PLOT X+Deltax*SIN(Angle),Y+Deltay*COS(Angle)
6270 NEXT Angle
6280 PENUP
6290 SUBEXIT
6300 Box:MOVE X+Deltax,Y+Deltay
6310 DRAW X-Deltax,Y+Deltay
6320 DRAW X-Deltax,Y-Deltay
6330 DRAW X+Deltax,Y-Deltay
6340 DRAW X+Deltax,Y+Deltay
6350 PENUP
6360 SUBEXIT
6370 Del:PENUP
6380 DEG
6390 FOR Angle=0 TO 360 STEP 120
6400 PLOT X+1.5*Deltax*SIN(Angle),Y+1.5*Deltay*COS(Angle)
6410 NEXT Angle
6420 PENUP
6430 SUBEND

```

## APPENDIX G. DESCRIPTION OF FLIP-CHIP PACKAGE

In conjunction with the resin cure and ion sensing studies, and with the aid of D. Fulginitti of Draper Laboratory, a flip-chip packaging scheme has been designed. Packaging of devices is being currently undertaken at Draper.

The flip-chip package offers two advantages over the TO-5 header. The first is the elimination of wire bonds. The second is the conversion of the shape of the package to that of a thin sliver. Both of these make the device more suitable for insertion into a vat of hardening resin.

The heart of the package is a 20 mil thick ceramic piece of 96% Alumina, onto which a pattern of conductor has been formed by the silk screening technique (Figure G1-3). The ceramic piece has eight .025" diameter holes surrounding a single .05" hole in the center. Platinum-gold conductor is patterned around each of the outer holes and leading toward the center hole. A layer of solder is screened over each of the outer pads, and onto the tips of the wires leading toward the center hole.

Devices are prepared for the package with the addition of two steps: 1) wafers are coated with a protective overglass (probably polyimide), and patterned using the overglass mask. Only the bonding pads and the lock and key on the device remain unprotected; 2) gold balls are bonded to each of the eight bonding pads on the device using a gold ball bonder. Tails are trimmed to be as short as possible.

A die is mounted by turning it upside down, and aligning its bonding pads to the tips of the conductor surrounding the center hole on

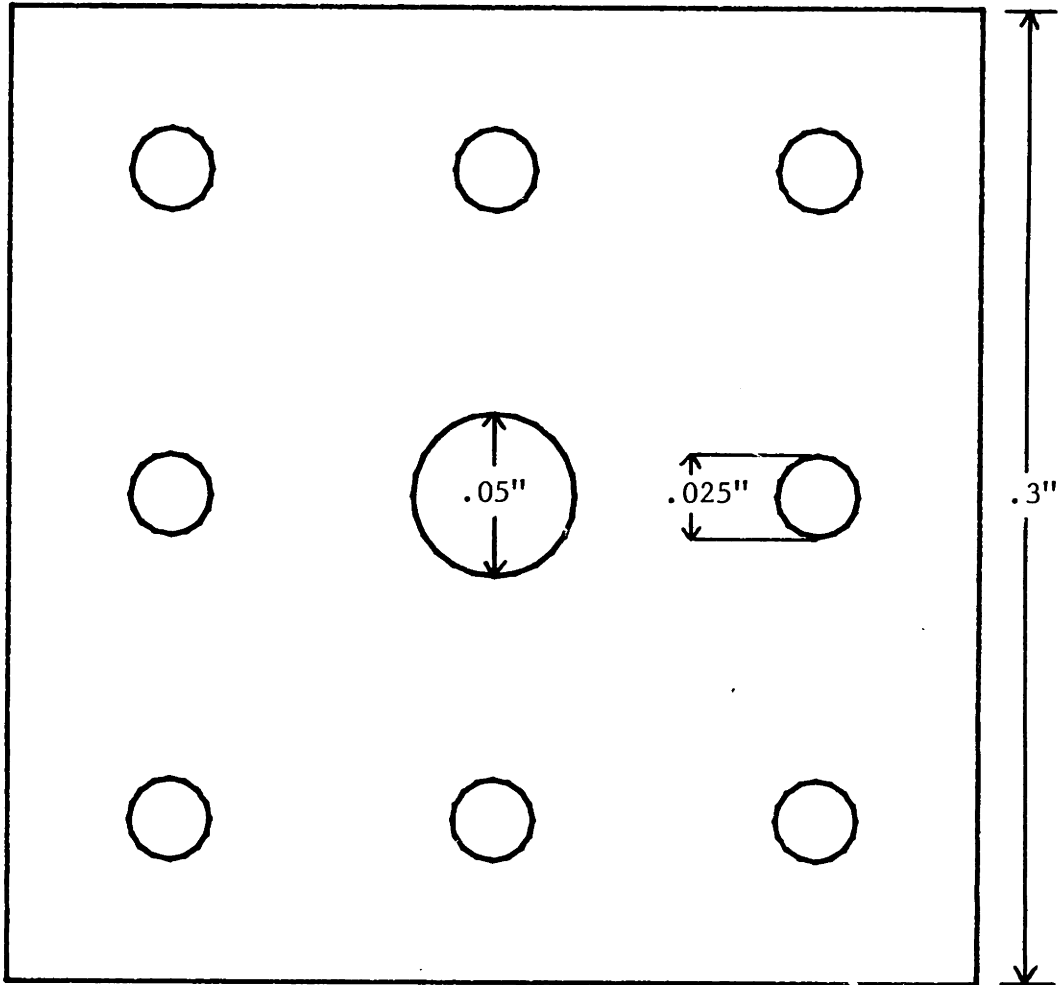


Figure G1) Ceramic Piece for Flip-Chip Package

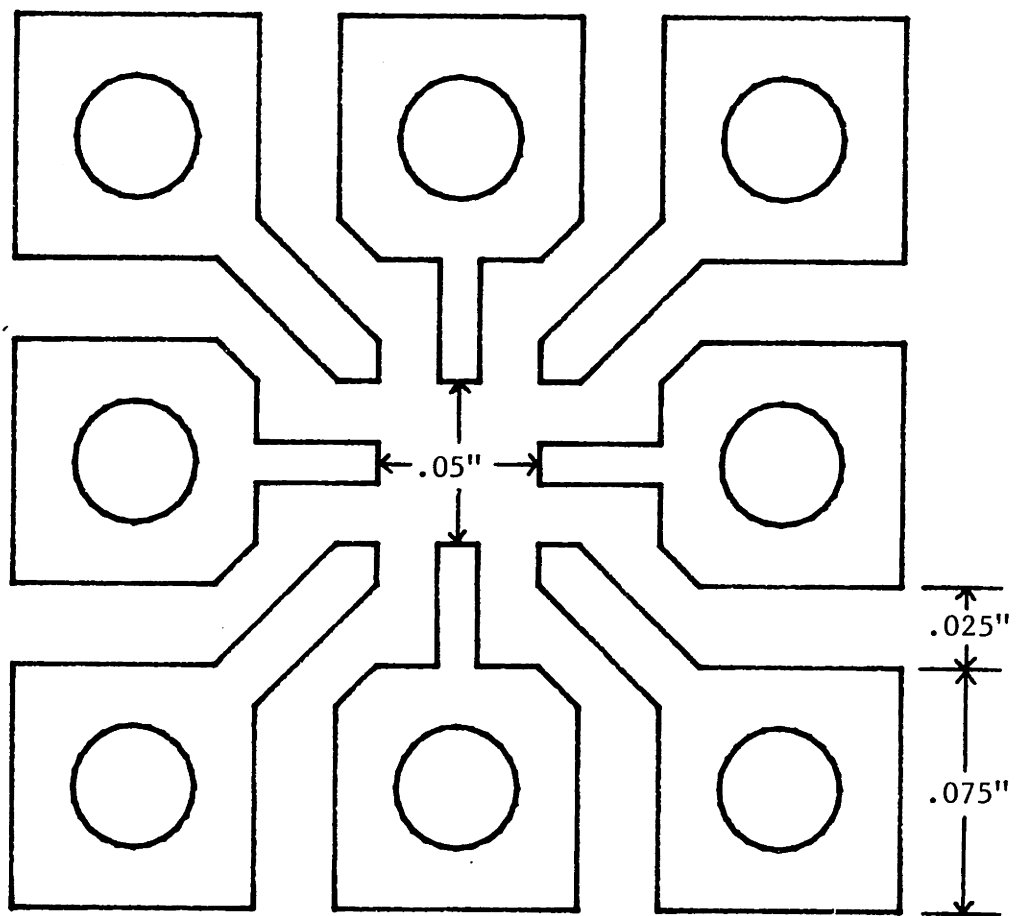


Figure G2) Silk Screen Layout of Conductive Pattern for Flip-Chip Package

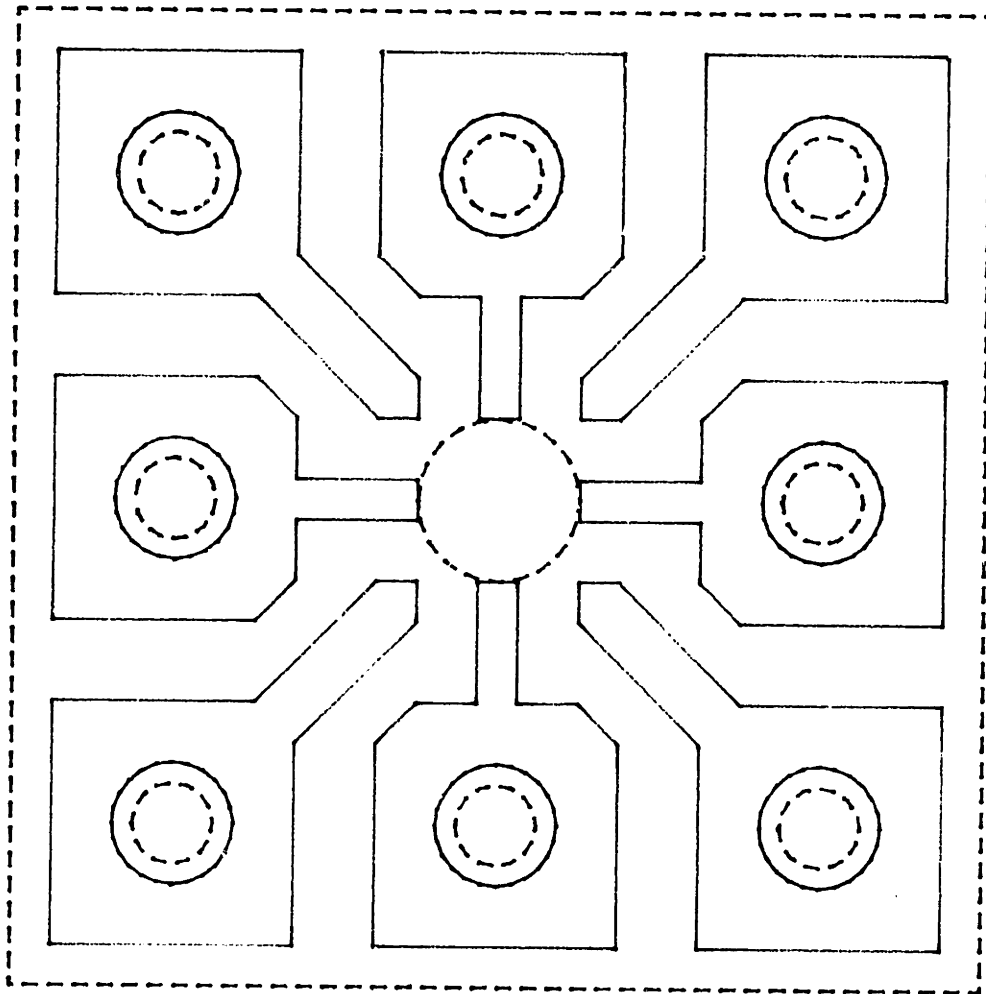


Figure G3) Overlay of Ceramic Piece and Conductive Pattern



the ceramic piece. While aligned, the assembly is heated until the solder melts, then cooled. If this is done properly, each bonding pad on the device will be electrically contacted to one of the big pads on the ceramic piece, via solder bonds to the gold balls. The purpose of the gold balls is twofold: 1) to provide an interface between the solder and the aluminum, since they do not adhere to one another, and 2) to lift the die slightly above the ceramic piece, thus helping to prevent short circuits that could occur if the solder flows.

Only the active surface area of the device is exposed through the center hole in the ceramic piece. If required by the device application, the gap between the die and the ceramic piece could be carefully sealed with epoxy along the inner rim of the center hole.

Contact to the outside world is to be made via thin ribbon cable. The wires are inserted from the back of the piece, through the hole in each pad. The tips of the wires are then soldered to the corresponding pads. This arrangement should guarantee sturdy electrical contacts.

If the device application demands it, the whole assembly could then be electrically insulated with epoxy, leaving exposed metal only on the active device area, and making the assembly immersible. This insulation is thus necessary for the ion-sensitive device.

## APPENDIX H. PLANS FOR AN IMMERSIBLE DEVICE

In conjunction with the ion-sensing studies, a device structure was designed for the purpose of surviving the rigors of immersion over long periods of time (Figures H1-2). The process was never used due to the lack of an appropriate pH-sensitive film. However, it is described here in a series of fifteen steps:

- 1) A thin layer of silicon dioxide is grown in dry  $O_2$  on a lightly-doped, p-type <100> silicon wafer. A layer of silicon nitride is deposited on top of the oxide, by the LPCVD (Low Pressure Chemical Vapor Deposition) technique.
- 2) Photoresist is spun onto the wafer. A masking step takes place in which the photoresist over field areas is removed. The exposed  $Si_3N_4$  is removed with a plasma etch in  $CF_4$  with 5%  $O_2$ . The remaining exposed oxide is stripped in buffered etch.
- 3) An ion implantation of boron dopes the exposed silicon heavily p-type, forming the channel-stop. The remaining photoresist is stripped.
- 4) A thick layer of oxide is grown in steam over the field areas. The  $Si_3N_4$  prevents this oxide growth over device areas.
- 5) The  $Si_3N_4$  is removed via a plasma etch as above, and the remaining oxide over device areas is again stripped with buffered etch.
- 6) An oxide of approximately 1000 Angstroms is grown in dry  $O_2$ . The wafer receives a light implant of arsenic, to dope the silicon under the thin oxide lightly n-type. This implant creates the depletion-mode devices.
- 7) Photoresist is applied and patterned, leaving openings only over the source/drain areas of the chip. Oxide is etched away here with buffered etch.
- 8) The source/drain areas of the wafer are doped heavily n-type with a second arsenic implant.
- 9) Photoresist is stripped, possibly requiring an  $O_2$  plasma etch,

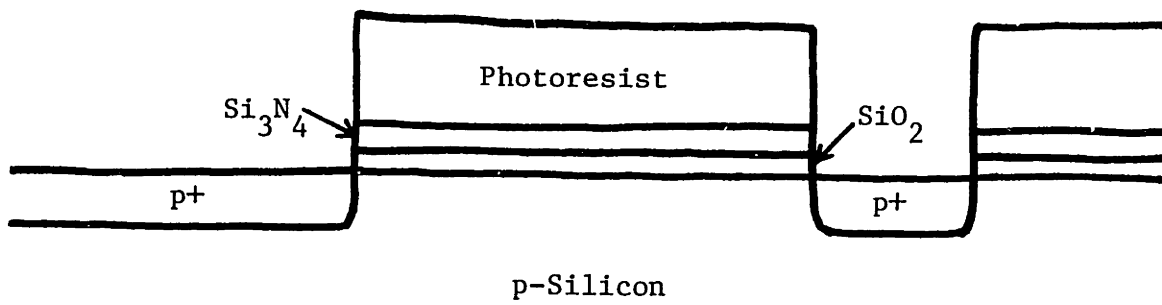


Figure H1A) Wafer Cross Section Following Implant of Step 3

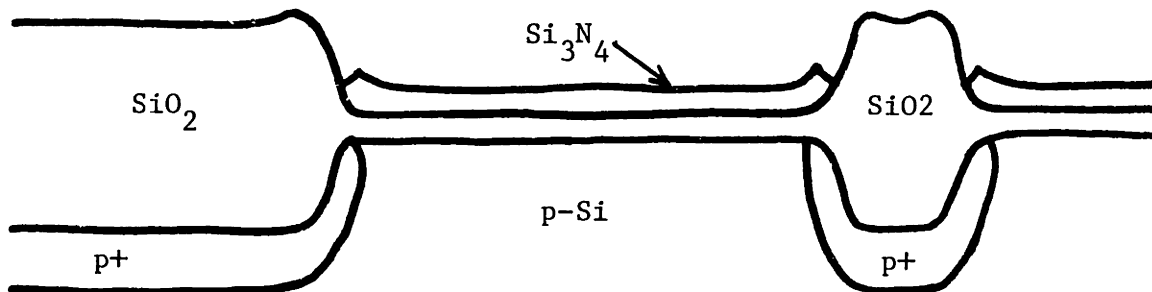


Figure H1B) Wafer Cross Section Following Step 4

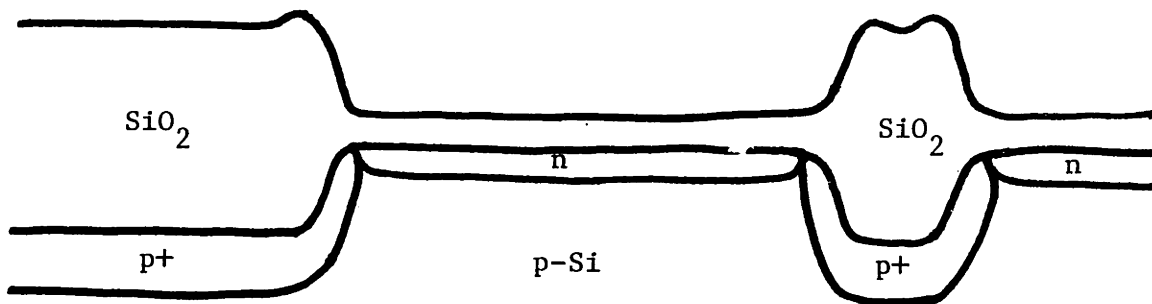


Figure H1C) Wafer Cross Section Following Step 6

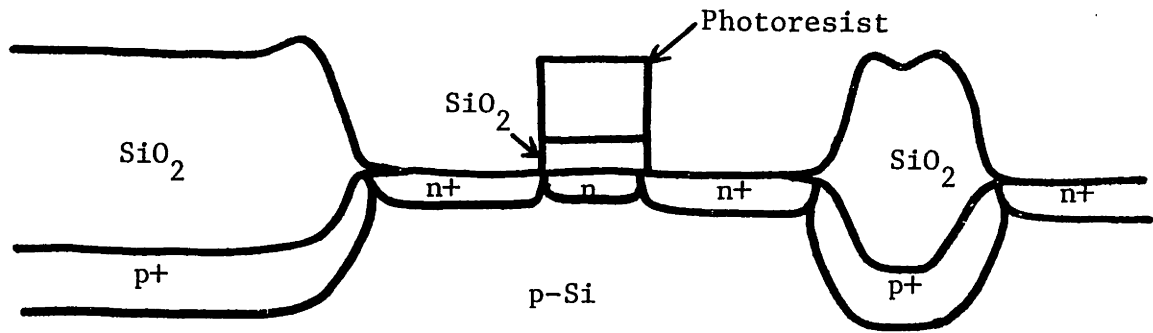


Figure H2A) Wafer Cross Section Following Step 8

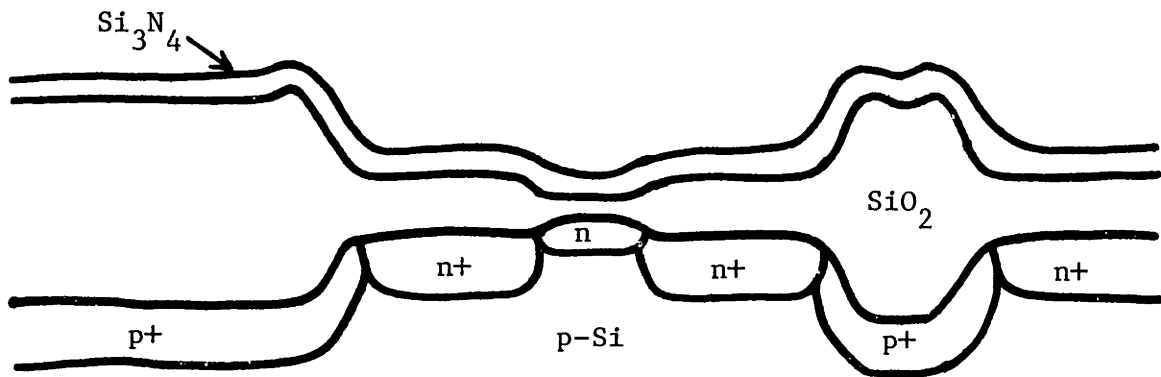


Figure H2B) Wafer Cross Section Following Step 10

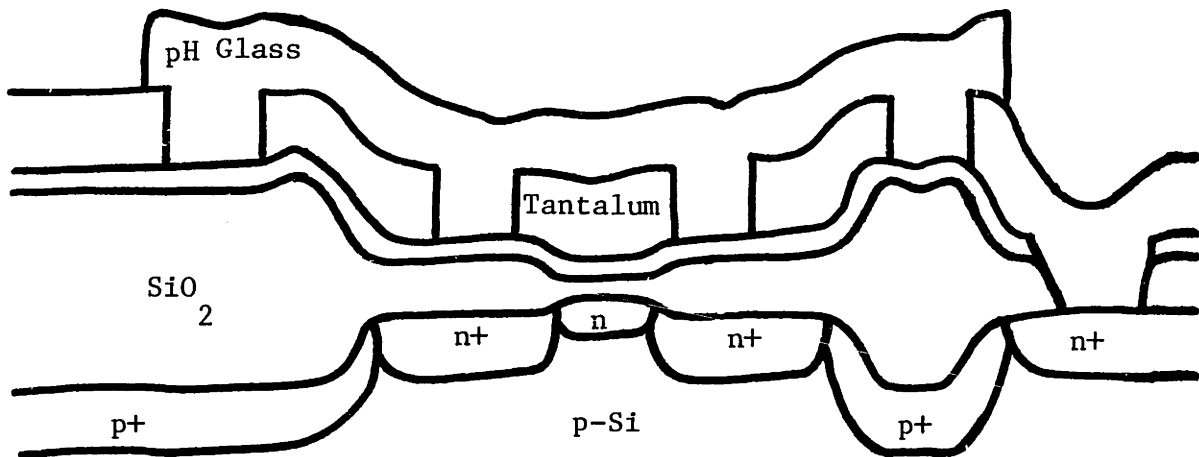


Figure H2C) Wafer Cross Section Following Step 14

due to the high implant dosage of the previous step. The thin oxide over the channel regions is stripped in buffered etch.

- 10) A new layer of 1000 Angstrom oxide is grown in dry  $O_2$ , followed by the deposition of a layer of  $Si_3N_4$ . This layer of silicon nitride will protect the oxide beneath from ions in the solution.
- 11) Photoresist is applied and patterned to have openings corresponding to contact holes. The exposed  $Si_3N_4$  is stripped with a plasma etch as before, and the remaining exposed oxide is stripped with buffered etch.
- 12) Photoresist is applied to the wafer and patterned such that photoresist is removed where metal is to lie. A layer of tantalum is deposited over the wafer, either by E-beam evaporation or sputtering. The tantalum is then patterned by "lifting off" the remaining photoresist. Tantalum was chosen as the metal because it resists corrosion, it adheres to silicon dioxide, and it makes a good contact to silicon.
- 13) The wafer is coated with a layer of pH-sensitive glass, by whatever means proves successful.
- 14) Photoresist is applied and patterned to leave openings above bonding pads, etc. The exposed pH glass is then removed above the tantalum by ion milling. The photoresist is stripped.
- 15) Contact pads are coated with a layer of aluminum, making bonding to the device possible. This could be done by evaporating the aluminum through a shadow mask since only course alignment is required.

## REFERENCES

- (1) Theory, Design, and Biomedical Applications of Solid-State Chemical Sensors, P.W. Cheung, D.G. Fleming, W.H. Ko, and M.R. Neuman, ed., CRC Press Inc., West Palm Beach, 1978.
- (2) J.M. Adcock III, "Evaluation of pH Glasses for Use in CFT Based Sensors", S.B. Thesis, MIT, May 1980, unpublished.
- (3) R.J. Johns, private communication.
- (4) N.L. Bowen, "The Study of the Electrical Conductivity of Poly (p-aminophenylacetylene) Using Charge-Flow Devices", S.M. Thesis, MIT, Sept. 1979, unpublished.
- (5) S.D. Senturia, N.F. Sheppard, S.Y. Poh, and H.R. Appelman, "The Feasibility of Electrical Monitoring of Resin Cure with the Charge-Flow Transistor", *Polymer Engineering and Science*, in press.
- (6) S.D. Senturia, C.M. Sechen, and J.A. Wishneusky, "The Charge-Flow Transistor: A New MOS Device", Appl. Phys. Lett. 30, 106-108, January 15, 1977.
- (7) S.D. Senturia, M.G. Huberman, and R. Van der Kloot, "Moisture Sensing with the Charge-Flow Transistor", Proc. ARPA/NBS Workshop on Moisture Measurement in Integrated Circuit Packages, Gaithersburg, Md., March 1978.
- (8) C.M. Sechen, "Charge-Flow Structures as Polymeric Early Warning Fire-Alarm Devices", S.M. Thesis, MIT, June 1977, unpublished.
- (9) N.F. Sheppard, "Electrical Monitoring of Epoxy Resin Polymerization", S.M. Thesis, in progress.
- (10) S.D. Senturia, "Fabrication and Evaluation of Polymeric Early-Warning Fire-Alarm Devices", NASA CR-134765, Final Contract Report, April 1975.
- (11) This result has been previously observed in another form: S.D. Senturia and R.J. Jachowicz, "Cooperative NBS-MIT Research on Capacitive Moisture Sensors", G8-9029, Final Grant Report, April 1979.
- (12) D.A. Antoniadis and R.W. Dutton, "Model for Computer Simulation of Complete IC Fabrication Process", IEEE Journal of Solid-State Circuits, Vol. SC-14, pp.412-422, April 1979.
- (13) A.G. Sabnis and J.T. Clemens, "Characterization of the Electron

Mobility in the Inverted <100> Silicon Surface", International Electron Device Meeting, December, 1979.

- (14) A. Jungreis, "Examination of a Moisture-Sensitive Co-polymer Matrix: PEO/PPO", MIT UROP Report, in progress.
- (15) S.Z. Hosain, "N-Channel Charge-Flow Transistors", S.B. Thesis, MIT, January 1979, unpublished.